

VACUUM STRUCTURE OF QCD IN AN EFFECTIVE LAGRANGIAN
APPROACH

By

Todd Darwin Fugleberg

B. Sc., The University of Saskatchewan, 1993

M. Sc., The University of British Columbia, 1996

A THESIS SUBMITTED IN PARTIAL FULFILLMENT OF
THE REQUIREMENTS FOR THE DEGREE OF
DOCTOR OF PHILOSOPHY

in

THE FACULTY OF GRADUATE STUDIES
DEPARTMENT OF PHYSICS

We accept this thesis as conforming
to the required standard

THE UNIVERSITY OF BRITISH COLUMBIA

August 2000

© Todd Darwin Fugleberg, 2000

In presenting this thesis in partial fulfilment of the requirements for an advanced degree at the University of British Columbia, I agree that the Library shall make it freely available for reference and study. I further agree that permission for extensive copying of this thesis for scholarly purposes may be granted by the head of my department or by his or her representatives. It is understood that copying or publication of this thesis for financial gain shall not be allowed without my written permission.

Department of Physics
The University of British Columbia
6224 Agricultural Road
Vancouver, B.C., Canada
V6T 1Z1

Date:

Aug. 21/00

Abstract

The vacuum structure of QCD is studied using an anomalous effective Lagrangian approach. This approach makes it possible to determine how physical observables depend on the strong CP violation parameter, θ . The θ -dependence of QCD and the phenomenology of the light pseudoscalar mesons in this theory are illustrated. The vacuum structure of QCD is shown to be quite complex with the prediction of a number of different types of nontrivial vacuum states. Two specific examples of nontrivial vacuum states are analysed in more detail. The decay rate of a metastable vacuum state for the $\theta = 0$ case is nonperturbatively calculated in both the zero and high temperature limits. The formation of a nontrivial θ -vacuum state in heavy ion collisions is predicted in a simplified numerical model. These results have implications for the study of the evolution of the early universe near the QCD phase transition and may be tested experimentally very soon in heavy ion collision experiments.

Table of Contents

| | |
|--|------------|
| Abstract | ii |
| Table of Contents | iii |
| List of Figures | v |
| Acknowledgement | vi |
| 1 Introduction | 1 |
| 1.1 Review of Quantum Chromodynamics and the θ -parameter | 2 |
| 1.2 Motivation | 9 |
| 1.3 Overview | 12 |
| 2 The Anomalous Effective Lagrangian and Implications | 15 |
| 2.1 The Anomalous Effective Lagrangian | 15 |
| 2.2 Theta Dependence | 20 |
| 2.3 Vacuum Structure | 21 |
| 2.3.1 $q=1$ | 23 |
| 2.3.2 $q\neq 1$ | 25 |
| 2.4 Phenomenology of the Pseudoscalar Mesons for Non-Zero θ | 25 |
| 3 False Vacuum Decay | 35 |
| 3.1 The Domain Wall Solution | 38 |
| 3.2 Semiclassical Theory | 40 |

| | | |
|----------|--|-----------|
| 3.3 | Quantum Corrections at Zero Temperature | 42 |
| 3.3.1 | Positive Eigenvalues | 43 |
| 3.3.2 | Zero and Negative Eigenvalues | 53 |
| 3.3.3 | Decay Rate for Zero Temperature | 54 |
| 3.4 | Quantum Corrections for High Temperature | 55 |
| 3.4.1 | Positive Eigenvalues | 55 |
| 3.4.2 | Zero and Negative Eigenvalues | 58 |
| 3.4.3 | Decay Rate for High Temperature | 59 |
| 3.5 | Summary | 59 |
| 4 | Production of Nontrivial Theta Vacua | 61 |
| 4.1 | DCC | 62 |
| 4.2 | Nontrivial θ -vacua | 64 |
| 4.3 | Numerical Evolution | 67 |
| 5 | Conclusions | 74 |
| 5.1 | Results | 74 |
| 5.2 | Future Research | 76 |
| | Bibliography | 79 |
| | Appendices | 84 |
| A | Derivation of the Effective Potential for QCD | 84 |
| A.1 | Anomalous Effective Lagrangian for QCD | 84 |
| A.2 | Determining the values of p and q | 91 |
| B | Hyperspherical Harmonics in Four Dimensions | 94 |

List of Figures

| | | |
|------|--|----|
| 2.1 | Branches of the effective potential before the infinite volume limit is taken. | 19 |
| 2.2 | Piecewise smooth effective potential after the infinite volume limit is taken. | 20 |
| 2.3 | Two flavour effective potential. | 24 |
| 2.4 | Vacuum energy as a function of vacuum angle θ | 24 |
| 2.5 | Effective potential for $q=2$ and $N_f = 2$ | 26 |
| 2.6 | π^0 mass as a function of θ | 31 |
| 2.7 | η mass as a function of θ | 31 |
| 2.8 | η' mass as a function of θ | 31 |
| 2.9 | The Euler θ angle as a function of θ | 33 |
| 2.10 | The Euler ϕ angle as a function of θ | 33 |
| 2.11 | The Euler ψ angle as a function of θ | 33 |
| 3.12 | Effective potential at $\theta = 0$ for equal chiral phases $\phi = \phi_u = \phi_d = \phi_s$. . . | 39 |
| 3.13 | The domain wall solution. | 40 |
| 3.14 | Expansion of the partition function. | 43 |
| 3.15 | The “potential” $U''(\phi_b(r))$ | 46 |
| 3.16 | Comparison of the perturbation $V_{pert}(r)$ and the approximate perturbation. | 48 |
| 3.17 | The phase shift $\delta_0(\omega_\lambda)$ shown as a function of ω_λ for various values of n . . | 49 |
| 4.18 | Time evolution of $ \phi_k $ shown for various $ \vec{k} $ | 69 |
| 4.19 | The Fourier distribution of the field is shown at three different times. . . | 70 |
| 4.20 | The zero mode and a non-zero mode are shown as a function of time for three different volumes. | 71 |

Acknowledgement

I would like to thank my supervisor, Dr. Ariel Zhitnitsky, for his help and guidance. I have learned a great deal through working with him and I am grateful to him for pushing me to make this thesis the very best it could be.

I would also like to thank the other members of my supervisory committee: Dr. Janis McKenna, Dr. John Ng and Dr. Gordon Semenoff for their invaluable help and comments. I would particularly like to thank Dr. McKenna for her advice on other career related matters.

I would like to thank Lori Paniak, Sebastian Jaimungal, Kirk Buckley, Mark Laidlaw, and Igor Halperin for their helpful advice and for many stimulating and enjoyable conversations. I would also like to thank all of my other friends here at U.B.C. for making my time in Vancouver very pleasant. In particular I would like to thank Jaret, Sofia, Greg, Mateo, Alison, Kevin and all the members of "Where's My Head".

Thanks are due to the entire faculty and staff of the Physics and Astronomy Department at U.B.C. for providing a stimulating and positive work environment.

I would like to acknowledge that this work was funded in part by the Natural Sciences and Engineering Research Council of Canada.

Words cannot express my gratitude to my family for the constant support and encouragement they have shown me throughout my studies and, indeed, throughout my life. I would especially like to thank my wonderful wife Lisa and my fantastic son Nathan for keeping me sane during this demanding process. This thesis is a testament to their love and support.

Chapter 1

Introduction

It is generally accepted that Quantum Chromodynamics (QCD) is the theory that describes the strong nuclear force. In this theory all hadrons are composite structures of particles called quarks, and quarks interact with other quarks via exchange of gluons¹. Quarks have a flavour, an electric charge and a colour charge, while gluons only carry colour charge.

The existence of quarks is supported by various experimental results. As well, all the observed hadronic particles can be described as colour singlet combinations of three quarks or quark-antiquark pairs. QCD can be used to calculate observables in the high energy (weak coupling) limit, such as in deep inelastic lepton-hadron scattering, and the theory agrees well with the experiments in this regime. Unfortunately, at low energies QCD exhibits essentially non-perturbative behaviour such as confinement and dynamical breaking of chiral symmetry. As well, QCD is asymptotically free, which means that the perturbative weak coupling limit applies in the high energy regime while the realm of ordinary nuclear matter is the nonperturbative strong coupling limit. Therefore, while QCD is an excellent candidate for a theory of the strong nuclear force, it is difficult to use it to obtain any quantitative low energy results for ordinary nuclear matter.

Anomalous effective Lagrangians are a useful tool for analysing QCD in the low energy limit. The anomalous effective Lagrangian used in this thesis makes it possible to study the vacuum structure of QCD, which could have important implications for study of the

¹As well as by the exchange of the electroweak force carriers

evolution of the early universe. As well, it allows us to make predictions that can be tested in heavy ion collisions. Probing the physics of the early universe directly in heavy ion collisions is certainly an exciting concept. We will return to the discussion of effective Lagrangians after a review of Quantum Chromodynamics.

1.1 Review of Quantum Chromodynamics and the θ -parameter

QCD is an $SU(N_c)$ gauge theory² defined by the QCD Lagrangian:

$$\mathcal{L} = -\frac{1}{4}G_{\mu\nu}^a G_a^{\mu\nu} + \sum_{i=1}^{N_f} \bar{\Psi}_\alpha^i (i\gamma^\mu D_\mu^{\alpha\beta} - m^i \delta^{\alpha\beta}) \Psi_\beta^i + \theta \frac{\alpha_s}{16\pi} G_{\mu\nu}^a \tilde{G}_a^{\mu\nu}, \quad (1.1)$$

where $G_{\mu\nu}^a$ is the field strength tensor of QCD, Ψ_α^i are the quark fields, $D_\mu^{\alpha\beta}$ is the covariant derivative and α_s is the QCD strong coupling parameter. The dual field strength tensor is defined as $\tilde{G}_a^{\mu\nu} = \varepsilon_{\sigma\rho\mu\nu} G_a^{\sigma\rho}$ where $\varepsilon_{\sigma\rho\mu\nu}$ is the totally antisymmetric four index tensor. The index i labels the quark flavour and the sum on i is over the number of quark flavours, N_f . The Greek indices α and β label the quark colour and run over the number of colours, N_c . The Greek indices μ and ν are Lorentz indices and run over the spacetime dimensions. The Roman index a on the field strength tensor is the colour index for the gluon fields and runs over the range: $a = 1 \dots N_c^2 - 1$. The theory of QCD has $N_c = 3$ and this value is used in this thesis even though we leave the symbol N_c in the formulas so that N_c dependence is explicit. We will be concerned with low energy physics so we will only include the light quarks. In Chapter 2 and Chapter 3 we will include the up, down, and strange quark flavours ($N_f = 3$) and in Chapter 4 our numerical results only include the up and down flavours ($N_f = 2$).

The field strength tensor in terms of the gluon (gauge) fields is:

$$G_{\mu\nu}^a = \partial_\mu A_\nu^a - \partial_\nu A_\mu^a - g_s f_{abc} A_\mu^b A_\nu^c, \quad (1.2)$$

² $SU(N_c)$ is the group of $N_c \times N_c$ unitary matrices with unit determinant

where $g_s^2 \equiv 4\pi\alpha_s$ and f_{abc} are the structure constants of the gauge group $SU(N_c)$. The quark covariant derivative is:

$$D_\mu^{\alpha\beta} \Psi_\beta^i = \left(\delta^{\alpha\beta} \partial_\mu + ig_s A_\mu^a \frac{\lambda_a^{\alpha\beta}}{2} \right) \Psi_\beta^i, \quad (1.3)$$

where $\lambda_a^{\alpha\beta}$ are the generators of $SU(N_c)$.

QCD is a $SU(N_c)$ gauge theory which means that the Lagrangian is invariant under coupled $SU(N_c)$ transformations of the quark and gluon fields similar to electromagnetism. We will not comment further on this fact other than to comment that physical observables must be invariant under these gauge transformations and are said to be gauge invariant.

The “extra” term in (1.1) involving the θ -parameter is a total derivative and thus is irrelevant to perturbation theory. However, nonperturbative effects due to instantons indicate that this term should be included in general. We will say more about this θ -parameter after discussing the symmetries of the Lagrangian.

In the chiral limit, which is defined by $m_i = 0$, this Lagrangian is invariant under the transformations:

$$\begin{aligned} \Psi_\alpha^i &\rightarrow \exp(iA\lambda_{ij}^b) \Psi_\alpha^j, \\ \Psi_\alpha^i &\rightarrow \exp(iA\lambda_{ij}^b \gamma^5) \Psi_\alpha^j, \end{aligned} \quad (1.4)$$

where A is an arbitrary real constant and λ_{ij}^b are the generators of the group of $N_f \times N_f$ unitary matrices, $U(N_f)$. The transformations correspond to the multiplication of a vector of quarks in flavour space by a member of $U(N_f)$. The invariance under these two types of transformations means that the Lagrangian has an $U(N_f)_{\text{Vector}} \times U(N_f)_{\text{Axial}}$ symmetry. The $U(N_f)$ matrices can be written as the product of the matrices corresponding to subgroups of $U(N_f)$:

$$U(N_f) = SU(N_f) \otimes U(1), \quad (1.5)$$

where $SU(N_f)$ has already been defined and $U(1)$ is simply an overall phase which also fixes the determinant of the $U(N_f)$ matrix. The symmetry group of the massless QCD Lagrangian is then³:

$$SU(N_f)_{\text{Vector}} \otimes U(1)_{\text{Vector}} \otimes SU(N_f)_{\text{Axial}} \otimes U(1)_{\text{Axial}}. \quad (1.6)$$

Symmetries of the Lagrangian can be shown to imply the existence of conserved currents. For example, the vector current defined in terms of the quark fields is conserved:

$$\partial_\mu J^\mu \equiv \partial_\mu (\bar{\Psi} \gamma^\mu \Psi) = 0. \quad (1.7)$$

The conserved currents lead to conserved charges:

$$\frac{d}{dt} Q \equiv \frac{d}{dt} \left(\int d^3x J^0 \right) = 0. \quad (1.8)$$

As well, current conservation leads to certain exact identities, called Ward Identities, which are very important and useful.

Symmetries of a field theory at the classical level may not be true symmetries of the quantised field theory. Quantising the fields and applying perturbation theory may reveal that the symmetry is not respected by the quantum theory. In this case the symmetry is said to have an anomaly. The associated currents and charges are no longer conserved, but the Ward Identities that come from the original symmetry are not lost, and are simply altered to include the effect of the anomaly. They are then referred to as anomalous Ward Identities. The $U(1)_{\text{Axial}}$ symmetry of massless QCD is anomalous and this anomaly is taken into account in anomalous effective Lagrangians, which we discuss in the next section.

As well, some of the symmetries of the Lagrangian may not be respected by the vacuum state. This is called spontaneous symmetry breaking and is indicated by the

³There is also the $SU(N_c)_{\text{Color}}$ gauge symmetry and a scaling symmetry that we ignore here.

existence of a non-zero vacuum expectation value of some combination of fields, which is called a condensate. Another result is the appearance of a massless particle, called a Goldstone boson, for every broken symmetry. In the QCD vacuum, the condensate:

$$\langle \bar{\Psi}\Psi \rangle \neq 0, \quad (1.9)$$

spontaneously breaks the $U(N_f)_{\text{Axial}}$ subgroup of the symmetry group (1.6). This corresponds to nine broken symmetries and should indicate the presence of nine Goldstone bosons. These symmetries, however, are explicitly broken by the mass terms which we will discuss next.

For non-zero quark masses, $m_i \neq 0$, the QCD Lagrangian is no longer invariant under the transformations (1.4) and we say that the symmetry is explicitly broken⁴. Fortunately the Ward Identities can again be simply altered to include the effects of the explicit breaking of the symmetry. Further, it can be shown that the Goldstone bosons will acquire small masses proportional to the square root of the quark masses and are then referred to as pseudo-Goldstones. The pions, kaons and the η -meson are identified as the 8 pseudo-Goldstones of the spontaneously broken $SU(N_f)_{\text{Axial}}$ symmetries. The η' meson, however, which should be the remaining pseudo-Goldstone of the broken $U(1)_{\text{Axial}}$ symmetry, is heavier than it should be. This is the famous $U(1)$ problem.

The last term in the QCD Lagrangian (1.1) involving the θ -parameter is related to the vacuum structure of QCD and the axial anomaly. This term is important for this thesis so we give a brief explanation of its origin (for a detailed discussion see [1]).

It can be shown that all possible configurations of the gauge field, A_μ^a , can be all be classified by an integer, n , called the winding number, which is determined by:

$$n = \frac{ig_s^3}{24\pi^2} \int d^3x \varepsilon^{ijk} (A_i^a A_j^b A_k^c) \text{Tr}(\lambda^a \lambda^b \lambda^c), \quad (1.10)$$

⁴For equal masses of the quarks there is a remnant $SU(N_f)$ flavour symmetry that will remain unbroken. This point will be relevant to the meson mixing angles in Chapter 2.

where Tr denotes the matrix trace over the generating matrices, λ^a of $SU(N_c)$. In particular the vacuum configurations of the fields fall into classes labelled by the winding number and these are referred to as winding vacua. However, there exist operators corresponding to physical observables that transform between winding vacua:

$$\mathcal{O}|n\rangle = |n+1\rangle, \quad (1.11)$$

which implies that the QCD vacuum should involve contributions from all winding vacua. The θ -vacuum states, which are coherent superpositions of winding vacua:

$$|\theta\rangle = \sum_n e^{-in\theta} |n\rangle, \quad (1.12)$$

are the vacuum states that allow no transitions between different vacuum states:

$$\langle\theta|\mathcal{O}|\theta'\rangle \sim \delta(\theta - \theta'). \quad (1.13)$$

Using these θ -vacuum states in QCD has a nontrivial effect on the Lagrangian which we illustrate next.

The vacuum-vacuum transition amplitude in terms of the $|\theta = 0\rangle$ -vacua is defined to be:

$$\langle\theta = 0|\mathcal{O}|\theta = 0\rangle \equiv \int \mathcal{D}A_\mu \mathcal{D}\bar{\Psi} \mathcal{D}\Psi \mathcal{O} \exp \left[i \int d^4x \mathcal{L} \right], \quad (1.14)$$

where \mathcal{L} is the QCD Lagrangian (1.1) without the θ term. This amplitude can be written in terms of the winding vacua as:

$$\langle\theta = 0|\mathcal{O}|\theta = 0\rangle = \sum_{m,n} \langle m|\mathcal{O}|n\rangle. \quad (1.15)$$

The presence of non-zero θ leads to an extra phase:

$$\langle\theta|\mathcal{O}|\theta\rangle = \sum_{m,n} e^{i(m-n)\theta} \langle m|\mathcal{O}|n\rangle. \quad (1.16)$$

It can be shown that:

$$\frac{g_s^2}{64\pi^2} \int d^4x G_{\mu\nu}^a \tilde{G}^{\mu\nu}_a = m - n, \quad (1.17)$$

which describes a gauge field configuration which changes winding number over time.

Combining equations (1.14), (1.15), (1.16) and (1.17) we obtain the result:

$$\langle \theta | \mathcal{O} | \theta \rangle = \int \mathcal{D}A_\mu \mathcal{D}\bar{\Psi} \mathcal{D}\Psi \mathcal{O} \exp \left[i \int d^4x \left\{ \mathcal{L} + \frac{\alpha_s}{16\pi} G_{\mu\nu}^a \tilde{G}_a^{\mu\nu} \right\} \right], \quad (1.18)$$

where we have used $g_s^2 \equiv 4\pi\alpha_s$. The integrand in the exponent is exactly the QCD Lagrangian we quoted in (1.1). This shows that the general QCD Lagrangian should include the θ -term.

The θ term is connected with the axial anomaly. The axial anomaly can be restated as the fact that the axial current:

$$J_{5\mu} = \sum_{i=1}^{N_f} \bar{\Psi}^i \gamma^5 \gamma^\mu \Psi^i, \quad (1.19)$$

is not conserved. It can be shown that the divergence of the axial current in the quantum theory is given by:

$$\partial_\mu J_5^\mu = \frac{N_f \alpha_s}{8\pi} G_{\mu\nu}^a \tilde{G}_a^{\mu\nu}. \quad (1.20)$$

As was mentioned earlier, $G_{\mu\nu}^a \tilde{G}_a^{\mu\nu}$ is a total divergence, which means it can be written:

$$G_{\mu\nu}^a \tilde{G}_a^{\mu\nu} = \partial_\mu K^\mu. \quad (1.21)$$

K^μ is defined in terms of the gauge fields, A_μ^a , and is not gauge invariant. This means that we can define a new conserved current:

$$\tilde{J}_{5\mu} = J_{5\mu} - \frac{N_f \alpha_s}{8\pi} K_\mu, \quad (1.22)$$

with a corresponding conserved charge:

$$\tilde{Q}_5 = \int d^3x \tilde{J}_{50}. \quad (1.23)$$

It can be shown that this charge generates changes of the θ parameter:

$$e^{iA\tilde{Q}_5}|\theta\rangle = |\theta - 2N_f A\rangle, \quad (1.24)$$

for arbitrary real constant A . This does not contradict our earlier comments because \tilde{Q}_5 is not gauge invariant and therefore does not correspond to a physical observable. If all the quarks are massless then the conservation of the anomalous axial current means that the θ -dependence of the physical theory can be removed by a $U(1)_{\text{Axial}}$ rotation.

The θ term in (1.1) breaks some discrete symmetries of the rest of the Lagrangian. Without this term, the Lagrangian is invariant under the charge conjugation (C) transformation, where particle and anti-particles are switched ($\bar{\Psi} \leftrightarrow \Psi$), and the Parity (P) transformation where all spatial vectors are reflected through the origin ($\vec{x} \rightarrow -\vec{x}$). The term involving the θ -parameter explicitly breaks P and CP invariance and we can say that the θ parameterises the amount of CP violation in the strong interaction. Stringent limits have been placed on the value of the θ -parameter in the universe today by measurements of the neutron electric dipole moment[2] which predict a value of $\theta < 10^{-10}$ [3].

The problems of the θ -parameter are not eliminated, however, as the θ -parameter in the full theory will contain, for instance, in addition to any fundamental parameter, contributions from the determinant of the quark mass matrix(see [1]):

$$\theta = \theta_{QCD} + \arg(\det M). \quad (1.25)$$

The strong CP problem can then be stated in the following way: “Why do completely unrelated contributions to the θ -parameter cancel each other out to such a high degree of accuracy?”. A solution to this problem can be found by promoting the θ -parameter to the status of a dynamical field called the axion. This field can be shown to dynamically relax to zero, providing a solution to the strong CP problem[4]. The axion is an extremely

weakly interacting particle and has so far evaded detection despite the best efforts of many physicists.

It is important to note, however, that this research does not require the existence of the axion. In fact, even if there is no dynamical axion to solve the strong CP problem, we will argue in Chapter 4 that it is possible to create regions of space where dynamical fields will behave as if the θ -parameter were non-zero. This “induced” θ -parameter could differ significantly from the θ -parameter in the universe as a whole. This type of non-zero θ -parameter is much more likely to be observed in heavy ion collisions and is perhaps a more important motivation for considering non-zero values of θ . We will not distinguish between the two types of θ for most of the results of this thesis.

1.2 Motivation

As was mentioned previously, it is difficult to use the full theory of QCD to calculate observables in the low energy regime. However, in this regime we are able to use effective Lagrangians which have proven to be a very powerful tool in Quantum Field Theory. These effective Lagrangians are not meant to be a complete theory, but are used to study the behaviour of the low energy degrees of freedom of QCD in order to understand the theory in this regime.

There are two main types of effective Lagrangians in use in Quantum Field Theory. The first type is the Wilsonian effective action which describes the low energy dynamics of the lightest particles in the theory. The heavier particles are in some sense “integrated out” as can actually be done in some quantum field theories. However, in many cases (such as QCD), it is not known how to do this and one simply writes down an effective Lagrangian based on constraints such as symmetries. Effective Chiral Lagrangians are of this type and are very useful in their domain of application.

Another type of effective Lagrangian is defined as the Legendre transformation of the generating functional for the connected Greens functions. This formulation implements (at the Lagrangian level) anomalous Ward identities relating vacuum condensates of the fields and is referred to as the anomalous effective Lagrangian. This type of approach is very useful in studying vacuum properties of the theory and is the approach used in this thesis.

The utility of the second type of approach was recognised long ago for supersymmetric gauge theories for both the pure gauge case [5] and for full supersymmetric QCD[6]. More recently it has been applied to non-supersymmetric Yang Mills theory[7] and generalised to QCD[8, 9]. The Witten-Veneziano-Di Vecchia effective chiral Lagrangian[10], which was studied even earlier, represents a hybrid of the two types of effective Lagrangians. It is based on symmetry properties, as are effective chiral Lagrangians, but it also represents the first attempt to include the effects of the anomaly which leads to the second type of approach.

It should be stressed that the form of the anomalous effective Lagrangian used in this thesis is only one possible candidate for a low energy effective Lagrangian for QCD. It is certainly a promising candidate, but we can not say with certainty that it is the only one.

Study of this anomalous effective Lagrangian approach is interesting for four reasons. First, this effective Lagrangian provides a generalisation of the large N_c Di Vecchia-Veneziano-Witten effective chiral Lagrangian (VVW ECL) for arbitrary N_c . The VVW ECL was determined purely from symmetry considerations and inclusion of the anomaly. The Lagrangian that we use is a generalisation in the sense that starting from this Lagrangian, integrating out the heavy degrees of freedom, and then passing to the large N_c limit, we reproduce the VVW ECL. Furthermore, this approach to the derivation of the VVW ECL fixes all dimensional parameters in terms of the measurable quark and

gluon condensates. I cannot stress enough that we are not saying that the VVW ECL is wrong. The effective Lagrangian we use is simply a possible generalisation of the VVW effective chiral Lagrangian to finite values of N_c .

Second, this approach makes it possible to address the problem of the θ -dependence of QCD. The θ -parameter is the strong CP violation parameter which was discussed in the previous section. The form of the effective Lagrangian that we use solves a number of puzzles relating to the θ -dependence of physical observables in general and the energy dependence of a nontrivial θ -vacuum. The θ -dependence of QCD is directly related to the axion potential since the axion arises by promoting the θ -parameter to the status of a dynamical field.

Third, this effective Lagrangian allows one to address the phenomenology of the light pseudoscalar mesons and the η' meson without any further phenomenological input. We obtain important results concerning the η' mass and we are able to calculate the masses of the light neutral pseudoscalar mesons (π^0 and η). We obtain values for the $\eta - \eta'$ mixing angle for unbroken SU(2) flavour symmetry and $\pi^0 - \eta - \eta'$ mixing angles for fully broken flavour symmetry. As well, we generalise the above results to include the effect of a non-zero θ -parameter. Finally, we show that the mesons cease to be pure pseudoscalars in the presence of a non-zero θ -parameter. The θ -dependence in the phenomenology of the pseudoscalar mesons is particularly important for the detection of some of the nontrivial vacuum states that we will discuss next.

The final, and perhaps the most important reason, for studying this effective Lagrangian, is that it predicts the possibility of a large variety of metastable vacua in certain regions of parameter space. Nontrivial vacua have been shown to exist in Yang Mills theories in the large N_c limit using the AdS/CFT correspondence[11]. The same phenomenon was observed in the analysis of soft breaking of supersymmetric models[12]. The existence of nontrivial vacua appears to be a general phenomenon for gauge theories in the strong

coupling limit. The metastable vacua could have played an important role in the evolution of the early universe at around the time of the QCD phase transition. The possible effects include dark matter (axions [13] and MACHOs [14]), baryogenesis[15, 16], the formation of large scale magnetic fields[17] and many others[18]. Therefore, understanding the physics of these nontrivial vacuum states could be important in understanding the early evolution of the universe. What is even more exciting is that most of the results of this thesis are potentially testable in heavy ion collisions at the Relativistic Heavy Ion Collider (RHIC) at Brookhaven National Laboratories. One of the results presented in this thesis suggests that a nontrivial θ -vacuum state is potentially observable at RHIC. The θ -dependence of the phenomenology of the pseudoscalar mesons discussed above provides a number of ways to look for this θ -vacuum state. Probing the physics of the early universe directly in heavy ion collisions is certainly an exciting possibility.

The reasons for believing that this effective Lagrangian might be physically meaningful are also fourfold. First, by construction, it reproduces the chiral and conformal Ward identities of QCD. Second, it reduces to the VVW ECL in the appropriate limits as was mentioned above. Third, it reproduces the known dependence of physical observables in θ for small values of θ , but also leads to 2π periodicity of physical observables in θ . Fourth, the related effective Lagrangian for gluodynamics [7] has the desirable property:

$$\left. \frac{d^{2k} E_{vac}(\theta)}{d\theta^{2k}} \right|_{\theta=0} \sim (1/N_c)^{2k}, \quad (1.26)$$

which was argued for by Veneziano in order for the $U(1)$ problem to be resolved [19].

1.3 Overview

The vacuum properties of QCD are studied starting from an anomalous effective Lagrangian.

First, the form of the anomalous effective Lagrangian is discussed.

Second, the θ -dependence of the vacuum of QCD is studied in this approach and shown that it has the correct θ -dependence for small θ and that it also produces 2π periodicity in θ of physical observables.

Third, the phenomenology of the pseudoscalar mesons is studied. We obtain a mass formula for the η' meson which is a generalisation of the mass formula from [8] to non-zero values of θ . We obtain values for the masses of the neutral pseudoscalars for arbitrary values of θ . We also obtain a formula for the $\eta - \eta'$ mixing angles and a method of calculating the $\pi_0 - \eta - \eta'$ mixing angles for non-zero θ . Finally we can show that for non-zero values of θ the pseudoscalar mesons cease to be pure pseudoscalars, but acquire scalar components.

Fourth, the decay rate is calculated for a false vacuum at $\theta = 0$ consisting of a chiral fields at a nontrivial minimum of the effective potential. We nonperturbatively calculate the decay rate per unit volume, Γ/V , for both the zero and high temperature theories. In addition, the method used in these calculations represents a new approach that could be useful in other calculations of this type.

Finally, a numerical study is presented of the evolution of the light degrees of freedom in regions of non-zero θ in order to show that it is possible to form a nontrivial θ -vacuum state in relativistic heavy ion collisions.

The goal of this thesis is develop the understanding of the vacuum structure of QCD in this particular effective Lagrangian approach and make predictions about observable consequences that could be tested in heavy ion collisions.

In Chapter 2 the anomalous effective Lagrangian is discussed and the θ -dependence of the vacuum, the vacuum structure and the phenomenology of the pseudoscalar mesons is studied in this theory. In Chapter 3 we calculate the decay rate of a chiral false vacuum for the low temperature theory and the high temperature theory. In Chapter 4 we discuss a numerical calculation performed to demonstrate the possibility of producing

a nontrivial θ -vacuum state in a heavy ion collision. Chapter 5 discusses conclusions and areas for future research.

Chapter 2

The Anomalous Effective Lagrangian and Implications

The purpose of this chapter is to introduce the anomalous effective Lagrangian for QCD and discuss some of its implications¹. In the first section we discuss the form of the anomalous effective Lagrangian. In the second section we discuss the θ -dependence of the vacuum energy. In the third section we discuss the structure of the QCD vacuum. In the fourth section we discuss the phenomenology of the light neutral pseudoscalar mesons and the η' meson, including the masses and mixing angles and the appearance of a scalar component of the mesons for non-zero θ .

2.1 The Anomalous Effective Lagrangian

The construction of the effective Lagrangian used in these studies was already accomplished before this research. The details of the effective Lagrangian necessary for the understanding of this work are presented here. For completeness, a review of the derivation by Zhitnitsky and Halperin[7, 8] is included in Appendix A.

A useful tool for studying the properties of the QCD vacuum in the presence of the θ -parameter is the anomalous effective Lagrangian for QCD. The anomalous effective Lagrangian is defined as the Legendre transform of the generating functional for zero momentum correlation functions. In QCD the relevant operators are $G_{\mu\nu}\tilde{G}^{\mu\nu}$ (topological density operator), $G^2 \equiv G_{\mu\nu}G^{\mu\nu}$ (gluon scalar current) and $\bar{\Psi}\Psi$ (quark condensate). The correlation functions of both gluon operators are fixed in terms of the gluon condensate:

¹Many of the results of this chapter were published in [9].

$\langle \alpha_s / \pi G^2 \rangle$ [20, 21]. Actually, only the potential part of this Lagrangian can be constructed as this is the only part that can be fixed by low energy theorems relating the zero momentum correlation functions. The potential part determines the whole Lagrangian, however, once the standard kinetic term is inserted, and so we will use the terms effective potential and effective Lagrangian interchangeably.

The most important point is that the effective potential constructed in this way will contain all the information provided in known low energy theorems of QCD.

In the effective Lagrangian approach the light² matter fields are described by the unitary matrix, U_{ij} , corresponding to the phases of the chiral condensate:

$$\langle \bar{\Psi}_L^i \Psi_R^j \rangle = -|\langle \bar{\Psi}_L \Psi_R \rangle| U_{ij}, \quad (2.27)$$

with ³:

$$U = \exp \left[i\sqrt{2} \frac{\pi^a \lambda^a}{f_\pi} + i \frac{2}{\sqrt{N_f}} \frac{\eta'}{f_{\eta'}} \right], \quad UU^\dagger = 1, \quad (2.28)$$

where λ^a are the Gell-Mann matrices of $SU(N_f)$, π^a is the octet of pseudoscalar fields (pions, kaons and the eta meson) and η' is the $SU(N_f)$ singlet pseudoscalar field (meson). We use the values $f_\pi = 132 \text{ MeV}$ [22] and $f_{\eta'} = 86 \text{ MeV}$ [20] for the meson decay constants⁴. The indices, i and j , of U_{ij} run over the quark flavour index, $i, j = 1 \dots N_f$, which correspond to the quark flavours up(u), down(d) and strange(s), respectively.

The effective potential in terms of these fields is given by:

$$W_{eff}(U, U^\dagger) = - \lim_{V \rightarrow \infty} \frac{1}{V} \log \left\{ \sum_{l=0}^{p-1} \exp \left[V E \cos \left[-\frac{q}{p} (\theta - i \log \det U) + \frac{2\pi}{p} l \right] + \frac{1}{2} V \text{Tr}(MU + M^\dagger U^\dagger) \right] \right\}, \quad (2.29)$$

²Note that the η' is not really very light, but it enters the theory in this way and the mass of the η' is one of the topics that we address in this thesis.

³Note that mixing of the flavour eigenstates is ignored at this level. See Section 2.4 for more details.

⁴It should be noted that what we refer to as $f_\pi / \sqrt{2}$ is sometimes denoted f_π in the literature. As well, what we refer to as $f_{\eta'}$, is $f_{\eta'} / \sqrt{3}$ in the notation of [20].

where V is the total four volume, $M = \text{diag}(m_i |\langle \bar{\Psi}^i \Psi^i \rangle|)$ and $E = b\alpha_s / (32\pi) \langle G^2 \rangle$ ⁵, $b = \frac{11}{3}N_c - \frac{2}{3}N_f$ is the first coefficient of the Gell-Mann - Low β -function of QCD (see Appendix A) and Tr denotes the matrix trace. The sum over the integer l arises in the full derivation (see Appendix A) and is a sum over different branches⁶ of the potential (see below). It is necessary in order that the full effective potential, including the gluon degrees of freedom, be single valued and bounded from below. The sum remains after the heavy gluon degrees of freedom are integrated out. The prescription of summing over all branches was first suggested in [23] and applied to the anomalous effective Lagrangian of [5] to cure problems similar to this case. As well, this prescription is consistent with the results of [11] where the problem of θ -dependence is studied using the AdS/CFT correspondence.

The parameters p and q are relatively prime integers of the order: $p = \mathcal{O}(N_c)$ and $q = \mathcal{O}(N_c^0) = \mathcal{O}(1)$. Different approaches to fixing these parameters give different results. For completeness, the details of these approaches are discussed in Appendix A. Here we simply give the two sets of parameters that have been derived:

- $q = 1$ and $p = N_c$,
- $q = 8$ and $p = 3b_{QCD} = 11N_c - 2N_f$,

where b_{QCD} is the first coefficient of the beta function of QCD. The first set of values is perhaps more natural and is in agreement with supersymmetric theories, but there are some difficulties with the arguments for transferring these results unchanged to non-supersymmetric theories⁷. The second set of values has been derived from a number of

⁵We use the values $\langle \alpha_s / \pi G^2 \rangle = 0.012 \text{ GeV}^4$, $\langle \bar{\Psi}^u \Psi^u \rangle = \langle \bar{\Psi}^d \Psi^d \rangle = -(240 \text{ MeV})^3$ and $\langle \bar{\Psi}^s \Psi^s \rangle = -0.8 (240 \text{ MeV})^3$, except in Chapter 3 where we use $\langle \bar{\Psi}^s \Psi^s \rangle = -(240 \text{ MeV})^3$.

⁶If a single value for l was used in this effective potential, instead of summing over l , then the effective potential would simply be the argument of the exponential for a specific value of l . This is what is meant by the branch of the effective potential and is labelled by the integer l .

⁷See Appendix A for brief details and references.

different approaches and cannot be ruled out. The question of which set of parameters is correct is very significant as different values of these parameters can lead to some different qualitative results. Most of the results of this thesis do not depend on specific values of these parameters. When results do depend on specific values, this fact will be pointed out and discussed.

The effective potential (2.29) may not be represented by a single analytic function in the $V \rightarrow \infty$ limit. The thermodynamic limit selects, at each value of $\theta - i \log \det U$, one particular branch (*ie.* a particular value of the integer l) and cusp singularities occur where the branches coincide. The different branches of the effective potential before the infinite volume limit is taken are shown in Figure 2.1. The infinite volume limit picks the lowest energy branch out from all the other branches of the effective potential (see Figure 2.2). The cusps are present because level crossing occurs and the branch which is the lowest energy changes due to this crossing.

The present form of the effective potential (2.29) is most conducive to discussing the topic of chiral rotations. Notice that one can perform the global transformation:

$$U \rightarrow \text{diag}(e^{i\psi_i}) U, \quad (2.30)$$

to transform to a Lagrangian of the same form since the kinetic term of the form, $\text{Tr}(\partial_\mu U \partial_\mu U^{-1})$, will be unaffected. This fact was used in [10] to introduce the θ -parameter into the effective potential. This fact was also used in [10] to show that if any of the quark masses vanish, the θ -parameter can have no effect on the physics. This result will be briefly touched on later in this chapter. Finally, we will use a chiral rotation of this type in Chapter 4 to introduce the concept of the induced θ -parameter.

Now we return to the effective potential for the light matter fields which, when we take $U = \text{diag}(e^{i\phi_i})$ ⁸, becomes a piecewise smooth potential for the phases of the chiral

⁸This is not a restriction since the quark mass matrix can always be diagonalised.

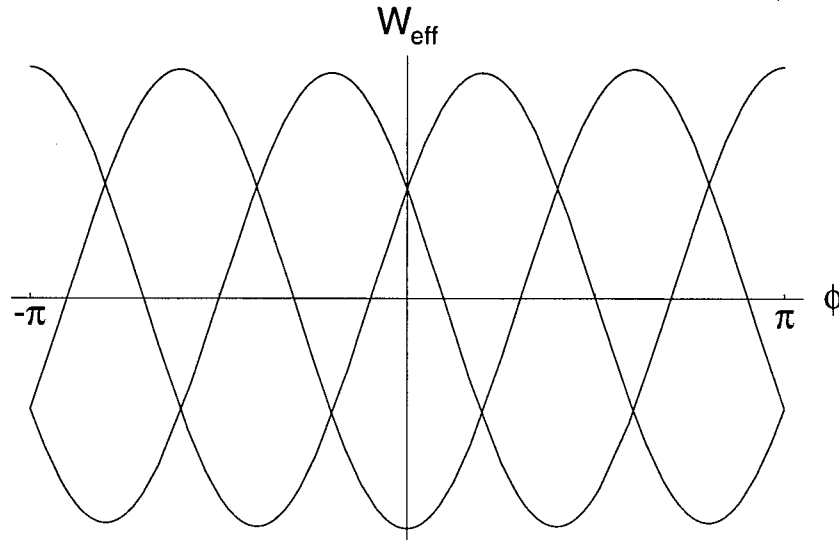


Figure 2.1: Branches of the effective potential before the infinite volume limit is taken for $\theta = 0$, $N_f = 1$, $q = 5$ and $p = 3b_{QCD}$.

condensate, with cusp singularities:

$$W_{eff}^{(l)} = -E \cos \left(-\frac{q}{p}\theta + \frac{q}{p} \sum \phi_i + \frac{2\pi}{p} l \right) - \sum M_i \cos \phi_i, \quad l = 0, 1, \dots, p-1, \quad (2.31)$$

if

$$(2l-1)\frac{\pi}{q} \leq \theta - \sum \phi_i < (2l+1)\frac{\pi}{q}. \quad (2.32)$$

The chiral phases of the quark condensate are denoted by ϕ_i where the index 'i' runs over the quark flavour index (*ie.* u, d, s). They are also referred to as the light chiral fields and are related to the pseudoscalar meson fields by recalling Eq. (2.28).

At this point it is useful to give some indication of what the parameters p and q mean in terms of the effective potential. The parameter ' p ' is the number of branches of the effective potential. It also corresponds to the number of distinct vacua before the infinite volume limit is taken. The parameter ' q ' determines the number of distinct vacua with different energies that exist before the infinite volume limit is taken. For q even there are $(q+2)/2$ different energy vacua; for q odd there are $(q+1)/2$ different energy vacua.

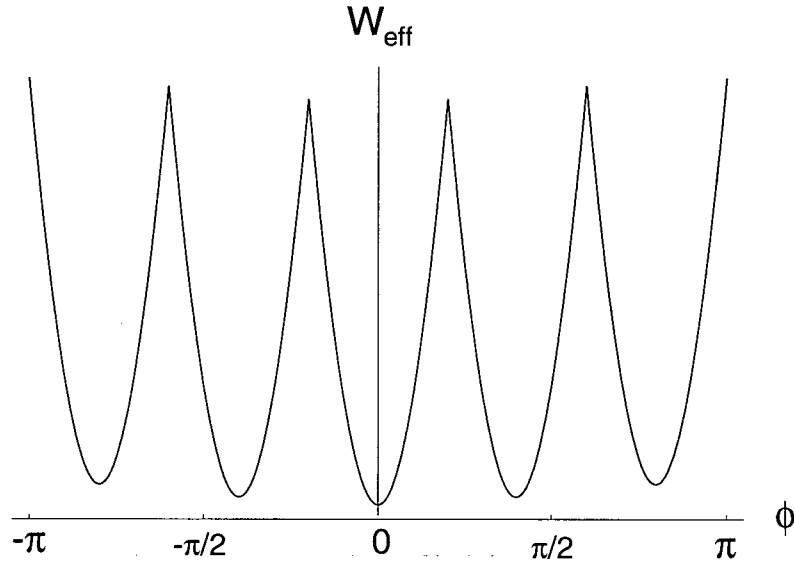


Figure 2.2: Piecewise smooth effective potential after the infinite volume limit is taken for $\theta = 0$, $N_f = 1$, $q = 5$ and $p = 3b_{QCD}$.

For $q = 1$ all ' p ' vacua are degenerate in energy. The parameter ' q ' is also the number of physically distinct vacua that exist at $\theta = 0$ in the infinite volume limit.

This form of the effective potential (2.31) for the light chiral fields is the starting point of all the research of this thesis.

2.2 Theta Dependence

The effective potential (2.31) for the phases of the chiral condensate described in the last section is a piecewise smooth potential with cusp singularities. The form of this potential is important because it satisfies two seemingly contradictory requirements. The first requirement is that for pure gluodynamics the vacuum energy should depend on θ only in the specific combination θ/N_c in order that the $U(1)$ problem be resolved. With $p = \mathcal{O}(N_c)$ the effective potential appears to have the correct form and in fact has exactly the desired form if we use the beta function of pure gluodynamics. The second

requirement is that since θ is an angular variable, all physical observables should be periodic in θ with period 2π . This requirement seems at first glance to be impossible to meet when the first requirement is met. This potential does satisfy both these properties, however, and the piecewise smooth structure turns out to be crucial (see Figure 2.2). The different branches of the effective potential each locally depend only on the combination θ/N_c , but the fact that in the infinite volume limit only the lowest energy state survives restores the 2π periodicity of physical observables.

2.3 Vacuum Structure

From the effective potential above (2.31) one can derive the equations of minimisation for each of the chiral fields in the $l = 0$ branch:

$$\sin\left(\frac{q}{p}\theta - \frac{q}{p}\sum\phi_i\right) = \frac{pM_i}{qE}\sin(\phi_i). \quad (2.33)$$

They coincide with those of [10] to lowest order in $1/N_c$ and can be used to find the solutions for the vacuum values of the chiral fields as a function of θ . For general values of $\varepsilon_i \equiv pM_i/qE$ an analytic solution is not possible. For three light quarks ($N_f = 3$) in the realistic case, $\varepsilon_u, \varepsilon_d \ll 1, \varepsilon_s \approx 1$, approximate solutions can be found as solutions of the equations:

$$\begin{aligned} \phi_s^{(l=0)} &= 0, \\ \phi_u^{(l=0)} + \phi_d^{(l=0)} &= \theta, \\ \varepsilon_u \sin \phi_u^{(l=0)} &= \varepsilon_d \sin \phi_d^{(l=0)}, \end{aligned} \quad (2.34)$$

where $\mathcal{O}(\varepsilon_u, \varepsilon_d)$ terms have been neglected in (2.33). The solution to these equations is:

$$\begin{aligned} \sin \phi_u^{(l=0)} &= \frac{m_d \sin \theta}{[m_u^2 + m_d^2 + 2m_u m_d \cos \theta]^{1/2}} + \mathcal{O}(\varepsilon_u, \varepsilon_d), \\ \sin \phi_d^{(l=0)} &= \frac{m_u \sin \theta}{[m_u^2 + m_d^2 + 2m_u m_d \cos \theta]^{1/2}} + \mathcal{O}(\varepsilon_u, \varepsilon_d), \end{aligned} \quad (2.35)$$

$$\sin \phi_s^{(l=0)} = \mathcal{O}(\varepsilon_u, \varepsilon_d).$$

This solution for the $l = 0$ branch agrees with the solution in [10]. Notice that for $\theta = 0$ the solutions are $\phi_i = 0$. Finally notice that for $m_i \equiv m \ll \Lambda_{QCD}$ the lowest energy state is:

$$\phi_i \approx \frac{\theta}{N_f}, \quad (2.36)$$

which, when substituted back into the effective potential for $l = 0$, produces a formula for the vacuum energy as a function of θ :

$$E_{vac} \approx -E - MN_f \cos\left(\frac{\theta}{N_f}\right). \quad (2.37)$$

This formula is the vacuum energy of the true vacuum state in a universe with a given value of θ and it is independent of the values of q and p . This relation actually has a very deep significance. It shows that the energy difference between the $\theta = 0$ vacuum and the $\theta \neq 0$ vacuum is proportional to the parameter M_i , in agreement with a general theorem that physical θ -dependence appears only in combination with m_q and goes away in the chiral limit.⁹ It is also important for the results in Chapter 4 that the θ -vacuum energy is not proportional to the parameter E , as suggested by the θ -dependence of (2.31), but is proportional to the smaller parameter M_i . This means that the formation of nontrivial θ -vacuum may be possible in heavy ion collisions.

It must now be stated that the exact form of the effective potential is not crucial to the θ -vacuum energy dependence. The crucial feature is that the θ -parameter occurs only in the very special form: $(\theta - \sum \phi)$. This feature is also present in [10] and in both cases we see that the large parameter in front of the term containing this combination does not prevent the formation of a state with nontrivial θ -value. Instead it means that the state will have nontrivial values of the chiral phases which will depend on θ and the vacuum energy will depend on $M_i \propto m_q$.

⁹This was shown in [10]: physical θ -dependence vanishes if any quark mass goes to zero.

For further discussion of the vacuum structure we will distinguish between two situations: $q = 1$ and $q \neq 1$.

2.3.1 $q=1$

In the case where $q = 1$ we find that the solution of the corresponding equation of minimisation for $l = 1$ does not lead to a minimum of the effective potential but instead leads to a saddle point. This is illustrated in Figure 2.3 for $\theta = 0$ and $N_f = 2$. The solutions for all other values of l coincide with one of these solutions(modulo 2π). Therefore there exists a unique vacuum.

We have checked numerically, using physical values of the quark masses in the case $N_f = 3$, that for all values of θ there is only one vacuum, in agreement with [10]. In particular, at $\theta = \pi$ no extra metastable vacua appear.

When the masses satisfy Dashen's constraint[24]:

$$m_u m_d > m_s |m_d - m_u|, \quad (2.38)$$

the vacuum doubling phenomenon—the appearance of a metastable vacuum state—occurs for values of θ near π . This metastable state is a “double” of the original vacua because at the critical point, $\theta = \pi$, the two vacua are exactly degenerate. These results agree with the results of [10]. For three ($N_f = 3$) light equal-mass quarks we find that the metastable state exists for θ values from $\pi/2$ to $3\pi/2$. This is in agreement with the results of [25]. The vacuum energy is shown as a function of θ in this case in Figure 2.4.

None of the results of this section are new, but they show that the form of the effective potential that we use reproduces previous results [10, 25] for the case $q = 1$.

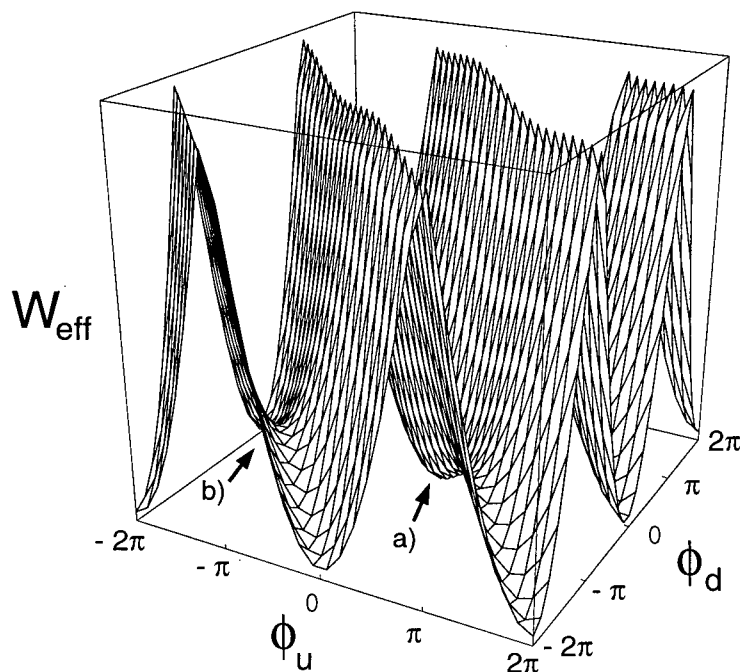


Figure 2.3: Two flavour effective potential. Indicated points are a) minimum and b) saddle point.

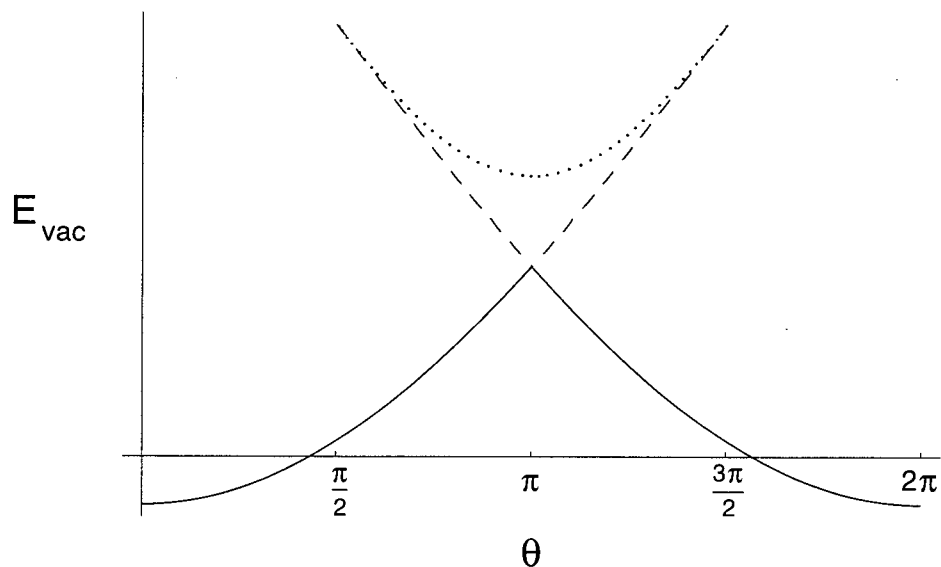


Figure 2.4: Vacuum energy as a function of vacuum angle θ for the case $q = 1$ with $N_f = 3$ light flavours of equal masses. The solid and dashed lines represent minima and the dotted line is the intermediate saddle point.

2.3.2 $q \neq 1$

Interesting vacuum structure arises when we allow $q \neq 1$. Notice that the effective potential (2.31) has the property that $\phi \rightarrow \phi + 2\pi$ simply corresponds to a relabelling of the branches $l \rightarrow l + q$. Therefore for $\theta = 0$ we have q physically distinct vacuum states corresponding to the minima of the branches $l = 0, \dots, q - 1$.

For illustrative purposes, consider the specific case $q = 2$, $N_f = 2$ and $\theta = 0$. The effective potential for this case is illustrated in Figure 2.5. Notice that there are $q = 2$ minima of the effective potential: one stable vacuum solution and one metastable. This behaviour carries over to all values of q , with $q - 1$ metastable vacua and 1 stable vacuum. This is a new feature of the theory and leads to the phenomenon of false vacuum decay which is discussed in the next chapter.

One desirable feature of this potential is that the vacuum doubling phenomenon, in which an extra metastable vacuum state appears and becomes degenerate with the highest energy metastable vacuum state at the critical values:

$$\theta = (2k + 1)\frac{\pi}{q}, \quad k = 0, 1, \dots, p - 1, \quad (2.39)$$

occurs for all values of the light quark masses. The extreme sensitivity of the theory to the values of the light quark masses is avoided when $q \neq 1$.

2.4 Phenomenology of the Pseudoscalar Mesons for Non-Zero θ

In this section we specialise to the case of $N_f = 3$ in order to calculate the θ -dependence of the π^0 , η and η' masses and the $\eta - \eta'$ and $\pi^0 - \eta - \eta'$ mixing angles. As well we show that the pseudoscalar mesons, which are pure pseudoscalars for $\theta = 0$, acquire scalar components for non-zero values of θ .

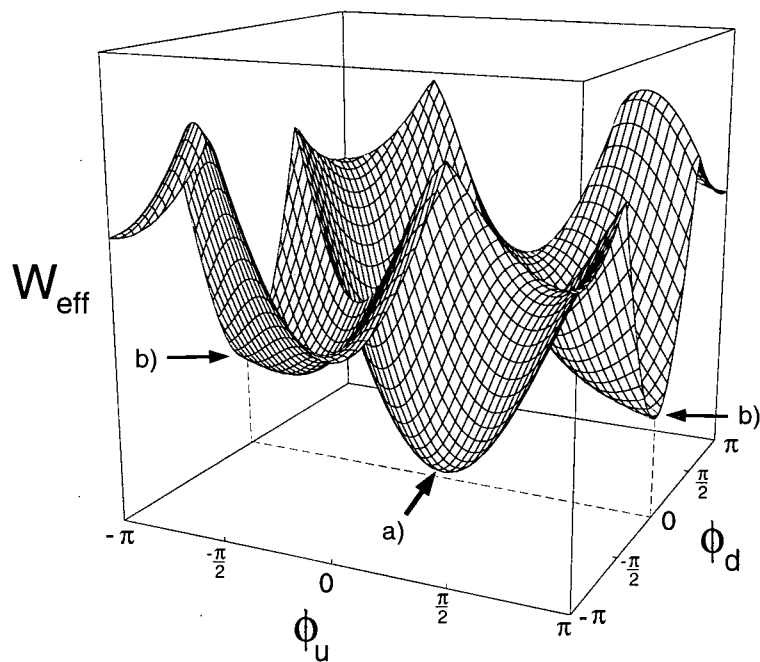


Figure 2.5: Effective potential for $q=2$ and $N_f = 2$. The point indicated as a) is the global minimum. The two local minima indicated as b) are identified.

The chiral condensate is parameterised in the following way:

$$U = U_0 \exp \left[i\sqrt{2} \frac{\pi^a \lambda^a}{f_\pi} + i \frac{2}{\sqrt{N_f}} \frac{\pi^9}{f_{\eta'}} \right], \quad (2.40)$$

where U_0 is the solution to the minimisation equations, λ^a are the Gell-Mann matrices of $SU(N_f)$, π^a is the pseudoscalar octet, π^9 is the singlet field that is identified with the η' in the absence of mixing. The π^a and π^9 fields have vanishing expectation values. Inserting this U into Eq. (2.29) and expanding this term to quadratic order in the fields we find that the linear terms vanish and we obtain the mass matrix from the terms of the form:

$$\frac{1}{2} \sum_{a,b=3,8,9} M_{ab} \pi^a \pi^b. \quad (2.41)$$

Note that the indices do not run over the quark flavour group but over the $U(3)$ indices associated with the Gell-Mann matrices¹⁰. The π^3 , π^8 and π^9 fields are associated with the Gell-Mann matrices:

$$\lambda_3 = \begin{pmatrix} 1 & 0 & 0 \\ 0 & -1 & 0 \\ 0 & 0 & 0 \end{pmatrix}, \quad \lambda_8 = \frac{1}{\sqrt{3}} \begin{pmatrix} 1 & 0 & 0 \\ 0 & 1 & 0 \\ 0 & 0 & -2 \end{pmatrix}, \quad \lambda_9 = \sqrt{\frac{2}{3}} \begin{pmatrix} 1 & 0 & 0 \\ 0 & 1 & 0 \\ 0 & 0 & 1 \end{pmatrix}, \quad (2.42)$$

which are matrices with respect to the quark flavour basis. These fields behave like: $(\bar{u}u - \bar{d}d)/\sqrt{2}$, $(\bar{u}u + \bar{d}d - 2\bar{s}s)/\sqrt{6}$ and $(\bar{u}u + \bar{d}d + \bar{s}s)/\sqrt{3}$, respectively. These are the flavour eigenstates usually associated with the neutral mesons π^0 , η and η' , respectively, in the absence of mixing. The components of the mass matrix are:

$$m_{33}^2 = \frac{2}{f_\pi^2} (M_u \cos \phi_u + M_d \cos \phi_d),$$

$$m_{88}^2 = \frac{2}{3f_\pi^2} (M_u \cos \phi_u + M_d \cos \phi_d + 4M_s \cos \phi_s),$$

¹⁰We include in this term the identity matrix, denoted by λ^9 , which is not properly a Gell-Mann matrix.

$$\begin{aligned}
m_{99}^2 &= 4 \left(\frac{q}{p} \right)^2 \frac{E}{f_{\eta'}^2} N_f \cos \left(-\frac{q}{p} \theta + \frac{q}{p} \sum \phi_i + \frac{2\pi l}{p} \right) + \frac{4}{N_f} \frac{1}{f_{\eta'}^2} \sum_{i=u,d,s} M_i \cos \phi_i, \\
m_{38}^2 &= m_{83}^2 = \frac{2}{\sqrt{3} f_{\pi}^2} (M_u \cos \phi_u - M_d \cos \phi_d), \\
m_{39}^2 &= m_{93}^2 = 2 \sqrt{\frac{2}{N_f f_{\pi} f_{\eta'}}} (M_u \cos \phi_u - M_d \cos \phi_d), \\
m_{89}^2 &= m_{98}^2 = 2 \sqrt{\frac{2}{3 N_f f_{\pi} f_{\eta'}}} (M_u \cos \phi_u + M_d \cos \phi_d - 2 M_s \cos \phi_s),
\end{aligned} \tag{2.43}$$

where the ϕ_i are the vacuum values of the particular vacuum about which we are expanding. Notice that the m_{99} component depends on θ explicitly and all of the components depend on θ implicitly through the vacuum values of ϕ_i . Neglecting mixing effects, m_{99} coincides with the physical mass of the η' . In fact for $\theta = 0$ and particular values, $p = 3b_{QCD}$ and $q = 8$, we reproduce exactly the relation derived in [8]:

$$f_{\eta'}^2 m_{\eta'}^2 = \frac{8}{9b} N_f \langle \frac{\alpha_s}{\pi} G^2 \rangle - \frac{4}{N_f} \sum_{u,d,s} m_i \langle \bar{\Psi}_i \Psi_i \rangle + \mathcal{O}(m_q^2). \tag{2.44}$$

This relation shows that the η' is heavier than the other pseudoscalar mesons because of the contribution from the gluon condensate. It also predicts that the strange quark contributes 20-40% of the mass of the η' . This suggests that perturbative corrections of $\mathcal{O}(m_s^2)$ (see below) could be quite significant. Taking the formal limit $N_c \rightarrow \infty$ and $m_q \rightarrow 0$ leads to the mass relation in [21] where $m_{\eta'}^2$ scales like N_f/N_c , in agreement with [26]. If we instead take the limit $N_c \rightarrow \infty$ with fixed quark mass $m_q \neq 0$, then $m_{\eta'}^2 = \mathcal{O}(m_q)$, as for ordinary pseudo-Goldstone bosons. The mass relation (2.44) gives the numerical result for $m_{99} (\approx m_{\eta'}) = 900$ MeV. This result is encouraging as it is of the right order of magnitude, (see below) and is the first connection between the unrelated quantities, $m_{\eta'}$ and $\langle G^2 \rangle$ ¹¹.

The fact that the mass matrix M_{ab} defined by (2.41) has off diagonal terms, as seen in (2.43), means that the physical fields are not the π^a fields, but linear combinations of

¹¹The gluon condensate is measured in the charmonium system which is totally unrelated to the η' .

them determined by the eigenvectors of the mass matrix. The eigenvalues of the mass matrix give the masses of the physical mass eigenstates corresponding to the π^0 , η and η' mesons. For $\theta = 0$, $p = N_c$, $q = 1$, and the standard values $m_u = 4$ MeV, $m_d = 7$ MeV and $m_s = 150$ MeV we obtain the values:

$$m_{\pi^0} = 131 \text{ MeV}, \quad m_{\eta} = 412 \text{ MeV}, \quad m_{\eta'} = 1015 \text{ MeV}. \quad (2.45)$$

Comparing these values to the measured masses of 135 MeV, 547 MeV and 958 MeV respectively, we see that the mass values are all of the right order of magnitude and in approximately the right ratios to one another, which is very encouraging. These values were obtained using specific values for gluon and strange quark condensates, the values of which are fairly uncertain. They could be off by 20% or more and this would have a significant effect on the masses. A change to either of the condensate values would have a similar relative effect on each of the η and η' masses, but little effect on the π^0 mass. In addition these values could be altered significantly by higher order perturbative corrections.

An analytical form for the masses of the neutral mesons as a function of θ would be extremely messy, but is obtained very easily numerically, and the results are shown in Figures 2.6, 2.7 and 2.8 (Note the different scales on the vertical axes.). We can see that there is a mild θ -dependence in the masses of the η and η' and a strong θ -dependence in the mass of the π^0 . This can be easily understood from the components of the mass matrix (2.43). The masses of the η and η' are predominantly determined by the diagonal terms m_{88}^2 and m_{99}^2 . The m_{88}^2 term is dominated by the M_s term, because the strange quark mass is so much larger than the up and down quark masses. This term is very weakly dependent on θ through the $\cos(\phi_s)$ term as can be seen by recalling the vacuum solution (2.35). The variation of the m_{99}^2 term with respect to θ is similarly determined by the M_s term because the term involving the larger parameter, E , is constant since

the vacuum solutions have $(\sum_i \phi_i - \theta) = 0$. The π^0 mass, however, is predominantly determined by the m_{33}^2 term which is determined solely by the up and down quark terms which are strongly dependent on the θ -parameter as illustrated by the vacuum solutions (2.35) for ϕ_u and ϕ_d . This θ -dependence of the masses is one of the possible signals of the formation of a nontrivial θ -vacuum discussed in Chapter 4.

In the limit of pure SU(2) flavour symmetry ($m_u = m_d = m$, which also means $\phi_u = \phi_d$) we can consider the simplest case of $\eta - \eta'$ mixing. For $\theta = 0$ the mixing matrix is:

$$m_{\eta-\eta'}^2 = \begin{pmatrix} -\frac{4}{3f_\pi^2}(2m_s\langle\bar{s}s\rangle + m\langle\bar{u}u\rangle) & \frac{4\sqrt{2}}{3f_\pi f_{\eta'}}(m_s\langle\bar{s}s\rangle - m\langle\bar{u}u\rangle) \\ \frac{4\sqrt{2}}{3f_\pi f_{\eta'}}(m_s\langle\bar{s}s\rangle - m\langle\bar{u}u\rangle) & -\frac{4}{3f_{\eta'}^2}\sum m_i\langle\bar{\Psi}_i\Psi_i\rangle + \frac{N_f b}{8}\left(\frac{q}{p}\right)^2 \frac{\langle(\alpha_s/\pi)G^2\rangle}{f_{\eta'}^2} \end{pmatrix}, \quad (2.46)$$

which can easily be shown to coincide with an accuracy $\mathcal{O}(m_q^2)$ with the matrix given by Veneziano[26]:

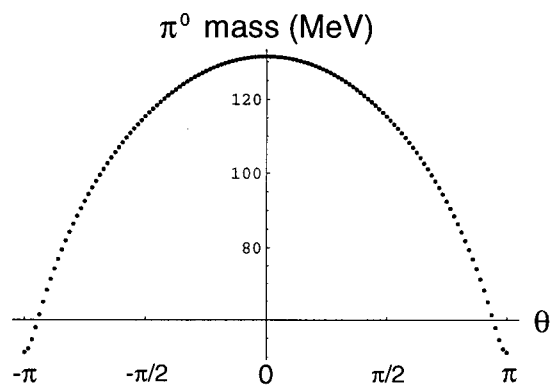
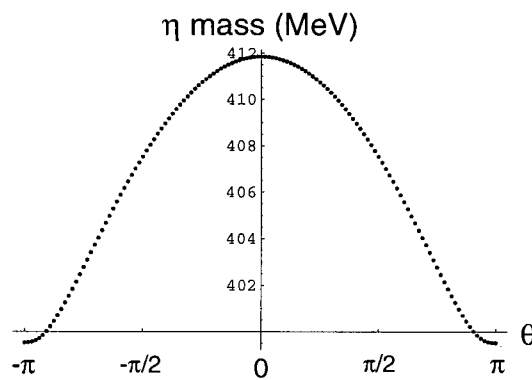
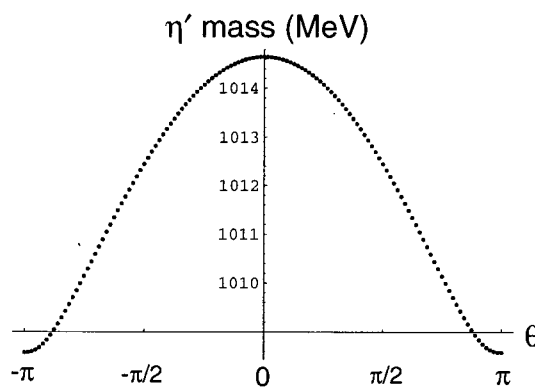
$$m_{\eta-\eta'}^2 = \begin{pmatrix} \frac{1}{3}(4m_K^2 - m_\pi^2) & -\frac{2\sqrt{2}}{3}(m_K^2 - m_\pi^2) \\ -\frac{2\sqrt{2}}{3}(m_K^2 - m_\pi^2) & \frac{2}{3}m_K^2 + \frac{1}{3}m_\pi^2 + \frac{\chi}{N_c} \end{pmatrix}, \quad (2.47)$$

where we replace the topological susceptibility, χ , evaluated in pure gluodynamics, with the value in QCD proportional to the gluon condensate. It should be stressed that the fact that both sides of the relation (2.44) depend on quantities evaluated in QCD represents a significant improvement in our understanding. A QCD analog of the Witten-Veneziano formula[26] can be written down for the particular values $p = 3b_{QCD}$ and $q = 8$:

$$\langle\frac{\alpha_s}{\pi}G^2\rangle = \frac{3b}{8}f_{\eta'}^2(m_{\eta'}^2 + m_\eta^2 - 2m_K^2) + \mathcal{O}(m_q^2). \quad (2.48)$$

This equation is a generalisation of the η' mass relation (2.44) to include the effects of $\eta - \eta'$ mixing. The $\eta - \eta'$ mixing angle as a function of θ is:

$$\alpha = \frac{1}{2} \sin^{-1}\left(\frac{2m_{89}^2}{m_{\eta'}^2 - m_\eta^2}\right), \quad (2.49)$$

Figure 2.6: π^0 mass as a function of θ Figure 2.7: η mass as a function of θ Figure 2.8: η' mass as a function of θ

where m_{89}^2 is given above in (2.43) and, $m_{\eta'}^2$ and m_{η}^2 , are eigenvalues of the mass matrix for a given value of θ . For $\theta = 0$ and ϕ_i given by the vacuum solutions in this case, we obtain an $\eta - \eta'$ mixing angle of about -22° . This value is reasonable as phenomenological estimates from experimental data range from -10° to -23° [27].

As well, we can study the full case of $\pi^0 - \eta - \eta'$ mixing angles when the $SU(2)$ flavor symmetry is broken. The mass eigenvector coordinate system, $\hat{\pi}_0 - \hat{\eta} - \hat{\eta}'$ is defined by the eigenvectors of the mass matrix. The orientation of the mass eigenvector coordinate system with respect to the $SU(3)$ flavor eigenstate system, $\hat{\pi}_3, \hat{\pi}_8$ and $\hat{\pi}_9$, can be specified by Euler angles. For the specific case where $\theta = 0$ and $m_u = 4$ MeV, $m_d = 7$ MeV and $m_s = 150$ MeV we obtain the Euler angles[28]:

$$\theta_{Euler} = 19^\circ, \quad \phi_{Euler} = -0.83^\circ, \quad \psi_{Euler} = 2.5^\circ. \quad (2.50)$$

These values show that at least for $\theta = 0$ the mixing of the π^0 meson with the η and η' is fairly small and breaking of the $SU(2)$ flavor symmetry does not have a large effect on the $\eta - \eta'$ mixing. In general, the Euler angles can be found numerically and they are shown as a function of θ in Figures 2.9, 2.10 and 2.11. We can see that there is a significant dependence on θ in the case of the full $\pi^0 - \eta - \eta'$ mixing. As in the case of the masses, the mixing angles would likely be significantly affected by changes to the values used for the gluon and strange quark condensates and by the inclusion of perturbative corrections.

The final topic of this section is the behaviour of the pseudoscalar mesons under the Parity Operation (P) for non-zero values of θ . For $\theta = 0$ they are eigenfunctions of Parity with eigenvalue -1 , which means they are pure pseudoscalars. For $\theta \neq 0$ they cease to be eigenstates of Parity and become mixtures of scalar and pseudoscalar states¹².

Recalling the definition (2.27) of the chiral condensate matrix, U , and the diagonal

¹²This fact was previously noted in [29].

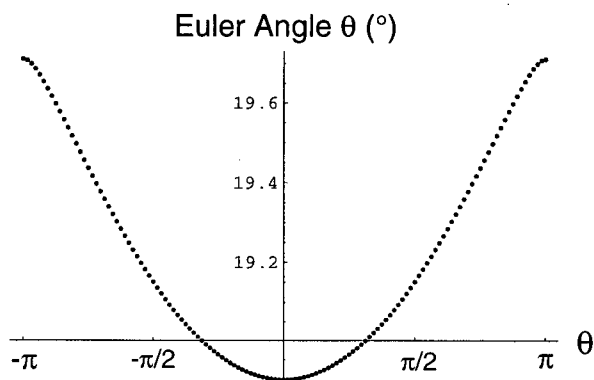


Figure 2.9: The Euler θ angle for the mass eigenvector coordinate system with respect to the flavor eigenstate coordinate system as a function of θ .

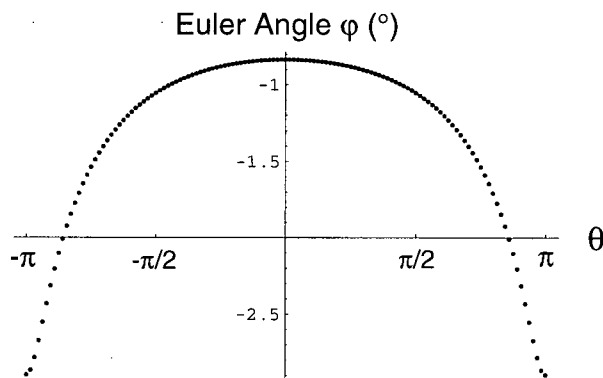


Figure 2.10: The Euler ϕ angle for the mass eigenvector coordinate system with respect to the flavor eigenstate coordinate system as a function of θ .

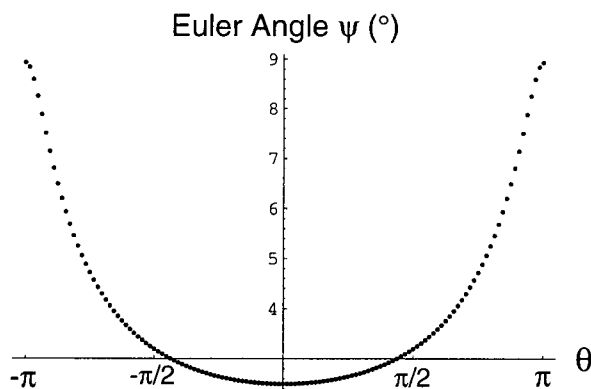


Figure 2.11: The Euler ψ angle for the mass eigenvector coordinate system with respect to the flavor eigenstate coordinate system as a function of θ .

form of the vacuum solution, the quark condensates in the θ -vacuum:

$$\langle \bar{\Psi}'_{Li} \Psi'_{Rj} \rangle_{\theta} \equiv \langle \bar{\Psi}_{Li} \Psi_{Rj} \rangle_{\theta=0} e^{i\phi_i}, \quad (2.51)$$

can be represented as a chiral rotation of the usual vacuum:

$$\Phi' = U_R \Phi U_L^\dagger, \quad \Phi'_{ij} = \langle \bar{\Psi}_{Li} \Psi_{Rj} \rangle_{\theta=0}, \quad (2.52)$$

with:

$$(U_R)_{ik} = \delta_{ik} e^{\frac{i}{2}\phi_i} \quad (U_L^\dagger)_{kj} = \delta_{kj} e^{\frac{i}{2}\phi_i}. \quad (2.53)$$

The quark fields transform under this rotation in the following way:

$$\Psi'_{Ri} = (U_R)_{ik} \Psi_{Rk}, \quad \Psi'_{Lj} = \Psi_{Lk}^\dagger (U_L^\dagger)_{kj}. \quad (2.54)$$

In the chirally rotated basis, the spin content of the pseudoscalars is the same as in the standard basis. However, in terms of the unrotated basis the spin content will generally have a very different form. Consider for example the π^0 field in the θ -vacuum:

$$|\pi^0\rangle \sim |\bar{u}' i \gamma_5 u' - \bar{d}' i \gamma_5 d'\rangle = \cos \phi_u |\bar{u} i \gamma_5 u\rangle - \sin \phi_u |\bar{u} u\rangle - (u \leftrightarrow d). \quad (2.55)$$

The second term in this equation, which vanishes for $\theta = 0$, is the additional scalar component which the π^0 field acquires for non-zero values of θ . The other pseudoscalar particles undergo a similar transformation.

The scalar component of the pseudoscalar mesons for non-zero values of θ could have extremely important implications. It may be possible to create regions with non-zero θ -parameter in heavy ion collisions. If pseudoscalar particles originating in this region manage to escape from the reaction volume, observation of their scalar admixture would provide very convincing proof of the existence of a region of non-zero θ -parameter.

In this chapter we have introduced the anomalous effective Lagrangian and discussed some of the interesting implications of this anomalous effective Lagrangian. In the following chapters we expand on some of these implications.

Chapter 3

False Vacuum Decay

In this chapter we discuss the decay of the lowest metastable vacuum for $\theta = 0$, described in Chapter 2, in both the zero and high temperature limits¹. The existence of this specific metastable vacuum is somewhat controversial, as it requires the counterintuitive parameter value, $q \neq 1$, as we will discuss further below. However, nontrivial vacua have been shown to exist in Yang-Mills theories in the large N_c limit using the AdS/CFT correspondence and the same phenomenon was observed in the analysis of soft breaking of supersymmetric models[12]. It appears that the existence of nontrivial vacua is a general phenomenon for gauge theories in the strong coupling regime. Therefore this calculation can be considered as one example of a general class of problems. Therefore, in addition to the specific results we obtain for this particular calculation, another important goal of this chapter is to develop techniques which could be useful in the study of this type of phenomenon.

The decay rate of the false vacuum in large N_c Yang Mills theory was estimated in [31]. The calculation of the decay rate of the false vacuum presented here differs from [31] because it is valid for finite N_c and because the heavy glueball degrees of freedom² have been integrated out in our approach, while their calculation derives entirely from gluodynamics. For more comments on the elimination of heavy degrees of freedom see below. The decay rate of a false vacuum was estimated in [25] in the case that $\theta \approx \pi$ and N_c is finite. Our calculation differs from [25] in the inclusion of the singlet η' field and

¹The results of this chapter are contained in [30]

²We use this term to refer to gluonic degrees of freedom which take into account colour confinement.

choice of parameters $q = 8$ and $p = 11N_c - 2N_f$. As well, both of these estimates only use the semiclassical approximation, while we determine the effect of the first quantum corrections. The form of the semiclassical decay rate in our case is identical to that of [31, 25]. We make no numerical comparisons as the false vacua involved are all different.

These false vacua and domain walls could lead to many interesting consequences in the study of the evolution of the early universe at around the time of the QCD phase transition. One example of this is related to baryogenesis and dark matter, and is described in [15]. The zero temperature decay rate of the false vacua calculated in this chapter is relevant to this particular application. As well, these metastable states hopefully can be experimentally studied at RHIC and the high temperature decay rate calculated in this chapter would be relevant to this research. Bubbles of this false vacuum would display CP odd signatures such as those described in [32] where the large N_c limit was assumed.

Even without consideration of these interesting applications, our method of calculation of the determinantal prefactor is useful as an alternative to previous methods. Previous calculations [33] [34] [35] [36] of bubble nucleation rates use a particular method for calculating the determinant ratio of operators of the form:

$$\mathcal{M} = -\nabla^2 + \omega^2 + \alpha V(r), \quad (3.56)$$

involving a theorem from [33]. We prefer to use a more direct approach. Our procedure provides a method for obtaining both analytical approximations and exact numerical calculations for this determinantal prefactor. Our numerical approximation involves only numerical integration, unlike the method of [37] which also involves numerical solution of differential equations and might not be reliable in some cases involving non-smooth perturbation potentials. Our methods are more along the lines of [38] but are sufficiently different to constitute independent results. As well, we use the same methods to calculate

the decay rate in the zero temperature theory which has not been done before.

We calculate the decay rate of the lowest metastable vacuum for $\theta = 0$ in the simplified setting where $m_i \equiv 4\text{MeV}$ and the chiral phases are equal. This amounts to studying only radial motion in ϕ -space. We analyse the problem in the spirit of [39] and only consider transitions between the lowest energy metastable state and the physical vacuum. The results should be easily generalisable to other transitions.

This calculation is an approximation for a number of reasons. Most obviously because we make several approximations in order to obtain an analytical answer, but we believe it should give the dominant contribution within a factor of the order of unity. It should be noted that this approximation is in some sense nonperturbative, since it should contain contributions from perturbation diagrams of all orders.

The second reason this calculation is an approximation is that we have ignored some complications so that we are able to carry out the calculation. The inclusion of fermions (nucleons) could drastically change the results, but they also drastically increase the difficulty of the calculation, so they are left out in this first approximation. As well, there is the consideration that heavy intrinsic degrees of freedom, such as glueballs, might play a role. It has been suggested[40] that the cusps in the effective potential are due to the integration out of heavy degrees of freedom, that the presence of cusps invalidates the construction of the domain wall from the effective Lagrangian and that a complete calculation must include the heavy degrees of freedom. The decay rate in both these cases can only be decreased by the inclusion of these heavy degrees of freedom. In order to calculate the decay rate, however, we must ignore these effects and content ourselves with calculating an upper bound for the decay rate.

The results of this chapter are the only results which depend on specific values for the integer parameters p and q . The very existence of the metastable vacuum state at $\theta = 0$ requires $q \neq 1$. The parameters p and q are left in the formulas and so are

otherwise arbitrary, but we must keep this restriction in mind throughout the chapter. When numerical results are given, the values $p = 3b_{QCD} = 11N_c - 2N_f$ and $q = 8$ are used.

3.1 The Domain Wall Solution

An approximate solution for the field configuration of the domain wall between the metastable and true vacua is needed to calculate the decay rate. For ease of calculation we re-scale and shift the chiral field $\phi \rightarrow (2/f_\pi\sqrt{N_f})\phi - \pi/(qN_f)$ in order to have the standard normalisation of the kinetic term and a symmetrised form of the potential.

The effective potential for $\theta = 0$ becomes:

$$W(\phi) = \begin{cases} E \left[1 - \cos \left(\frac{2q\sqrt{N_f}}{pf_\pi} \phi - \frac{\pi}{p} \right) \right] - Mf(\phi) & \text{if } \phi \geq 0 \\ E \left[1 - \cos \left(\frac{2q\sqrt{N_f}}{pf_\pi} \phi + \frac{\pi}{p} \right) \right] - Mf(\phi) & \text{if } \phi \leq 0 \end{cases},$$

$$f(\phi) = N_f \left[\cos \left(\frac{2}{f_\pi\sqrt{N_f}} \phi - \frac{\pi}{qN_f} \right) - \cos \left(\frac{2\pi}{qN_f} \right) \right]. \quad (3.57)$$

The effective potential (3.57) has a global minimum at $\phi_+ = (\pi f_\pi)/(2q\sqrt{N_f})$ and a local minimum at $\phi_- = -(\pi f_\pi)/(2q\sqrt{N_f})$, with a cusp singularity between them (see Figure 3.12). The minima are interpreted as two vacua separated by a high potential barrier ($\sim G^2$) which is fairly wide, while the energy splitting, ΔE , between the states is fairly small in comparison:

$$\Delta E = m_q N_f \left| \langle \bar{\Psi} \Psi \rangle \right| \left(1 - \cos \frac{2\pi}{qN_f} \right) + 0(m_q^2). \quad (3.58)$$

Therefore we can use the thin wall approximation [39] in our calculations. The domain wall solution in this approximation corresponding to the effective potential (3.57) is:

$$\phi_{d.w.}(x) = \frac{pf_\pi}{2q\sqrt{N_f}} \left[-\frac{\pi}{p} + 4 \arctan \left\{ \tan \left(\frac{\pi}{4p} \right) \exp[\mu(x - x_0)] \right\} \right] \text{ if } x < x_0,$$

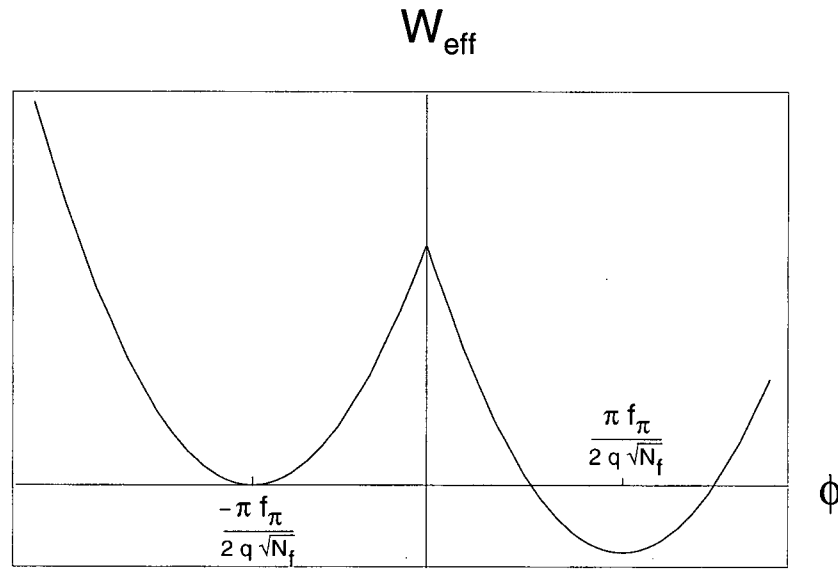


Figure 3.12: Effective potential at $\theta = 0$ for equal chiral phases $\phi = \phi_u = \phi_d = \phi_s$.

$$= \frac{pf_\pi}{2q\sqrt{N_f}} \left[\frac{\pi}{p} - 4 \arctan \left\{ \tan \left(\frac{\pi}{4p} \right) \exp [-\mu(x - x_0)] \right\} \right] \text{ if } x > x_0, \quad (3.59)$$

where x_0 is the position of the centre of the domain wall and:

$$\mu \equiv \sqrt{\left. \frac{d^2 W_{eff}}{d\phi^2} \right|_{min}} = \frac{2q\sqrt{N_f}\sqrt{E}}{pf_\pi}, \quad (3.60)$$

is the inverse width of the wall. The solution (3.59) is shown as a function of $x - x_0$ in Figure (3.13). Its first derivative is continuous at $x = x_0$, but the second derivative exhibits a discontinuity. The energy density of the wall is given by:

$$\sigma = \frac{4p}{q\sqrt{N_f}} f_\pi \sqrt{\langle \frac{b\alpha_s}{32\pi} G^2 \rangle} \left(1 - \cos \frac{\pi}{2p} \right) + \mathcal{O}(m_q f_\pi^2). \quad (3.61)$$

In what follows we use this domain wall solution in our calculation of the decay rate per unit volume of the false vacuum for both zero and high temperature field theory. The next section describes the semiclassical calculation.

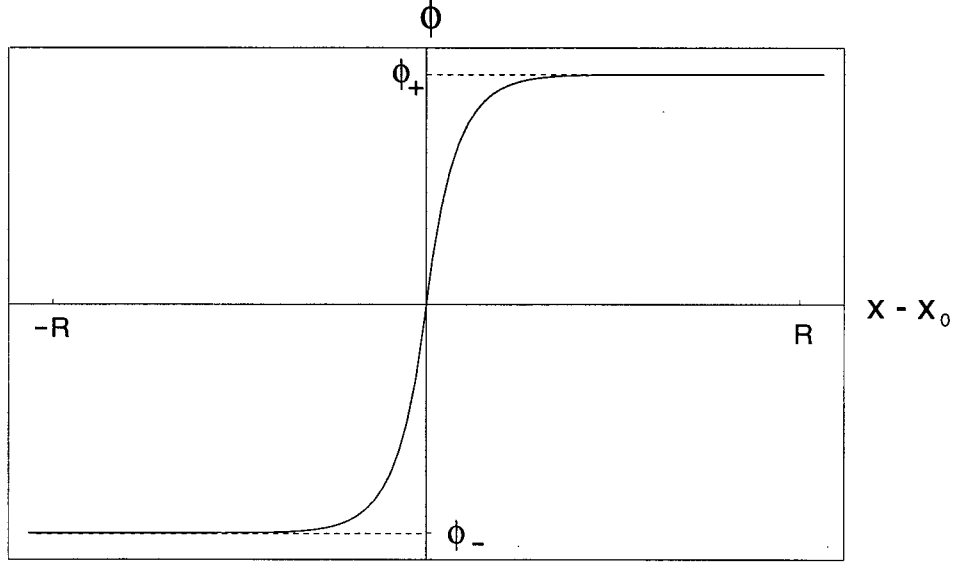


Figure 3.13: The domain wall solution.

3.2 Semiclassical Theory

The decay of a false vacuum was discussed in [39] and the formula for the decay rate per unit volume, Γ/V , was shown to be:

$$\Gamma/V = Ae^{-B/\hbar}[1 + O(\hbar)]. \quad (3.62)$$

The semiclassical approximation at zero temperature tells us that B is given by the Euclidean action of ϕ :

$$B = S_4 = \int d\tau d^3\vec{x} \left[\frac{1}{2} \left(\frac{\partial\phi}{\partial\tau} \right)^2 + \frac{1}{2} (\nabla\phi)^2 + U(\phi) \right], \quad (3.63)$$

where $U(\phi)$ is the potential, W_{eff} , for the chiral phases described in the previous section neglecting the energy difference, ΔE , between the two vacua:

$$U(\phi) = \begin{cases} E \left[1 - \cos \left(\frac{2q\sqrt{N_f}}{pf\pi} \phi - \frac{\pi}{p} \right) \right] & \text{if } \phi \geq 0 \\ E \left[1 - \cos \left(\frac{2q\sqrt{N_f}}{pf\pi} \phi + \frac{\pi}{p} \right) \right] & \text{if } \phi \leq 0. \end{cases} \quad (3.64)$$

In order for this to be finite we must have $\lim_{r \rightarrow \infty} \phi(r) = \phi_- \equiv -\pi f_\pi / 2q \sqrt{N_f}$ where $r = \sqrt{x^2 + y^2 + z^2 + t^2}$. The solution of this problem is the four dimensional equivalent to the solution which Coleman calls “the bounce” [39]. It describes a bubble of the true vacuum in the false vacuum at the origin which forms, grows to a maximum size and then shrinks to nothing again (*ie.* an $O(4)$ invariant bubble). In the thin wall approximation the bounce solution describing a false vacuum bubble with radius, R , is:

$$\phi_b(r) = \begin{cases} \phi_+ & \text{for } r \ll R \\ \phi_{d.w.}(R-r) & \text{for } r \approx R \\ \phi_- & \text{for } r \gg R \end{cases}, \quad (3.65)$$

and the value of B is calculated to obtain [39]:

$$\Gamma/V \propto \exp(-S_4[\phi_b]) = \exp\left(-\frac{27\pi^2\sigma^4}{2(\Delta E)^3}\right), \quad (3.66)$$

where σ is the domain wall energy and:

$$S_4[\phi_b] = \frac{3^3 \cdot 2^7 \cdot \pi^2 p^4}{q^4 N_f^5} \frac{f_\pi^4 E^2}{M^3} \frac{(1 - \cos \frac{\pi}{2p})^4}{(1 - \cos \frac{2\pi}{qN_f})^3} \simeq \frac{27}{256} \frac{\pi^4 q^2 N_f}{p^4} \frac{f_\pi^4 \langle \frac{b\alpha_s}{32\pi} G^2 \rangle^2}{m_q^3 |\langle \bar{\Psi}\Psi \rangle|^3}, \quad (3.67)$$

is the Euclidean action of the 4D bounce solution.

The thin wall approximation is valid because the radius of the 4D bubble, which is found to be $R = 3\sigma/\Delta E$ by minimising the value $S_4[\phi_b]$, is much larger than the width of the domain wall, $1/\mu$.

For finite temperature QCD, the semiclassical approximation is slightly different. At sufficiently high temperature the bubble solution becomes a stable $O(3)$ invariant bubble with radius [41]:

$$R(T) = \frac{2S_1(T)}{\Delta E}. \quad (3.68)$$

where the temperature dependence of the domain wall energy, $S_1(T)$, is not known. In

this case the calculation of B gives[41]:

$$\Gamma/V \propto \exp(-S_3[\phi_b]/T) = \exp\left(-\frac{16\pi S_1(T)^3}{3(\Delta E)^2 T}\right). \quad (3.69)$$

It should be noted that this decay rate is for the ground state of the metastable well. The decay rate for excited energy states above the metastable vacuum via thermally activated transitions, while similar in form, is not the same[42].

In the next section we calculate the quantum corrections and determine the decay rate for the zero temperature theory. The section following that presents the same calculations for the high temperature theory.

3.3 Quantum Corrections at Zero Temperature

The quantum corrections at zero temperature correspond to the coefficient A in Equation(3.62)[43]:

$$A = \left| \frac{\det[-\partial_\mu \partial^\mu + U''(\phi_b)]}{\det[-\partial_\mu \partial^\mu + U''(\phi_-)]} \right|^{-1/2}. \quad (3.70)$$

This is the determinantal prefactor mentioned at the beginning of this chapter. The spectrum of the operator in the numerator consists of a discrete spectrum with zero and negative eigenvalues and a continuous positive eigenvalue spectrum starting at $\omega^2 \equiv U''(\phi_-)$. These two parts of the spectrum must be analysed separately and it can be shown that this factor separates into three parts:

$$A = \left(\omega^4 \int d^4x \left(\frac{B}{2\pi} \right)^2 \right) \frac{\omega}{\sqrt{\lambda_-}} \left| \frac{\det'[-\partial_\mu \partial^\mu + U''(\phi_b)]}{(\omega^{-2})^5 \det[-\partial_\mu \partial^\mu + \omega^2]} \right|^{-1/2}. \quad (3.71)$$

The first term comes from the zero eigenvalues. The second term comes from the negative eigenvalue. The third term is the determinant of the continuous positive eigenvalue spectrum where \det' signifies that the zero and negative eigenvalues are to be omitted. With these eigenvalues omitted, the perturbed operator in the numerator has five less

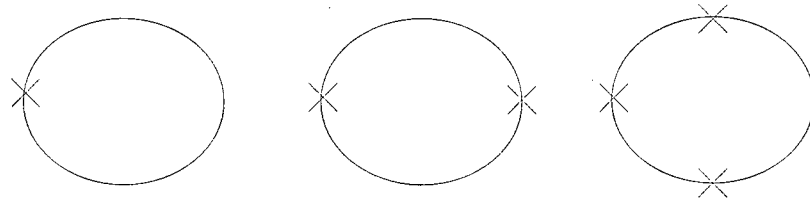


Figure 3.14: Expansion of the partition function.

eigenvalues in the spectrum because five of the eigenvalues of the unperturbed operator in the denominator have become part of the discrete spectrum of the perturbed operator. Assuming these eigenvalues have originated from the bottom of the unperturbed continuous spectrum we divide the third term by a factor of ω^2 for each omitted eigenvalue. The contributions from the zero and negative eigenvalues are normalised with a factor of ω keeping each of the three terms dimensionless.

3.3.1 Positive Eigenvalues

The contribution of the positive eigenvalues requires evaluation of the determinant ratio:

$$\left| \frac{\det'[-\partial_\mu \partial^\mu + U''(\phi_b)]}{(\omega^{-2})^5 \det[-\partial_\mu \partial^\mu + \omega^2]} \right|. \quad (3.72)$$

However, since the $(\omega^{-2})^5$ in the denominator corresponds to a set of measure zero in the continuous eigenvalue spectrum, we can omit it and the notation \det' which indicates omission of a discrete set of eigenvalues.

This determinant ratio is infinite, and to obtain a finite answer we must divide by an infinite factor. The determinant in the numerator can be expanded as:

$$\begin{aligned} \det | -\partial_\mu \partial^\mu + U''(\phi_b) | &= \exp \left[Tr \log \left\{ -\partial_\mu \partial^\mu + \omega^2 + V_{pert}(r) \right\} \right] \\ &= \det | -\partial_\mu \partial^\mu + \omega^2 | \times \\ &\exp Tr \left[\frac{V_{pert}(r)}{-\partial_\mu \partial^\mu + \omega^2} - \frac{1}{2} \left(\frac{V_{pert}(r)}{-\partial_\mu \partial^\mu + \omega^2} \right)^2 + \frac{1}{3} \left(\frac{V_{pert}(r)}{-\partial_\mu \partial^\mu + \omega^2} \right)^3 + \dots \right]. \end{aligned} \quad (3.73)$$

It should be noted that the determinant is equal to the partition function of the self interacting massive scalar particle and that the second factor in the last line is expanded up to one loop contributions involving three interactions with the effective external potential (see Figure 3.14). Tracing over a Cartesian basis, we can see that the one and two interaction contributions are divergent but the three interaction contribution is finite:

$$\text{Tr} \left[\frac{V_{\text{pert}}(r)}{-\partial_\mu \partial^\mu + \omega^2} \right] = \int d^4x d^4k \frac{V_{\text{pert}}(r)}{k^2 + \omega^2}, \quad (3.74)$$

$$\text{Tr} \left[\left(\frac{V_{\text{pert}}(r)}{-\partial_\mu \partial^\mu + \omega^2} \right)^2 \right] = \int d^4k d^4p \frac{\mathcal{V}_{\text{pert}}(k)}{(k^2 + \omega^2)} \frac{\mathcal{V}_{\text{pert}}(-k)}{((k+p)^2 + \omega^2)}, \quad (3.75)$$

$$\text{Tr} \left[\left(\frac{V_{\text{pert}}(r)}{-\partial_\mu \partial^\mu + \omega^2} \right)^3 \right] = \int d^4k d^4p d^4q \frac{\mathcal{V}_{\text{pert}}(k)}{(k^2 + \omega^2)} \frac{\mathcal{V}_{\text{pert}}(p)}{(p^2 + \omega^2)} \frac{\mathcal{V}_{\text{pert}}(-k-p)}{((k+p+q)^2 + \omega^2)} \quad (3.76)$$

where $\mathcal{V}_{\text{pert}}(k)$ is the Fourier transform of the $V_{\text{pert}}(r)$. We only get a finite answer if we divide through by the infinite factors.

The actual calculation is most easily done using hyperspherical coordinates in four dimensions, (r, θ, ϕ, ψ) , and expanding the eigenfunctions $\chi(r, \theta, \phi, \psi)$ in terms of the 4D hyperspherical harmonics:

$$\chi(r, \theta, \phi, \psi) = \sum_{n=0}^{\infty} \sum_{l=-n}^n \sum_{m=-|l|}^{|l|} C_{nlm} \frac{u(r)}{r^{3/2}} Y_{nlm}(\theta, \phi, \psi), \quad (3.77)$$

which are discussed in Appendix B.

In this situation, the Laplacian, when operating on each term of (3.77) with quantum number, n , becomes:

$$\partial_\mu \partial^\mu \rightarrow \frac{1}{r^{3/2}} \left[\frac{d^2}{dr^2} - \frac{4n^2 + 8n + 3}{4r^2} \right] r^{3/2} \equiv \frac{1}{r^{3/2}} \mathcal{D}_n r^{3/2}. \quad (3.78)$$

There are $2n(n+2) + 1$ such terms corresponding to different values of l and m but with the same eigenvalue. Therefore:

$$\det[-\partial_\mu \partial^\mu + U''] = \prod_{n=0}^{\infty} (\det[-\mathcal{D}_n + U''])^{2n(n+2)+1}. \quad (3.79)$$

First consider the denominator of (3.72), $\det[-\mathcal{D}_n + \omega^2]$. In order to calculate this determinant we need to solve the eigenvalue equation:

$$[\mathcal{D}_n - \omega^2 + \lambda]u(r) = 0. \quad (3.80)$$

The solutions to this differential equation that are well behaved at $r = 0$ and $r = \infty$ are:

$$u(r) = (\omega_\lambda r)^{3/2} J_n(\omega_\lambda r) \equiv \sqrt{\frac{\pi \omega_\lambda r}{2}} J_{n+1}(\omega_\lambda r), \quad (3.81)$$

where $\omega_\lambda \equiv \sqrt{\lambda - \omega^2}$. J_n are the 4D analogs of the spherical Bessel functions and $J_{n+1}(x)$ are Bessel functions of the first kind. These solutions become purely oscillatory as $r \rightarrow \infty$. Notice that this solution is only well defined for $\lambda > \omega^2$ and indeed there are no solutions for values of $\lambda \leq \omega^2$ which are well behaved at $r = 0$ and $r = \infty$. Therefore the continuous spectrum of eigenvalues can be written as $\lambda = \omega^2 + \omega_\lambda^2$ and:

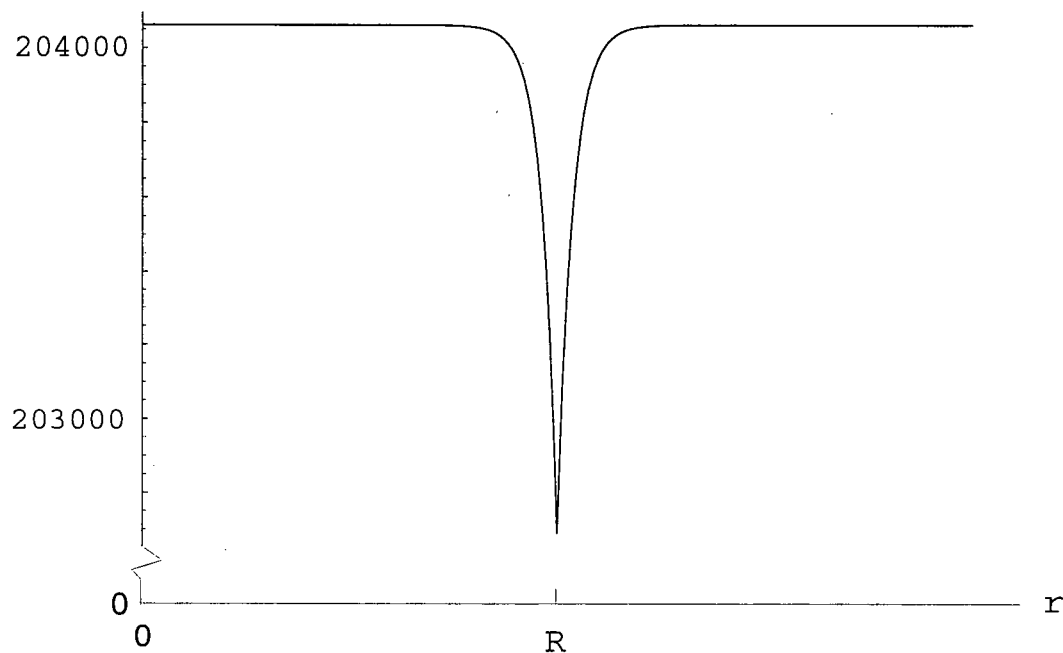
$$\det[-\mathcal{D}_n + \omega^2] = \prod (\omega^2 + \omega_\lambda^2). \quad (3.82)$$

The numerator of (3.72) involves the ‘‘potential’’ $U''(\phi_b(r))$. For the symmetrised effective potential (3.64), the ‘‘potential’’ for this problem is approximately constant except for a small perturbation in a small region near the bubble wall (see Figure 3.15). The constant potential has been analysed above. The solutions with or without the perturbations are identical for $r \ll R$ and almost identical for $r \gg R$. The perturbed solution differs from the unperturbed solution in this latter region at most by normalisation and a phase shift, $\tilde{\omega}_\lambda r = \omega_\lambda r + \delta(\omega_\lambda)$. In this situation, for each value of n , we can obtain the ratio of determinants for a discrete spectrum by [44]:

$$\prod \frac{\omega^2 + \tilde{\omega}_\lambda^2}{\omega^2 + \omega_\lambda^2} = \exp \left(\sum \ln \frac{\omega^2 + \tilde{\omega}_\lambda^2}{\omega^2 + \omega_\lambda^2} \right) \approx \exp \left(\sum \frac{2\omega_\lambda(\tilde{\omega}_\lambda - \omega_\lambda)}{\omega^2 + \omega_\lambda^2} \right), \quad (3.83)$$

which becomes in the continuum:

$$\exp \left[\frac{1}{\pi} \int_0^\infty d\omega_\lambda \frac{2\omega_\lambda \delta(\omega_\lambda)}{\omega^2 + \omega_\lambda^2} \right]. \quad (3.84)$$

Figure 3.15: The “potential” $U''(\phi_b(r))$.

This formula gives the determinant ratio for a particular value of n if we know the phase shifts, $\delta(\omega_\lambda)$. In order to calculate the phase shifts, however, we must make further approximations.

Consider both the perturbed and the unperturbed equations:

$$\left[\frac{d^2}{dr^2} - \frac{4n^2 + 8n + 3}{4r^2} + (\lambda - \omega^2) \right] u(r) = 0, \quad (3.85)$$

$$\left[\frac{d^2}{dr^2} - \frac{4n^2 + 8n + 3}{4r^2} + (\lambda - \omega^2 + V_{pert}(r)) \right] v(r) = 0. \quad (3.86)$$

Multiply (3.85) by $v(r)$ and (3.86) by $u(r)$, subtract, and integrate over r from 0 to ∞ to obtain:

$$\int_0^\infty (u''(r)v(r) - v''(r)u(r)) dr = (u'(r)v(r) - v'(r)u(r)) \Big|_0^\infty = \int_0^\infty V_{pert}(r)u(r)v(r) dr. \quad (3.87)$$

Using the fact that both solutions vanish at $r = 0$ and using the asymptotic form of the

Bessel functions we obtain an exact formula for the phase shift, $\delta(\omega_\lambda)$:

$$\sin \delta(\omega_\lambda) = \frac{1}{\omega_\lambda} \int_0^\infty V_{pert}(r) u(r) v(r) dr. \quad (3.88)$$

Since the perturbed differential equation is extremely difficult to solve, we use perturbation theory to obtain:

$$\delta(\omega_\lambda) \approx \delta(\omega_\lambda)_0 = \frac{1}{\omega_\lambda} \int_0^\infty V_{pert}(r) u(r)^2 dr = \frac{\pi}{2} \int_0^\infty V_{pert}(r) r J_{n+1}(\omega_\lambda r)^2 dr, \quad (3.89)$$

for small phase shifts. Using this result for the phase shift in Equation (3.84), we obtain the ratio of determinants:

$$\left| \frac{\det[-\mathcal{D}_n + U''(\phi_b)]}{\det[-\mathcal{D}_n + \omega^2]} \right| \approx \exp \left[\int_0^\infty \int_0^\infty d\omega_\lambda dr \frac{\omega_\lambda r}{\omega^2 + \omega_\lambda^2} V_{pert}(r) J_{n+1}(\omega_\lambda r)^2 \right], \quad (3.90)$$

for each value of n . The complete determinant ratio then becomes:

$$\left| \frac{\det[-\partial_\mu \partial^\mu + U''(\phi_b)]}{\det[-\partial_\mu \partial^\mu + \omega^2]} \right| = \exp \sum_{n=0}^\infty (2n(n+2) + 1) \left[\int_0^\infty \int_0^\infty d\omega_\lambda dr \frac{\omega_\lambda r}{\omega^2 + \omega_\lambda^2} V_{pert}(r) J_{n+1}(\omega_\lambda r)^2 \right], \quad (3.91)$$

for an arbitrary perturbation potential. The next step in our analysis is to take into account the specific potential in our problem.

It should be noted that this approximation, (3.91), gives the same result as the exact answer expanded to one loop (see Eq.3.73 and 3.74) where the trace is taken instead over $|rnlm\rangle, |knlm\rangle$ bases.

This formula is suitable for numerical evaluation, but in order to obtain an analytical answer we must approximate the perturbation in the potential U'' by:

$$\tilde{V}_{pert}(r) = \begin{cases} -\beta \frac{10(r - \frac{11R}{10})^2}{R^2} & \text{if } R > r > \frac{11R}{10} \\ -\beta \frac{10(r - \frac{9R}{10})^2}{R^2} & \text{if } \frac{9R}{10} > r > R \\ 0 & \text{otherwise} \end{cases}, \quad (3.92)$$

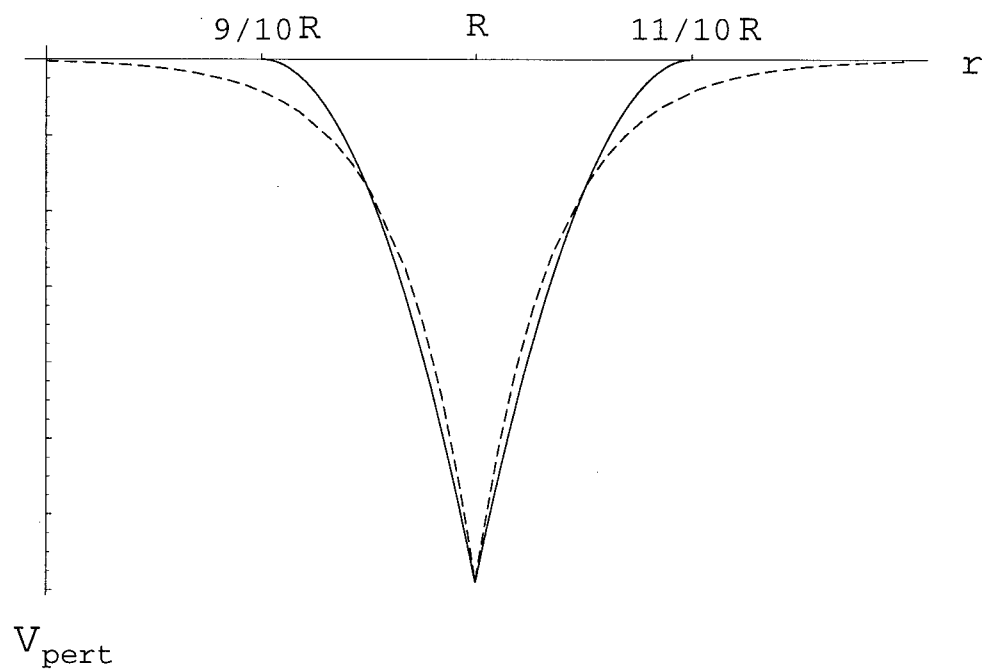


Figure 3.16: Comparison of the perturbation $V_{\text{pert}}(r)$ and the approximate perturbation. The perturbation $V_{\text{pert}}(r)$ is the dotted line and the approximate perturbation $\tilde{V}_{\text{pert}}(r)$ is the solid line.

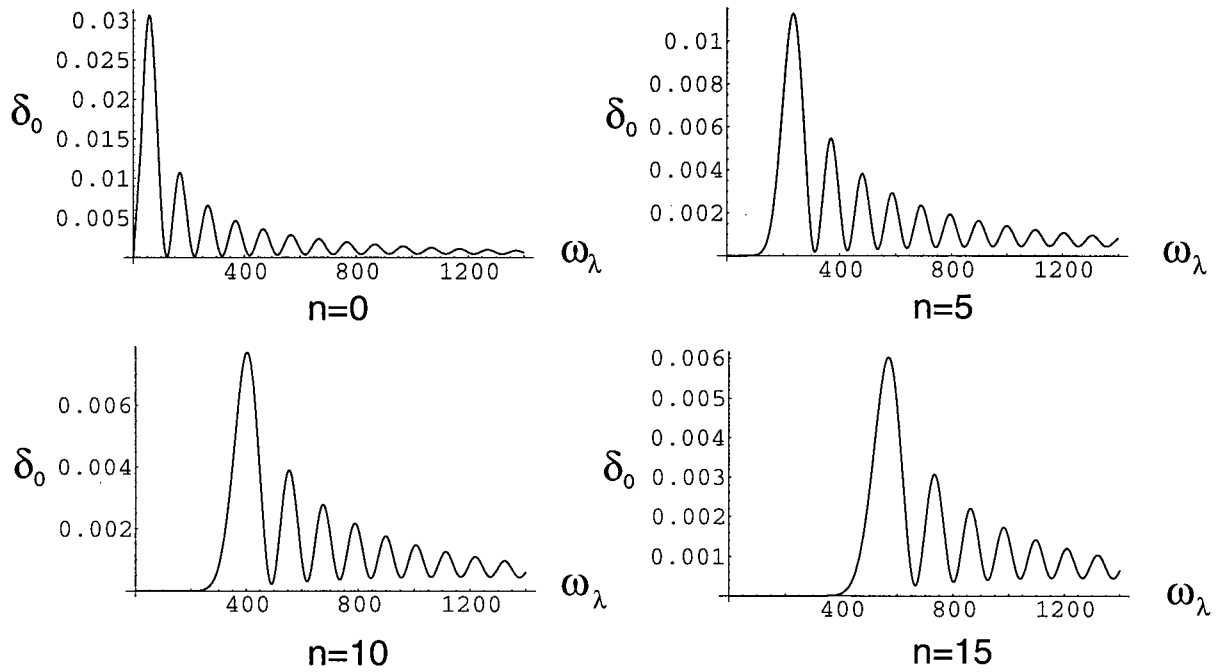


Figure 3.17: The phase shift $\delta_0(\omega_\lambda)$ shown as a function of ω_λ for various values of n . Notice the changing vertical scale.

where $\beta = (U''(\phi(0)) - U''(\phi(R)))$ (see Figure 3.16). With this approximate potential we find the phase shift via (3.89):

$$\begin{aligned} \delta_0(\omega_\lambda) = & -200 \frac{\beta}{R^2} \left[\frac{121}{200} r^2 R^2 (J_{n+1}(r\omega_\lambda)^2 - J_n(r\omega_\lambda)J_{n+2}(r\omega_\lambda)) \right. \\ & + \frac{2^{-4-2n} r^4 (r\omega_\lambda)^{2+2n}}{(n+4)!(n+1)!} \left\{ 2(n+2)(n+4) {}_1F_2 \left(n + \frac{3}{2}, n+4, 2n+3; -r^2\omega_\lambda^2 \right) \right. \\ & \left. \left. - r^2\omega_\lambda^2 {}_1F_2 \left(n + \frac{5}{2}, n+5, 2n+4; -r^2\omega_\lambda^2 \right) \right\} \right. \\ & \left. \frac{11}{10} \frac{2^{-2-2n} r^3 R (r\omega_\lambda)^{2+2n}}{(n + \frac{5}{2})[(n+1)!]^2} {}_2F_3 \left(n + \frac{3}{2}, n + \frac{5}{2}, n+2, n + \frac{7}{2}, 2n+3; -r^2\omega_\lambda^2 \right) \right]^{11/10R}. \quad (3.93) \end{aligned}$$

Using this result we can verify that $\delta(\omega_\lambda) \ll 1$ which means that the approximations of (3.89) are justified. The phase shift as a function of ω_λ is shown for a few values of n in Figure (3.17). However, (3.93) is very difficult to work with so we make another approximation. For ω_λ large enough, we can use the asymptotic approximation for the

Bessel function in (3.89),

$$J_{n+1}(x) = \sqrt{\frac{2}{\pi x}} \left\{ P_{n+1}(x) \cos \left[x - \left(n + \frac{3}{2} \right) \frac{\pi}{2} \right] - Q_{n+1}(x) \sin \left[x - \left(n + \frac{3}{2} \right) \frac{\pi}{2} \right] \right\}, \quad (3.94)$$

where:

$$P_{n+1}(x) = 1 - \frac{(\mu-1)(\mu-9)}{2!(8x)^2} + \frac{(\mu-1)(\mu-9)(\mu-25)(\mu-49)}{4!(8x)^4} - \dots, \quad (3.95)$$

$$Q_{n+1}(x) = \frac{(\mu-1)}{1!(8x)} - \frac{(\mu-1)(\mu-9)(\mu-25)}{3!(8x)^3} + \dots, \quad (3.96)$$

$$\mu = 4(n+1)^2. \quad (3.97)$$

In this way we find:

$$\delta_0(\omega_\lambda) \approx \frac{2R\beta}{30\pi\omega_\lambda} + \frac{(-1)^n \beta \cos(2R\omega_\lambda)}{\pi \omega_\lambda^2} + \mathcal{O}(1/\omega_\lambda^3). \quad (3.98)$$

This estimate for $\delta_0(\omega_\lambda)$ has an infrared cutoff in ω_λ , below which it is not a good estimate, and this will be true no matter how many terms in the approximation of the Bessel function we keep. Therefore, as a first approximation we keep only the first term and cut off the ω_λ integral at the position of the first peak in $\delta_0(\omega_\lambda)$. Using this approximation for $\delta_0(\omega_\lambda)$ we obtain a first estimate of the ratio of determinants for each value of the quantum number n given by:

$$\frac{\det[-\mathcal{D}_n + U''(\phi_b)]}{\det[-\mathcal{D}_n + U''(\phi_-)]} \approx \exp \left[\frac{2R\beta}{30\pi\omega} \arctan \left(\frac{\omega}{\bar{\omega}(n)} \right) \right], \quad (3.99)$$

where:

$$\bar{\omega}(n) \approx 33.16n + 72 = an + b, \quad (3.100)$$

is the infrared cutoff given by the location of the first peak in $\delta_0(\omega_\lambda)$. Using the result (3.99) we can calculate a first approximation for the complete determinant ratio. For large values of n the terms of the sum in the exponent of (3.91) approach:

$$\frac{4R\beta}{30\pi\omega} n^2 \left(\frac{\omega}{an} \right), \quad (3.101)$$

and therefore the sum is infinite. The first estimate for the complete determinant ratio based on (3.91) is infinite. This was to be expected based on comments at the beginning of this section and, since this approximation exactly coincides with (3.74), we subtract this term from the exponent of (3.91) as our normalisation prescription for the complete determinant ratio. Note that we have used the approximation of (3.98) to calculate the infinite factor, but the equality with (3.74) holds before this approximation was made.

In order to find a finite result for the determinant ratio we adjust our earlier approximation for the phase shift:

$$\delta(\omega_\lambda) = \arcsin(\delta_0(\omega_\lambda)) = \delta_0(\omega_\lambda) + \frac{1}{6}\delta_0(\omega_\lambda)^3 + \frac{3}{40}\delta_0(\omega_\lambda)^5 + \dots, \quad (3.102)$$

which would add correction terms to the exponent in (3.99). The second term in (3.102) leads to a factor of the form:

$$\exp \left[\frac{\pi^2}{24} \int_0^\infty d\omega_\lambda \frac{\omega_\lambda \delta_0(\omega_\lambda)^3}{\omega^2 + \omega_\lambda^2} \right], \quad (3.103)$$

for each value of n . This term is also divergent but does **not** exactly coincide with the next term in the expansion (3.73). However, the divergent contribution in each must be the same.

Therefore dividing through by the previously obtained infinite factor (*ie.* the right hand side of (3.99)) leads to the renormalised value:

$$\frac{\det[-\mathcal{D}_n + U''(\phi_b)]}{\det[-\mathcal{D}_n + U''(\phi_-)]} \approx \exp \left[\frac{\pi^2}{24} \left(\frac{2R\beta}{30\pi\omega} \right)^3 \left\{ \frac{\omega}{\bar{\omega}(n)} - \arctan \left(\frac{\omega}{\bar{\omega}(n)} \right) \right\} \right]. \quad (3.104)$$

For large values of n the terms of the sum in (3.91) approach:

$$\frac{\pi^2}{24} \left(\frac{2R\beta}{30\pi\omega} \right)^3 (2n^2 + 4n + 1) \left(\frac{\omega^3}{3a^3n^3} \right). \quad (3.105)$$

which also leads to a divergent sum and therefore an infinite value for the determinant ratio. The divergence here must be contained in the divergence in the two interaction

term of the expansion (3.73), as are other logarithmic divergences obtained from keeping more terms in the approximation of the Bessel function (3.94). However, subtracting the two interaction term will almost certainly leave a finite contribution at the next order in n . We assume this is the case, but since we are doing an approximate calculation, we will not calculate the finite contribution from the two interaction term or any correction terms to our approximation, since they will have the same physical dependence as the approximation we will give. We should further note that correction terms are probably not calculable analytically and are not likely to be a problem for our results. They are obtained from integrating oscillatory functions (see second term in (3.98)) over ω_λ in (3.103) and should not contribute very much. The renormalised approximation to the complete determinant ratio (3.91) that we obtain from (3.104) is given by:

$$\begin{aligned} & \exp \frac{\pi^2}{24} \left(\frac{2R\beta}{30\pi\omega} \right)^3 \left[\sum_{n=0}^{\infty} (2n(n+2) + 1) \left\{ \frac{\omega}{\bar{\omega}(n)} - \arctan \left(\frac{\omega}{\bar{\omega}(n)} \right) \right\} - \sum_{n=1}^{\infty} 2n^2 \frac{\omega^3}{3a^3 n^3} \right] \quad (3.106) \\ & = \exp \frac{\pi^2}{24} \left(\frac{2R\beta}{30\pi\omega} \right)^3 \left[\sum_{n=0}^{100} (2n(n+2) + 1) \left\{ \frac{\omega}{\bar{\omega}(n)} - \arctan \left(\frac{\omega}{\bar{\omega}(n)} \right) \right\} \right. \\ & \quad \left. - \sum_{n=1}^{100} \left\{ (2n(n+2) + 1) \frac{\omega^3}{3a^3 n^3} \right\} + \frac{4\omega^3}{3a^3} \zeta(2) + \frac{\omega^3}{3a^3} \zeta(3) \right], \quad (3.107) \end{aligned}$$

where ζ is the Riemann Zeta function:

$$\zeta(i) = \sum_{n=1}^{\infty} \frac{1}{n^i}. \quad (3.108)$$

Evaluating gives:

$$\exp \left[-5300 \frac{\pi^2}{24} \left(\frac{2R\beta}{30\pi\omega} \right)^3 \right] \approx \exp[-2 \times 10^{-5}]. \quad (3.109)$$

Because of the small value of the exponent we can see that the exponential is extremely well approximated by:

$$\exp \left[\frac{-5300\pi^2}{24} \left(\frac{2R\beta}{30\pi\omega} \right)^3 \right] \approx 1 - \frac{5300\pi^2}{24} \left(\frac{2R\beta}{30\pi\omega} \right)^3, \quad (3.110)$$

which is our result for the determinant ratio (3.72).

This is a nonperturbative calculation because Eq.(3.84) is a nonperturbative resummation of the perturbation expansion (3.73) of the determinant. While we make an approximation through Eq.(3.102), this expansion is nonperturbative since the terms of the expansions do not coincide. Our approximate calculation should therefore have contributions from all perturbative diagrams. This nonperturbative resummation of diagrams in the determinantal prefactor is very similar in spirit to that of [45].

This result constitutes the contribution of the positive eigenvalues to the quantum corrections to the decay rate in the zero temperature theory. In the next section we consider the zero and negative eigenvalues.

3.3.2 Zero and Negative Eigenvalues

The zero eigenvalues contribute $\sqrt{B/2\pi}$ per collective coordinate[39]. The action of the 4D bubble is independent of the centre of the bubble which means there are 4 collective coordinates leading to the first factor in Eq.(3.71).

The eigenfunctions of zero eigenvalue are:

$$\chi_{o\mu}(x, y, z, t) = \frac{d}{dx^\mu} \phi_b(r) = \frac{dr}{dx^\mu} \frac{d}{dr} \phi_b(r) = \frac{x^\mu}{r} \frac{d}{dr} \phi_b(r), \quad (3.111)$$

where $r = \sqrt{x^2 + y^2 + z^2 + t^2}$ and:

$$t = r \cos(\psi) \quad \sim Y_{100}, \quad (3.112)$$

$$z = r \cos(\theta) \sin(\psi) \quad \sim Y_{110}, \quad (3.113)$$

$$y = r \cos(\phi) \sin(\theta) \sin(\psi) \quad \sim Y_{111} + Y_{11-1}, \quad (3.114)$$

$$x = r \sin(\phi) \sin(\theta) \sin(\psi) \quad \sim Y_{111} - Y_{11-1}. \quad (3.115)$$

Therefore these eigenfunctions all correspond to $n = 1$ and since there are no radial nodes we can be sure that there are no negative eigenvalues with $n \neq 0$:

In [46] Coleman argued that there is only a single negative eigenvalue for an $O(4)$ invariant bounce. We assume this³ and determine its value. We use the method of Coleman in [39] with a slight modification. As was argued by Coleman, the only possible eigenfunctions of negative eigenvalue are those that are bound to the bubble wall. For such eigenfunctions we can approximate the centrifugal potential in (3.78) by a constant determined by its value at the bubble wall ($r = R$):

$$\lambda_{pn} = \lambda_p + \frac{4n^2 + 8n + 3}{4R^2}, \quad (3.116)$$

where λ_p is a number independent of n . We know that for $n = 1$ the lowest eigenvalue is zero:

$$\lambda_{01} = \lambda_0 + \frac{15}{4R^2} = 0. \quad (3.117)$$

Therefore we can obtain the lowest eigenvalue for $n = 0$:

$$\lambda_- = \lambda_{00} = \lambda_0 + \frac{3}{4R^2} = -\frac{15}{4R^2} + \frac{3}{4R^2} = -\frac{3}{R^2}. \quad (3.118)$$

This value is different from the value obtained by Coleman, but only by a factor of 2. We cannot explain this discrepancy but can only stand by our calculation.

3.3.3 Decay Rate for Zero Temperature

Therefore combining the zero temperature semiclassical result (3.66) with the quantum corrections obtained in the last section, we estimate the decay rate per unit volume of the false vacuum in the zero temperature theory to be:

$$\Gamma/V = \exp(-S_4) \left(\omega^4 \left(\frac{S_4}{2\pi} \right)^2 \right) \frac{\omega}{\sqrt{\lambda_-}} \left| \frac{\det'[-\partial_\mu \partial^\mu + U''(\phi_b)]}{(\omega^{-2})^5 \det[-\partial_\mu \partial^\mu + \omega^2]} \right| \quad (3.119)$$

$$= \exp\left(-\frac{27\pi^2\sigma^4}{2(\Delta E)^3}\right) \left(\frac{27\pi^2\sigma^4\omega^2}{4\pi(\Delta E)^3}\right)^2 \frac{R\omega}{\sqrt{3}} \left[1 - \frac{5300\pi^2}{24} \left(\frac{2R\beta}{30\pi\omega}\right)^3\right]^{-1/2} \quad (3.120)$$

$$= 1.55 \times 10^{-18} \text{MeV}^4 \approx 3 \times 10^{-4} \text{fm}^{-3} \text{s}^{-1}. \quad (3.121)$$

³This is most likely a good assumption but not proven due to the cusp in our potential. For more details see [43],[46] and [47].

It should be noted that the quantum corrections are negligible so the decay rate is basically determined by the semiclassical result. We believe that this observation would be unchanged by the inclusion of corrections that we have ignored in this calculation. While the quantum corrections did not turn out to be significant in this case, the fact that they are not is relevant to the baryogenesis mechanism mentioned at the start of this chapter. As well, the techniques applied to the problem may prove useful in other calculations of this type.

In the next section we perform the same calculation in the high temperature limit.

3.4 Quantum Corrections for High Temperature

The quantum corrections to the decay rate at high temperature are[41]:

$$A = T \left(\omega^3 \int d^3x \left(\frac{S_3[\phi_b]}{2\pi T} \right)^{3/2} \right) \frac{\omega}{\sqrt{\lambda_-}} \left| \frac{\det'[-\partial_i \partial^i + U''(\phi_b)]}{(\omega^{-2})^3 \det[-\partial_i \partial^i + U''(\phi_-)]} \right|^{-1/2}. \quad (3.122)$$

which again factors into three parts corresponding to zero, negative and positive eigenvalues respectively.

3.4.1 Positive Eigenvalues

The calculation in three dimensions is extremely similar. The expansion of the determinant ratio is exactly the same as in 4D (3.73). Tracing over a Cartesian basis, we can see that the one loop term is divergent while the two loop term is finite:

$$Tr \left[\frac{V_{pert}(r)}{-\partial_\mu \partial^\mu + \omega^2} \right] = \int d^3x d^3k \frac{V_{pert}(r)}{k^2 + \omega^2}, \quad (3.123)$$

$$Tr \left[\left(\frac{V_{pert}(r)}{-\partial_\mu \partial^\mu + \omega^2} \right)^2 \right] = \int d^3k d^3p \frac{\mathcal{V}_{pert}(k)}{(k^2 + \omega^2)} \frac{\mathcal{V}_{pert}(-k)}{((k+p)^2 + \omega^2)}. \quad (3.124)$$

The calculation is done using spherical coordinates and the eigenfunctions are expanded in terms of the spherical harmonics:

$$\chi(r, \theta, \phi) = \sum_{n=0}^{\infty} \sum_{l=-n}^n \sum_{m=-|l|}^{|l|} C_{lm} \frac{u(r)}{r} Y_{lm}(\theta, \phi). \quad (3.125)$$

The Laplacian, when operating on each term of (3.125) with quantum number l , becomes:

$$\partial_i \partial^i \rightarrow \frac{1}{r} \left[\frac{d^2}{dr^2} - \frac{l(l+1)}{r^2} \right] r \equiv \frac{1}{r} \mathcal{D}_l r. \quad (3.126)$$

Therefore:

$$\det[-\partial_i \partial^i + U''] = \prod_{l=0}^{\infty} (\det[-\mathcal{D}_l + U''])^{2l+1}. \quad (3.127)$$

The solutions to this differential equation that are well behaved at $r = 0$ and $r = \infty$ are:

$$u(r) = \omega_\lambda r j_l(\omega_\lambda r) \equiv \sqrt{\frac{\pi \omega_\lambda r}{2}} J_{l+1/2}(\omega_\lambda r), \quad (3.128)$$

where j_l are the usual 3D spherical Bessel functions and $\omega_\lambda \equiv \sqrt{\lambda - \omega^2}$. We obtain:

$$\delta(\omega_\lambda) \approx \frac{1}{\omega_\lambda} \int_0^\infty V_{pert}(r) u(r)^2 dr = \frac{\pi}{2} \int_0^\infty V_{pert}(r) r J_{l+1/2}(\omega_\lambda r)^2 dr, \quad (3.129)$$

thus giving^{4 5}:

$$\left| \frac{\det[-\partial_i \partial^i + U''(\phi_b)]}{\det[-\partial_i \partial^i + \omega^2]} \right| = \exp \sum_{l=0}^{\infty} (2l+1) \left[\int_0^\infty \int_0^\infty d\omega_\lambda dr \frac{\omega_\lambda r}{\omega^2 + \omega_\lambda^2} V_{pert}(r) J_{l+1/2}(\omega_\lambda r)^2 \right]. \quad (3.130)$$

As in the zero temperature case we can find the exact expression for the phase shift with the approximate potential but it is too difficult to work with. Instead we approximate the Bessel functions as in (3.94) where $(n+1) \rightarrow (l+1/2)$. In this way we find:

$$\delta(\omega_\lambda) \approx \delta_0(\omega_\lambda) = \frac{2R\beta}{30\pi\omega_\lambda} + \mathcal{O}(1/\omega_\lambda^2). \quad (3.131)$$

⁴Note that we have again dropped the factor of $(\omega^{-2})^3$ and the “det” notation, as the omitted eigenvalues correspond to a set of measure zero.

⁵The summand in this expression appears in [33], but is only used for the high energy modes. The non-divergent term in what follows does not appear in [33].

A first estimate of the ratio of determinants for each value of the quantum number, l , is given by:

$$\frac{\det[-\mathcal{D}_l + U''(\phi_b)]}{\det[-\mathcal{D}_l + U''(\phi_-)]} \approx \exp \left[\frac{2R\beta}{30\pi\omega} \arctan \left(\frac{\omega}{\bar{\omega}(l)} \right) \right], \quad (3.132)$$

where $\bar{\omega}(l) \approx 49.5l + 82 = cl + d$ is the infrared cutoff given by the location of the first peak in $\delta_0(\omega_\lambda)$ as a function of ω_λ . For large values of l the terms of the sum in (3.130) approach:

$$\frac{4R\beta}{30\pi\omega} l \left(\frac{\omega}{cl} \right), \quad (3.133)$$

and the sum is infinite and therefore the complete determinant ratio is also infinite. Again, this was to be expected and, since this approximation exactly coincides with the one loop term, our renormalisation prescription is to remove the one loop term from the exponent of (3.130).

Again we adjust our earlier approximation for the phase shift:

$$\delta(\omega_\lambda) = \arcsin(\delta_0(\omega_\lambda)) = \delta_0(\omega_\lambda) + \frac{1}{6}\delta_0(\omega_\lambda)^3 + \frac{3}{40}\delta_0(\omega_\lambda)^5 + \dots, \quad (3.134)$$

and the correction is implemented as in (3.103). Evaluating the contribution to the determinant ratio leads to:

$$\frac{\det[-\mathcal{D}_l + U''(\phi_b)]}{\det[-\mathcal{D}_l + U''(\phi_-)]} \approx \exp \left[\frac{\pi^2}{24} \left(\frac{2R\beta}{30\pi\omega} \right)^3 \left\{ \frac{\omega}{\bar{\omega}(l)} - \arctan \left(\frac{\omega}{\bar{\omega}(l)} \right) \right\} \right]. \quad (3.135)$$

For large values of l the terms of the sum in (3.130) approach:

$$\frac{\pi^2}{24} \left(\frac{2R\beta}{30\pi\omega} \right)^3 (2l+1) \left(\frac{\omega^3}{3c^3l^3} \right). \quad (3.136)$$

The sum is finite so we do not need to further normalise and the result for the complete determinant ratio (3.130) is:

$$\begin{aligned} & \exp \frac{\pi^2}{24} \left(\frac{2R\beta}{30\pi\omega} \right)^3 \left[\sum_{l=0}^{100} (2l+1) \left\{ \frac{\omega}{\bar{\omega}(l)} - \arctan \left(\frac{\omega}{\bar{\omega}(l)} \right) \right\} \right. \\ & \quad \left. - \sum_{l=1}^{100} \left\{ (2l+1) \frac{\omega^3}{3c^3l^3} \right\} + \frac{2\omega^3}{3a^3} \zeta(2) + \frac{\omega^3}{3a^3} \zeta(3) \right]. \end{aligned} \quad (3.137)$$

Evaluating gives:

$$\exp \left[82 \frac{\pi^2}{24} \left(\frac{2R\beta}{30\pi\omega} \right)^3 \right] \approx \exp[3 \times 10^{-7}]. \quad (3.138)$$

Because of the small value of the exponent, we can see that the exponential is extremely well approximated by:

$$\exp \left[\frac{82\pi^2}{24} \left(\frac{2R\beta}{30\pi\omega} \right)^3 \right] \approx 1 + \frac{82\pi^2}{24} \left(\frac{2R\beta}{30\pi\omega} \right)^3. \quad (3.139)$$

This result constitutes the contribution of the positive eigenvalues to the quantum corrections to the decay rate in the high temperature theory. In the next section we consider the zero and negative eigenvalues.

3.4.2 Zero and Negative Eigenvalues

In the $O(3)$ invariant bubble there are 3 collective coordinates leading to the first term in (3.122). The eigenfunctions of zero eigenvalue are:

$$\chi_{0\mu}(x, y, z) = \frac{d}{dx^\mu} \phi_b(r) = \frac{dr}{dx^\mu} \frac{d}{dr} \phi_b(r) = \frac{x^\mu}{r} \frac{d}{dr} \phi_b(r), \quad (3.140)$$

where $r = \sqrt{x^2 + y^2 + z^2}$ and:

$$z = r \cos(\theta) \sim Y_{10}, \quad (3.141)$$

$$y = r \cos(\phi) \sin(\theta) \sim Y_{11} + Y_{1-1}, \quad (3.142)$$

$$x = r \sin(\phi) \sin(\theta) \sim Y_{11} - Y_{1-1}. \quad (3.143)$$

Therefore these eigenfunctions all correspond to $l = 1$ and since there are no radial nodes we can be sure that there are no negative eigenvalues with $l \neq 0$.

We assume, as in the previous section, that there is only a single negative eigenvalue and concentrate on obtaining an approximation. The only possible eigenfunctions of

negative eigenvalue are those that are bound to the bubble wall. For such eigenfunctions we can approximate the centrifugal potential in (3.126) by a constant:

$$\lambda_{pn} = \lambda_p + \frac{l(l+1)}{R^2}, \quad (3.144)$$

where λ_p is a number independent of l . We know that for $l = 1$ the lowest eigenvalue is zero:

$$\lambda_{01} = \lambda_0 + \frac{2}{R^2} = 0. \quad (3.145)$$

Therefore we can obtain the lowest eigenvalue for $l = 0$:

$$\lambda_- = \lambda_{00} = \lambda_0 = -\frac{2}{R^2}. \quad (3.146)$$

3.4.3 Decay Rate for High Temperature

Therefore combining the high temperature semiclassical result (3.69) with the quantum corrections obtained in the last section we estimate the decay rate per unit volume of the false vacuum in the high temperature theory to be:

$$\Gamma/V = \frac{R\omega}{\sqrt{2}} \left(\omega^3 \left(\frac{16\pi S_1(T)^3}{3(\Delta E)^2 T} \right)^{3/2} \right) \exp \left(-\frac{16\pi S_1(T)^3}{3(\Delta E)^2 T} \right) \left[1 + \frac{82\pi^2}{24} \left(\frac{2R\beta}{30\pi\omega} \right)^3 \right]^{-1/2}. \quad (3.147)$$

We cannot obtain a numerical estimate for the decay rate at this time since the temperature dependence of the semiclassical result is not currently known. This result could be important to the study of false vacuum states of this type in heavy ion collisions.

3.5 Summary

In this chapter we nonperturbatively calculated the decay rate of a particular metastable vacuum state for $\theta = 0$ predicted by the form of the effective potential for the light chiral fields. We calculated the decay rate in both the zero and high temperature theories. The

low temperature result is significant to the baryogenesis mechanism described in [15]. The high temperature results could be important for testing the theory in heavy ion collisions. Both results could have important implications for the study of the development of the early universe near the time of the QCD phase transition. In addition the method used in these calculations represents a new approach that could be useful in other calculations of this type.

Chapter 4

Production of Nontrivial Theta Vacua

In this chapter we show in a simplified numerical model that nontrivial θ -vacua can be realized¹. This nontrivial vacuum is very different from the metastable vacuum discussed in the previous chapter, in which we had $\theta = 0$ throughout space and the metastable vacuum was definitely metastable. The nontrivial θ -vacuum that we discuss in this chapter has $\theta \neq 0$ by definition and is the true vacuum state in a universe with $\theta \neq 0$ everywhere. The energy of this vacuum state is given by Equation (2.37). As we have mentioned previously, we live in a universe where it is known that $\theta < 10^{-10}$ [3] so the true vacuum state of our universe corresponds very closely to the $\theta = 0$ vacuum state. However, it is possible that nontrivial θ -vacua can be produced inside a high temperature fireball created in heavy ion collisions. While this is a simplified model which differs somewhat from the real physics associated with high energy ion collisions, there is no reason to believe that the nontrivial θ -vacua cannot be realized at RHIC. Our results also give a rough estimate of the time it takes for these nontrivial θ -vacua to be formed. In order to have a hope of observing them, they must form within the time that the central region of the fireball is isolated from the true vacuum.

The real importance of observing effects of non-zero θ vacua in relativistic heavy ion collisions is that it provides us with an opportunity to study the physics of the early universe at around the time of the QCD phase transition. In the very early universe the conditions would have been similar to the inside of the heavy ion collisions and the

¹The results of this chapter were published in [48]

existence of a θ -parameter could have had significant implications to the evolution of the early universe.

Note that the formulas in this chapter are valid for arbitrary values of the parameters p and q . The numerical results were obtained using the specific values $p = N_c$ and $q = 1$.

In the next section we will discuss the Disoriented Chiral Condensate (DCC) which is closely related to the θ -vacuum state and is fairly well understood. In the section after that we will show how to extend the idea of the DCC to obtain the θ -vacuum state.

4.1 DCC

The creation of a θ -vacuum state is very similar to the creation of the Disoriented Chiral Condensate (DCC) in heavy ion collisions, which has been a subject of interest for some time [49, 50, 51] (among many others, see also a nice review [52] for a discussion of DCC as an example of an out of equilibrium phase transition). Therefore, we discuss the DCC first and then develop the idea of a θ -vacuum state afterwards. DCC refers to regions of space in which the chiral condensate points in a different direction from that of the ground state. The DCC could exist inside a hot shell of debris produced in heavy ion collisions and be protected from the true vacuum by this shell. For both the DCC and the θ -vacuum state, the difference in energy between the created state and the true vacuum state is proportional to the small parameter m_q and negligible at high temperature.

The chiral condensate, $\langle \bar{q}q \rangle$, is the vacuum expectation value of the composite operator $\bar{q}q$ made up of quark(q) and antiquark(\bar{q}) fields. Mesons are bound states of quarks and anti-quarks, and so the chiral condensates are just vacuum expectation values of the meson fields. The low energy dynamics of pions was modelled in [50] by a linear sigma model involving the four-component field $(\sigma, \vec{\pi})$. The potential of the four component field is a steep 4D Mexican hat potential with a slight extra slope ($\sim m_q$) in the σ

direction. In the region exterior to the hot shell of debris created in a heavy ion collision, the fields have the vacuum values $(v, 0)$. In the interior region, which has recently been in contact with the extremely high energy decay products, the pion fields can initially take non-zero values and the $(\sigma, \vec{\pi})$ vector can point in an arbitrary direction in the four dimensional configuration space. In particular the vacuum expectation value of the fields differs from the vacuum value: $(v, 0)$. Non-zero vacuum expectation values are defined as condensates and the four vector of field condensates differs from the vacuum direction or vacuum orientation. This is what is meant by a Disoriented Chiral Condensate. The condensates of course eventually relax to the vacuum values.

The absolute value of the chiral condensate right after the phase transition is expected to be close to its final (zero temperature) magnitude because of the steepness of the Mexican hat potential. However, the vacuum orientation of the formed condensate takes a longer time to relax due to the small free energy difference $\sim m_q$ between the DCC state and the vacuum state.

The high energy products of the collision expand outwards at relativistic speeds. Inside this shell is a region of DCC isolated from the true vacuum and at effectively zero temperature. If the cooling process of the interior is very rapid the system is initially out of equilibrium, but its evolution can be determined using the zero temperature equations of motion. It has been shown[50] that in the quenched approximation, where the temperature goes from ~ 200 MeV to zero instantaneously, the subsequent evolution exhibits a temporary growth of long wavelength spatial modes of the pion field corresponding to domains where the chiral condensate is approximately correlated, but oriented differently from the vacuum value.

It is useful to discuss the DCC in an effective Lagrangian approach to emphasise the similarity with a nontrivial θ -vacuum state. Due to the fact that the absolute value of the chiral condensate right after the phase transition is expected to be close to the

zero temperature magnitude, we can parameterise Goldstone fields by the same unitary matrix, U , introduced in Chapter 2:

$$U = e^{i\phi(\vec{n}\cdot\vec{\tau})}, \quad \langle \bar{\Psi}_L^i \Psi_R^j \rangle = -|\langle \bar{\Psi}_L \Psi_R \rangle| U_{ij}. \quad (4.148)$$

The energy density of the DCC is determined by the mass term in an effective Lagrangian:

$$E_\phi = -\frac{1}{2} \text{Tr}(MU + M^\dagger U^\dagger) = -2m|\langle \bar{\Psi}\Psi \rangle| \cos(\phi), \quad (4.149)$$

where we put $m_u = m_d = m$ for simplicity. Eq.(4.149) implies that any $\phi \neq 0(\text{mod } 2\pi)$ is not a stable vacuum state because $\frac{\partial E_\phi}{\partial \phi}|_{\phi \neq 0} \neq 0$, and therefore the vacuum is misaligned. On the other hand, the energy difference between the misaligned state and true vacuum ($\phi = 0$) is small and proportional to m_q . Therefore, the probability to create a state with an arbitrary ϕ at high temperature $T \sim T_c$ is proportional to $\exp[-V(E_\phi - E_0)/T]$, where V is 3D volume, and depends on ϕ only very weakly, i.e. ϕ is a quasi-flat direction. Right after the phase transition when $\langle \bar{\Psi}\Psi \rangle$ becomes non-zero, the pion field begins to roll down the potential slope toward $\phi = 0$, and of course overshoots it. Thereafter, the ϕ field oscillates. One should expect coherent oscillations of the π meson field which would correspond to a zero-momentum condensate of pions. This is exactly what was found in[50]. Eventually these classical oscillations produce real π mesons which hopefully can be observed.

4.2 Nontrivial θ -vacua

Now we turn to the nontrivial θ -vacuum state when the θ term is also non-zero and therefore the θ -vacuum state can be formed.

In the evolution of the early universe this non-zero θ -parameter could be a fundamental θ associated with a dynamical axion. In the case of heavy ion collisions, however, it is much more likely that we might observe what is called an ‘‘induced’’ θ -parameter.

The induced θ -parameter could arise if a region is created in a heavy ion collision over which the chiral phases are significantly correlated about a non-zero value. If this occurs then we perform a chiral rotation of the type discussed in Chapter 2:

$$U \rightarrow e^{-iN_f\phi_0}U = e^{i\theta}, \quad (4.150)$$

where $-\phi_0$ is the non-zero value about which the chiral phases are correlated and we obtain a new theory with an effective value of θ induced by the initial conditions. The fields behave as if the θ -parameter were non-zero. As we said above, we are far more likely to observe an induced θ vacuum in heavy ion collisions, so we have this type of θ parameter in mind throughout this chapter.

The production of nontrivial θ -vacua occurs in much the same way as for the DCC discussed above. The new element is that, in addition to chiral fields differing from their true vacuum values, the θ -parameter of QCD, which is zero in the real world, becomes effectively non-vanishing in a large region of space.

The starting point is again the effective potential for the chiral fields (2.31). The energy density of the misaligned vacuum is given by the potential:

$$V(\phi_i, \theta) = -E \cos \left[\frac{p}{q} \left(\sum_{i=1}^{N_f} \phi_i - \theta \right) + \frac{2\pi}{q} l \right] - \sum_{i=1}^{N_f} M_i \cos \phi_i$$

$$l = 0, 1, \dots, p-1, \quad (4.151)$$

for

$$(2l-1)\frac{\pi}{q} \leq \theta - \sum \phi_i < (2l+1)\frac{\pi}{q}. \quad (4.152)$$

As discussed previously in Chapter 3, and stress again here, the crucial point is that the θ -parameter appears only in the combination, $\sum \phi_i - \theta$. The most important difference between Eqs. (4.149) and (4.151) is the presence of the parametrically large term $\sim E \gg m_q |\langle \bar{\Psi}\Psi \rangle|$ in the expression for energy (4.151). This term does not go away in the chiral limit and provides a non-zero mass for the η' meson which is expressed

in terms of the parameter, E . It was for exactly this reason that it was thought until recently[53] that the nontrivial θ -vacua would involve too large an energy cost to be produced because of the large parameter associated with the θ -parameter.

The key point is that, for arbitrary phases ϕ_i , the energy of a misaligned state with non-zero θ differs by a huge amount ($\sim E$) from the vacuum energy. However, when the relevant combination ($\sum_i \phi_i - \theta$) from Eq.(4.151) is close by an amount of the order $\mathcal{O}(m_q)$ to its vacuum value, a Boltzmann suppression due to the term proportional to E is absent, and an arbitrary misaligned θ -state can be formed. Indeed, in the limit $M_i \ll E$, because of the large parameter in the first term, the vacuum state that is favoured for non-zero θ is the solution $\bar{\phi}_i \approx \theta/N_f$. Substituting this back into the potential we reproduce the well-known result[10] for the vacuum energy as a function of θ :

$$V(\theta) \approx -E - \sum M_i \cos(\theta/N_f). \quad (4.153)$$

This shows that the energy cost of creating a nontrivial θ -vacuum is proportional to the much smaller parameter, $M_i \propto m_q$, as in the case of the DCC. This is a very important result because it means that it may be possible to create a nontrivial θ -vacuum state in heavy ion collisions.

At this point we can apply the same philosophy as for the DCC. The chiral fields², ϕ_i , are allowed to take random values and after the phase transition roll toward the true solution $\bar{\phi}_i \approx \theta/N_f$ and of course overshoot it. The situation is very similar to what was described for the DCC with the only difference that, in general, we expect an arbitrary θ -disoriented state to be created in heavy ion collisions, not necessarily the $|\theta = 0\rangle$ state. The difference in energy between these states is proportional to m_q from (4.153).

Now we study the evolution of the chiral fields with time. For this study we assume

²As was discussed in Chapter 2, for $\theta \neq 0$ the meson fields are not pure pseudoscalar fields, but rather have a scalar component as well; the mixing angle between the singlet and octet combinations also depends on θ .

the following situation. The rapid expansion of the high energy shell leaves behind an effectively zero temperature region in the interior which is isolated from the true vacuum. The high temperature non-equilibrium evolution is very suddenly stopped, or “quenched”, leaving the interior region in a non-equilibrium initial state that then begins to evolve according to (almost) zero temperature Lagrangian dynamics. Starting from an initial non-equilibrium state we can study the behaviour of the chiral fields using the zero temperature equations of motion. The equations of motion are non-linear and cannot be solved analytically but we can solve them numerically in order to determine the behaviour of the fields. The production of a nontrivial θ -vacuum is indicated by the fact that the chiral fields relax to constant and equal non-zero values on a time scale over which spatial oscillations of the fields vanish. This indicates the presence of a condensate parameterised by the θ -parameter.

The formation of a non-perturbative condensate is also supported by observation of the phenomenon of coarsening (see below) and by a test of volume-independence of our results.

4.3 Numerical Evolution

The equations of motion for the phases of the chiral condensate with two quark flavours consist of two coupled, second-order, nonlinear partial differential equations:

$$\ddot{\phi}_i - \nabla^2 \phi_i + \gamma \dot{\phi}_i + \frac{d}{d\phi_i} V(\phi_j, \theta) = 0, \quad i = 1, 2 \quad (4.154)$$

where ∇^2 is the three dimensional spatial Laplacian and the potential is given in (4.151). Emission of pions and expansion of the domain contribute to the damping, γ , as might other processes. We do not know exactly how they would contribute, but we simulate these unknown effects by including a damping term with a natural value for the damping constant, $\gamma \sim \Lambda_{QCD} \sim 200 \text{ MeV}$.

In this section we present the results of a numerical solution of the equations of motion. The initial data for each of the chiral fields ϕ_i was chosen on a 3D grid of 16^3 points. The initial data consisted of random values of ϕ_i and $\dot{\phi}_i = 0$. The initial data was evolved in time steps using a Two-Step Adams-Bashforth-Moulton Predictor-Corrector method[54] for each grid point with the spatial Laplacian approximated at each grid point using a finite difference method. We used periodic spatial boundary conditions.

The grid spacing was determined by the length of a side of the spatial grid which was varied in order to vary the volume. The size of the time step between successive spatial grids was much smaller than the spatial grid spacing and was fixed at about $10^{-5} MeV^{-1}$.

We evolved the data for 8000 time steps and then applied a Fast Fourier Transform [55] to the spatial data at evenly spaced time steps. We then binned the data in small increments of the magnitude of the wave vector and averaged over the values in each bin in order to obtain the angular averaged power spectrum.

This procedure was carried out for different volumes. In all cases the results were qualitatively the same. We saw an initial growth of long wavelength modes as in [50] and subsequent damped oscillation of all modes. The $|\vec{k}| = 0$ modes oscillate and approach the non-zero equilibrium values of the fields. They exhibit this behaviour in the same time frame in which the Fourier coefficients of the modes with non-zero wave vectors fall to a tiny fraction of the zero mode coefficient. This qualitative behaviour occurs for different total volumes and grid sizes suggesting that this behaviour is not due to finite size effects.

The Fourier zero mode corresponds to a spatially constant field value. Therefore the fact that the zero-mode goes to non-zero constant value means that the field approaches a classical spatially constant field configuration. This clearly corresponds to a non-vanishing vacuum expectation value of the field which is the definition of a condensate. Therefore we can say that a condensate has been formed. This state is the ground state

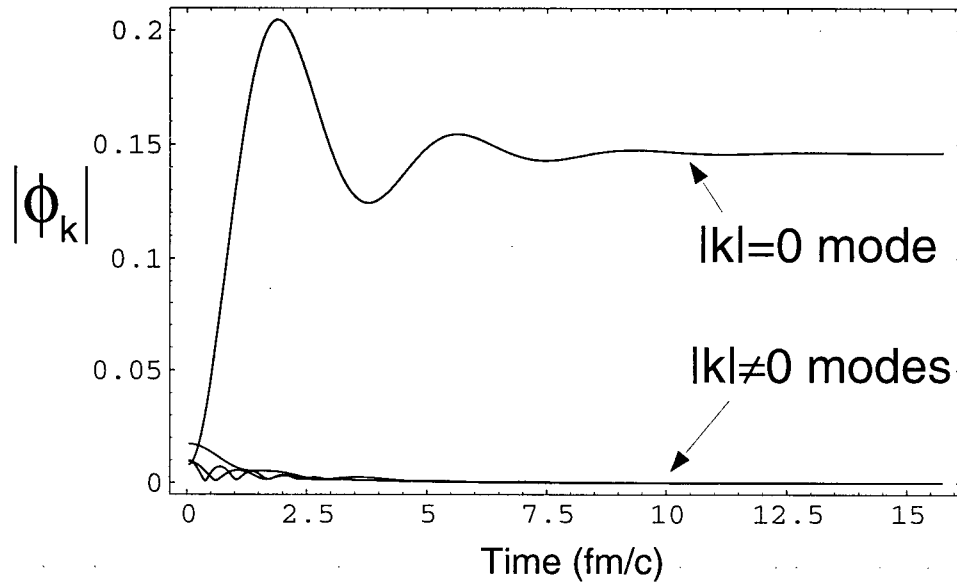


Figure 4.18: Time evolution of $|\phi_k|$ shown for various $|\vec{k}|$. Notice that the zero mode settles down to $\bar{\phi}_i \approx \theta/N_f$.

within the region where $\theta \neq 0$. We refer to this condensate as the nontrivial θ -vacua.

We should note that the $|\vec{k}| = 0$ mode is really only a quasi-zero mode as it is obtained in a finite spatial volume with periodic boundary conditions. However, the quasi-zero mode approaches the same value irrespective of the total spatial volume indicating that this really is a condensate. If it were not, we would expect the value of the coefficient to decrease when the volume of the system increases.

The evolution of the Fourier modes of the ϕ fields is shown in Figure 4.18 for the specific case of $\theta = 2\pi/16$ and a spatial grid of 10 fm on a side. The initial values of the ϕ fields were randomly chosen within the range $-7\pi/16$ to $7\pi/16$. The zero mode clearly settles down to a non-zero value. All higher momentum modes vanish extremely rapidly and are negligible long before the zero mode settles down to its equilibrium value.

The instantaneous distribution of Fourier modes for the evolution above is shown in Figure 4.19 at a few different times. This graph clearly shows the amplification of the zero mode as time increases. This phenomenon of coarsening and the formation of a

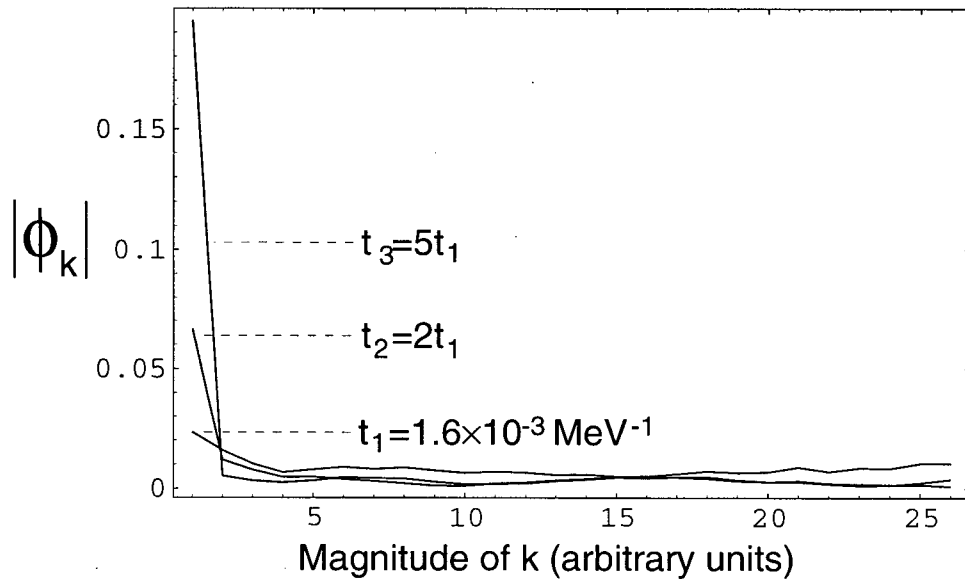


Figure 4.19: The Fourier distribution of the field is shown at three times within the first 1000 time steps of the evolution. The amplification of the zero mode demonstrates that the system exhibits the coarsening phenomenon.

nonperturbative condensate is very similar to earlier discussions in [52].

In Figure 4.20, $|\phi_k|$ is shown as a function of time for three different volumes. We chose $\theta = \pi/16$ and the volumes $(8 \text{ fm})^3$, $(16 \text{ fm})^3$, and $(32 \text{ fm})^3$. For each volume, we plotted the zero mode and the same non-zero mode. Notice that the zero mode is independent of the volume of the system, while the magnitude of the non-zero mode decreases with increasing volume. This is the signature that a real condensate has been formed.

For a total volume of $(10 \text{ fm})^3$ and $\theta = 2\pi/16$ the time for relaxation from the initial non-equilibrium state following the quench to the nontrivial θ -vacuum is approximately $10 \text{ fm}/c \approx 4 \times 10^{-23} \text{ s}$. This is of the same order of magnitude as the time which we might expect the central region of the fireball in a heavy ion collision to be isolated from the usual vacuum. In order to be able to observe a nontrivial θ -vacuum in a relativistic heavy ion collision, it must form before the protective shell breaks down.

As we have stated from the beginning, this is a simplified model. We have not

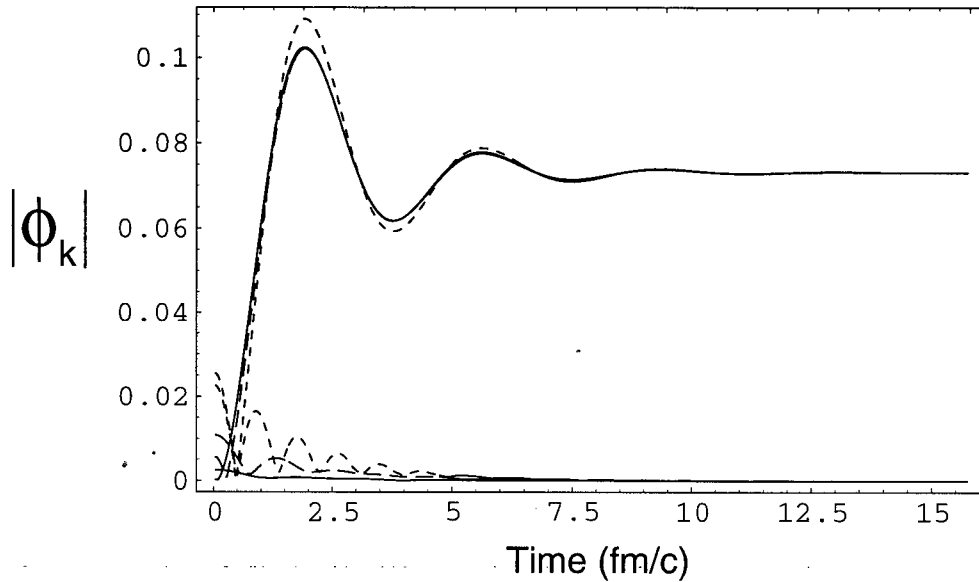


Figure 4.20: The zero mode and a non-zero mode are shown as a function of time for three different volumes. The heavily dashed line represents the smallest volume, the medium dashed line the middle volume, and the solid line represents the largest volume. This graph illustrates the volume independence of the zero mode.

attempted to correctly account for the collision geometry in heavy ion collisions since we have used a cubic lattice for our simulations. This fact is probably not relevant since the qualitative features of the behaviour are very robust under changes to the periodic lattice. This implies the behaviour is independent of the boundaries and as such would occur in any geometry. The volume we have used is just at the upper limit of what we would expect in heavy ion collisions at RHIC. Finally, we only included a phenomenological damping term. A complete calculation would have to include a better understanding of the effects of the expansion of the domain and emission of pions. However, our simplified calculation suggests the possibility of producing nontrivial θ -vacua in heavy ion collisions at RHIC.

The most natural question to ask at this point is: “If a nontrivial θ -vacuum state can be formed in heavy ion collisions on a time scale over which they might be observable,

how would we detect them?”. One of the first suggestions of how to detect them was that, due to the fact that the θ -vacua are odd under charge conjugation times parity (CP), their decay must produce some CP odd correlations suggested in [32]. However, one should expect that the signal will be considerably (if not completely) washed out by the re-scattering of the pions and their interactions in the final states, which mimic true CP-odd effects. In practice it is quite difficult to overcome the problem of separating a true CP violation from its simulation due to the final state interactions[56]. A more promising direction is to look at $\eta(\eta') \rightarrow \pi\pi$ decays[32, 57] which are strongly forbidden in our world, but nevertheless, will be of order one if $\theta \neq 0$ due to the presence of a scalar component in the pseudo-scalar mesons as discussed in Chapter 2. Calculations in [57] indicate that this effect could be quite noticeable and provide a definitive signature of a nontrivial θ -vacuum state. One could also look for electromagnetic decays of the pseudoscalar mesons which show the effects of shifted meson masses and lack of definite parity. This signature[57] might be easier to detect, as photons have a much better chance of penetrating the protective shell since they do not interact strongly. Finally, one could look for signatures related to the decay of the θ -vacuum state itself[57, 58]. These signatures range from production of axions to the enhancement of low energy photons and dileptons. The photons and dileptons could be produced indirectly, from the decay of the pseudoscalar mesons which are produced in predominantly low momentum modes or, directly, from the decay of an electromagnetic condensate coupled to the QCD condensate. In a recent paper[58] we obtained simple estimates for the π^0 , η and η' production in the decay of a θ -vacuum. These results show an amplification of production in the 10 MeV momentum range with many more η' mesons produced than either π^0 or η mesons. This would result in the enhancement of low energy dileptons which could possibly provide an explanation for the problem of the excess of low energy dileptons seen at CERN[59]. Indeed, it was shown in [60] that a sufficiently large enhancement of the

η' -production³ could easily explain the excess of dileptons seen at CERN. In summary, there are a number of different ways that nontrivial θ -vacuum states could be detected.

Therefore we have shown, through a numerical calculation of the zero temperature equations of motion with a non-zero induced θ parameter, that the chiral fields, ϕ , after a quench from high temperature go to a spatially constant non-zero value related to the θ -parameter. This occurs on a time scale of the order of 10^{-23} seconds. The fact that all other non-zero modes fall to negligible values long before, indicates that we have formed a condensate or a nontrivial θ -vacuum state. This prediction is testable in heavy ion collisions at RHIC.

³Note that the η' enhancement mechanism in [60] was very different from that described here.

Chapter 5

Conclusions

5.1 Results

The overall result of this thesis is a better understanding of the complexity of the QCD vacuum.

The θ -dependence of the vacuum energy has been clarified by analysis in the anomalous effective Lagrangian approach. The form of the effective potential in this approach simultaneously satisfies the naively contradictory requirements that the vacuum energy should depend only on the combination θ/N_c and should also be periodic in θ with period 2π . Furthermore, we have discussed the fact that the θ -vacuum energy is determined by a small parameter proportional to the quark mass m_q , which is similar to the disoriented chiral condensate. This is despite the fact that θ appears in the effective Lagrangian associated with a large parameter independent of m_q . This feature actually does not require the use of the anomalous effective Lagrangian we use, and is true for any effective chiral Lagrangian which respects the anomalous Ward Identities. This vacuum energy dependence is actually very significant to the possibility of production of nontrivial θ -vacua in heavy ion collisions. We have presented results related to the phenomenology of the pseudoscalar mesons in a nontrivial θ -vacuum. We obtained a generalisation of the η' mass formula expressed in terms of $\langle G^2 \rangle$ and $\langle \bar{\Psi}\Psi \rangle$ to non-zero θ . We obtained values for the masses in this model for the light neutral pseudoscalars for arbitrary values of θ . We obtained $\eta - \eta'$ and $\pi_0 - \eta - \eta'$ mixing angles for non-zero θ . Finally we showed

that for non-zero values of θ the pseudoscalar mesons cease to be pure pseudoscalars, but acquire scalar components. This θ -dependence of the phenomenology of the pseudoscalar mesons is particularly important to the detection of nontrivial θ -vacua.

Analysis of the vacuum structure of QCD in the anomalous effective Lagrangian approach leads to the realization that the vacuum structure may be very complex. The analysis shows the existence of metastable vacua (possibly a large number of them) for non-zero values of θ and the possible existence of metastable vacuum states even for $\theta = 0$. This is in agreement with the predictions of supersymmetric models. There is even the possibility of stable solitonic configurations between all the different vacuum states. All of these different vacuum configurations are potentially producible in relativistic heavy ion collisions and the increased understanding of the vacuum structure of QCD from this research will be crucial to their observation.

The decay rate for a single metastable vacuum for $\theta = 0$ to the true vacuum was calculated in both the low and high temperature limits. The results we obtained are given by Eqs. (3.119) and (3.147). These results are important for testing the theory in heavy ion collisions. In addition, the method used in these calculations represents a new approach that could be useful in other calculations of this type.

The final results we have obtained concern the formation of nontrivial θ -vacua in heavy ion collisions. Our numerical results in a simplified model suggest that a nontrivial θ -vacuum will likely be formed in heavy ion collisions. We also calculated a formation time of about 10^{-23} seconds, which is short enough that this nontrivial θ -vacuum state could be formed inside the shell of hot debris before the shell breaks down, while the interior region is still isolated from the exterior vacuum. This means that it may be possible to detect the nontrivial θ -vacua in heavy ion collisions.

As has been emphasised so far in this conclusion, all of the results of this thesis could be testable in and have important implications for the physics of heavy ion collisions.

The even more exciting implication of this fact is that we may have the opportunity to study the physics of the early universe at the time of the QCD phase transition in experiments at RHIC in the near future. The presence of nontrivial vacuum structure could have important implications for this epoch in the evolution of the early universe[13, 14, 15, 16, 17, 18].

5.2 Future Research

There are many possible areas of future research which expand upon the results of this thesis.

There are many methods by which the masses and the mixing angles of the pseudoscalar mesons we obtained could be altered. For instance, perturbative corrections to the mass matrix could have quite a significant effect on these values. The inclusion in the effective Lagrangian of terms of higher order in the quark mass would also lead to corrections. These corrections are expected to be quite small and are less important than perturbative corrections. It might be useful to determine how these corrections would affect these values and if they could bring about better agreement with measured masses.

As was mentioned above, the method used in the calculation of the decay rate of the false vacuum in Chapter 3 represents a new approach. The method could be applied to other decay problems already analysed using different techniques to test their agreement. As well, there is currently interest in other types of domain walls in low energy QCD for which these techniques might be well suited.

The inclusion of heavy degrees of freedom in the calculation of the false vacuum decay would be highly desirable for a complete understanding of the decay process. The inclusion of nucleons or heavy intrinsic degrees of freedom (glueballs) could have a significant effect on the decay rate of the false vacuum. Unfortunately, it is not clear

at present how to include these effects and whether they would complicate the problem beyond the hope of a solution.

The chiral false vacua at $\theta = 0$ studied in Chapter 3 was only the most simple of the possible metastable vacua of this type. For $q = 8$ there are three other metastable vacua that one could study. As well, there is the added possibility of metastable solitonic configurations that interpolate between different vacua. All of these different vacuum states are potentially producible in heavy ion collisions and could have implications for the study of the development of the early universe.

As was stated in Chapter 4, the numerical calculation presented there was done in a simplified model system. While the results are certainly important, it would be more satisfying to do the calculation in a more realistic model. The cubic lattice that we studied is highly unrealistic as the reaction volume in a heavy ion collision is shaped more like an elongated ellipsoid. The qualitative result of the formation of the condensate is almost certainly unaffected by the shape of the lattice. It is unlikely that the formation time of the condensate would be affected by the shape of the lattice but definitely possible. It would be useful to attempt to repeat this calculation taking into account the collision geometry and compare the results with those shown in this thesis.

A potentially important improvement to this simple model would be developing a more physically motivated understanding of the way in which the system is damped. We have included the effects of expansion of the domain and emission of pions in a very simple phenomenological damping term. Better understanding of how these processes would affect the dynamics will almost certainly be important in determining the formation time of, and thus the likelihood of observing, nontrivial θ -vacua in heavy ion collisions.

Another important area where more research is required is in the area of determining experimental signatures of the nontrivial vacuum structure. There have been a number of ideas put forward about how we might detect nontrivial θ -vacua[32, 57, 58]. These ideas

must be studied in more detail and used to derive testable predictions for experimentalists at RHIC to measure. As well, it has been suggested that some of these signatures[57, 58] may already be present in existing data for lower energy heavy ion collisions performed at CERN[59]. Demonstration of this claim would certainly provide further impetus for research in this area. In particular, in a recent paper[58], we have obtained simple estimates for the π^0 , η and η' production in the decay of a θ -vacuum state which show enhancement in the 10 MeV momentum range with many more η' 's produced than π^0 's or η 's. This would result in an enhancement of low energy dileptons would could explain the excess of low energy dileptons seen at CERN[59]. In fact, it has already been shown in [60] that a sufficiently large enhancement of the η' production¹ could easily explain the excess of dileptons seen at CERN.

¹Note that the η' enhancement mechanism in [60] was very different from that described here.

Bibliography

- [1] J. Donoghue, E. Golowich and B. Holstein, **Dynamics of the Standard Model** Cambridge University Press (1992).
- [2] P. Harris, *et al*, Phys. Rev. Lett. **82** (1999) 904.
K. Smith, *et al*, Phys. Lett. **B234** (1990) 191.
- [3] B. Borasoy, Phys. Rev. **D61** (2000) 114017, hep-ph/0004011.
R. Crewther, P. Di Vecchia, G. Veneziano and E. Witten, Phys. Lett. **B88** (1979) 123.
- [4] R. Peccei and H. Quinn, Phys. Rev. Lett. **38** (1977) 1440; Phys. Rev. **D16** (1977) 1791.
S. Weinberg, Phys. Rev. Lett. **40** (1978) 223.
F. Wilczek, Phys. Rev. Lett. **40** (1978) 279.
- [5] G. Veneziano and S. Yankielowicz, Phys. Lett. **B113** (1982) 231.
- [6] T. Taylor, G. Veneziano and S. Yankielowicz, Nucl. Phys. **B218** (1983) 439.
- [7] I. Halperin and A. Zhitnitsky, Phys. Rev. **D58** (1998) 054016.
- [8] I. Halperin and A. Zhitnitsky, Phys. Rev. Lett. **81** (1998) 4071, hep-ph/9803301.
- [9] T. Fugleberg, I. Halperin, and A. Zhitnitsky, Phys. Rev. **D59** (1999) 074023.
- [10] E. Witten, Ann. Phys. **128** (1980) 363.
P. Vecchia and G. Veneziano, Nucl. Phys. **B171** (1980) 253.
- [11] E. Witten, Phys. Rev. Lett. **81** (1998) 2862.
- [12] M. Shifman, Prog. Part. Nucl. Phys. 39 (1997) 1, hep-th/9704114.
- [13] J. E. Kim, Phys. Rep. **150** (1987) 1.
P. Sikivie, "Dark matter axions '96" (1996) hep-ph/9611339.
E. Shellard and R. Battye, Phys. Rept. **307** (1998) 227, astro-ph/9808220.
E. Shellard and R. Battye, "Cosmic Axions" (1998) astro-ph/9802216.

- [14] S. Banerjee, *et al*, "The Cosmological Quark-Hadron Transition and Massive Compact Halo Objects" (2000) astro-ph/0002007.
N. Borghini, W. Cottingham and R. Vinh Mau, J. Phys. **G26** (2000) 771, hep-ph/0001284.
A. Bhattacharyya, *et al*, Nucl. Phys. **A661** (1999) 629, hep-ph/9907262.
H. Kim, B.H. Lee and C. H. Lee, "Relics of Cosmological Quark-Hadron Phase Transition" (1999) astro-ph/9901286.
E. Witten, Phys. Rev. **D30** (1984) 272.
and references therein.
- [15] R. Brandenberger, I. Halperin and A. Zhitnitsky, "Baryogenesis at the QCD Scale", hep-ph/9903318, based on a plenary talk by R.B. at SEWM-98 and an invited talk by A.Z. at COSMO-98, published in the proceedings of SEWM-98.
- [16] S. Nayak and U. Yajnik, "Baryogenesis through Axion Domain Wall" (2000), hep-ph/0002219.
- [17] M. Forbes and A. Zhitnitsky, "Primordial galactic magnetic fields from axion domain walls at the QCD phase transition", hep-ph/0004051.
- [18] G. Fuller, G. Mathews and C. Alcock, Phys. Rev. **D37** (1988) 1380.
D. Enström, "Gamma-Ray Bursts and Dark Matter - A Joint Origin?" (1998) hep-ph/9810335.
B. Kämpfer, Annalen Phys. **9** (2000) 1.
A. Coley and T. Trappenberg, Phys. Rev. **D50** (1994) 4881.
M. Hindmarsh, Phys. Rev. **D45** (1992) 1130.
- [19] G. Veneziano, Nucl. Phys. **B159** (1979) 213.
- [20] V.A. Novikov, M.A. Shifman, A.I. Vainshtein and V.I. Zakharov, Nucl. Phys. **B191** (1981) 301.
- [21] I. Halperin and A. Zhitnitsky, Mod. Phys. Lett. **A13** (1998) 1955, hep-ph/9707286.
- [22] D.E. Groom, *et al*, The European Physical Journal **C15** (2000) 1.
- [23] A. Kovner and M. Shifman, Phys. Rev. **D56** (1997) 23961, hep-th/9702174.
- [24] R. Dashen, Phys. Rev. **D3** (1971) 1879.
- [25] A. Smilga, Phys. Rev. **D59** (1999) 114021, hep-ph/9805214.
- [26] E. Witten, Nucl. Phys. **B156** (1979) 269.
G. Veneziano, Nucl. Phys. **B159** (1979) 213.

- [27] F-G. Cao and A. I. Signal, Phys. Rev. **D60** (1999) 114012, hep-ph/9908481.
L. Burakovsky and T. Goldman, Phys. Lett. **B427** (1998) 361, hep-ph/9802404.
T. Feldmann and P. Kroll, Phys. Rev. **D58** (1998) 114006, hep-ph/9802409.
E.P. Venugopal and B. R. Holstein, Phys. Rev. **D57** (1998) 4397, hep-ph/9710382.
and references therein.
- [28] H. Goldstein, **Classical Mechanics**, Addison-Wesley Publishing Co. (1980) 143.
- [29] Z. Huang, K.S. Viswanathan and D.-d. Wu, Mod. Phys. Lett. **A7** (1992) 3147.
- [30] T. Fugleberg, "False Vacuum Decay in QCD within an Effective Lagrangian Approach", hep-ph/9906430.
- [31] M. Shifman, Phys. Rev. **D59** (1999) 021501.
- [32] D. Kharzeev, R.D. Pisarski, and M. Tytgat, Phys. Rev. Lett. **81** (1998) 512.
D. Kharzeev, R.D. Pisarski, Phys. Rev. **D61** (2000) 111901, hep-ph/9906401.
- [33] W. Cottingham, D. Kalafatis and R. Vinh Mau, Phys. Rev **B48** (1993) 6788.
- [34] J. Baacke and V.G. Kiselev, Phys. Rev. **D48** (1993) 5648.
- [35] J. Baacke, Phys. Rev. **D52** (1995) 6760.
- [36] A. Strumia and N. Tetradis, Nucl. Phys. **B542** (1999) 719.
- [37] J. Baacke and A. Surig, Z. Phys. **C73** (1997) 369.
- [38] L. Carson, X. Li, L. McLerran and R.T. Wang, Phys. Rev. **D42** (1990) 2127.
- [39] M.B. Voloshin, I. Yu. Kobzarev and L.B. Okun, Sov. J. Nucl. Phys. **20** (1975) 644.
S. Coleman, Phys. Rev. **D15** (1977) 2929.
- [40] I. Kogan, A. Kovner and M. Shifman, Phys. Rev. **D57** (1998) 5195.
- [41] A. Linde, Phys. Lett. **B100** (1981) 37.
A. Linde, Nuc. Phys. **B216** (1983) 421.
- [42] I. Affleck, Phys. Rev. Lett. **46** (1981) 388.
- [43] C. Callan and S. Coleman, Phys. Rev. **D16** (1977) 1762.
- [44] A. Vainshtein, V. Zakharov, V. Novikov and M. Shifman, Sov. Phys. Usp. **25(4)**
(1982) 195.
- [45] K. Kiers and M. Tytgat, Phys. Rev. **D57** (1998) 5970, hep-ph/9807412.

- [46] S. Coleman, *The Uses of Instantons in Aspects of Symmetry*, Cambridge University Press (1985).
- [47] S. Coleman, V. Glaser and A. Martin, *Comm. Math. Phys.* **58** (1978) 211.
- [48] K. Buckley, T. Fugleberg and A. Zhitnitsky, *Phys. Rev. Lett.* **84** (2000) 4814, hep-ph/9910229.
- [49] A.A. Anselm and M.G. Ryskin, *Phys. Lett.* **B266** (1991) 482.
J.-P. Blaizot, A. Krzywicki, *Phys. Rev.* **D46** (1992) 246.
J. Bjorken, *Int. J. Mod. Phys.* **A7** (1992) 561.
- [50] K. Rajagopal and F. Wilczek, *Nucl. Phys.* **B404** (1993) 577.
- [51] K. Rajagopal, "The Chiral Phase Transition in QCD: Critical Phenomena and Long Wavelength Pion Oscillations", in **Quark Gluon Plasma 2** edited by R. Hwa, World Scientific (1995), hep-ph/9504310.
- [52] D. Boyanovsky and H.J. de Vega, "Dynamics of Symmetry Breaking Out of Equilibrium: From Condensed Matter to QCD and the Early Universe" in ANSI-2000 published by the National Academy of Sciences of India, hep-ph/9909372.
- [53] I. Halperin and A. Zhitnitsky, *Phys. Lett.* **B440** (1998) 77.
- [54] R. Burden and J. Faires, **Numerical Analysis**, PWS-KENT Publishing Co. (1989) 257.
- [55] W. Press, S. Teukolsky, W. Vetterling and B. Flannery, **Numerical Recipes in C**, Cambridge University Press (1992).
- [56] R. Peccei, "CP Violation: A Theoretical Review", hep-ph/9508389; "Overview of Kaon Physics" published in the Proceedings of Kaon99, hep-ph/9909236.
- [57] A. Zhitnitsky, "Signatures of the Induced Θ vacuum state in Heavy Ion Collisions", hep-ph/0003191.
- [58] K. Buckley, T. Fugleberg and A. Zhitnitsky, "Induced theta-vacuum states in heavy ion collisions: A possible signature", hep-ph/0006057.
- [59] G. Agakichiev *et al*, CERES collaboration, *Phys. Rev. Lett.* **75** (1995) 1272.
N. Masera for the HELIOS-3 collaboration, *Nucl. Phys.* **A 590** (1995) 93c.
- [60] J. Kapusta, D. Kharzeev and L. McLerran, *Phys. Rev.* **D53** (1996) 5028, hep-ph/9507343.

- [61] C. Callan, R. Dashen and D. Gross, Phys. Lett. **B63** (1976) 172.
R. Jackiw and C. Rebbi, Phys. Rev. Lett. **37** (1976) 172.
- [62] F. Sannino and J. Schechter, Phys. Rev. **D57** (1998) 170, hep-th/9708113.
- [63] J. H. Kühn and V.I. Zakharov, Phys. Lett. **B252** (1990) 615.
- [64] I. Halperin and A. Zhitnitsky, Nucl. Phys. **B539** (1999) 166, hep-th/9802095.
- [65] K. Intriligator, R.G. Leigh, and N. Seiberg, Phys. Rev. **D50** (1994) 1092.
K. Intriligator, Phys. Lett. **B336** (1994) 409.
- [66] K. Intriligator and N. Seiberg, Nucl. Phys. Proc. Suppl. **45BC** (1996) 1, hep-th/9509066.

Appendix A

Derivation of the Effective Potential for QCD

The purpose of this appendix is to review the details of the derivation of the Effective Potential for the light fields in QCD. The first section reviews the derivation. The second section discusses some methods of determining two unknown parameters, p and q , of the Lagrangian.

A.1 Anomalous Effective Lagrangian for QCD

The derivation of the anomalous effective Lagrangian was originally presented in [8]. It relies heavily on the derivation of the anomalous effective Lagrangian for Yang Mills theory[7].

The Anomalous Effective Lagrangian is defined as the Legendre transform of the generating functional for zero momentum correlation functions. In Yang Mills theory the relevant operators are the $G_{\mu\nu}\tilde{G}_{\mu\nu}$ (topological density operator) and $G^2 \equiv G_{\mu\nu}G_{\mu\nu}$ (gluon scalar current). The correlation functions of these operators are fixed in terms of the gluon condensate: $\langle\alpha_s/\pi G^2\rangle$ [20, 21]. Actually only the potential part of this Lagrangian can be constructed as this is the only part that can be fixed by the Low Energy Theorems. This effective Lagrangian, while not useful for calculating the S-matrix, is just what we need to study the vacuum properties.

Construction of the effective Lagrangian is considerably simplified by defining new

complex fields, H and \bar{H} , which are linear combinations of the relevant operators:

$$H = \frac{1}{2} \left(\frac{\beta(\alpha_s)}{4\alpha_s} G^2 + i \frac{1}{\xi_{YM}} \frac{\alpha_s}{4\pi} G\tilde{G} \right), \quad \bar{H} = \frac{1}{2} \left(\frac{\beta(\alpha_s)}{4\alpha_s} G^2 - i \frac{1}{\xi_{YM}} \frac{\alpha_s}{4\pi} G\tilde{G} \right), \quad (\text{A.155})$$

where $\beta(\alpha_s) = -b_{YM}\alpha_s^2/(2\pi) + O(\alpha_s^3)$ is the Gell-Mann - Low β -function for gluodynamics¹ and the first coefficient of the β -function is given by $b_{YM} = (11/3)N_c$. ξ_{YM} is a generally unknown parameter which parameterises the correlation function of the topological density:

$$\lim_{q \rightarrow 0} i \int dx e^{iqx} \langle 0 | T \left\{ \frac{\alpha_s}{8\pi} G\tilde{G}(x) \frac{\alpha_s}{8\pi} G\tilde{G}(0) \right\} | 0 \rangle_{YM} = \xi_{YM}^2 \left\langle \frac{\beta(\alpha_s)}{4\alpha_s} G^2 \right\rangle_{YM}. \quad (\text{A.156})$$

The reason for using these composite fields has to do with the holomorphic structure of zero momentum correlation functions:

$$\begin{aligned} \lim_{q \rightarrow 0} i \int dx e^{iqx} \langle 0 | T \{ H(x) H(0) \} | 0 \rangle &= -4 \langle H \rangle, \\ \lim_{q \rightarrow 0} i \int dx e^{iqx} \langle 0 | T \{ \bar{H}(x) \bar{H}(0) \} | 0 \rangle &= -4 \langle \bar{H} \rangle, \\ \lim_{q \rightarrow 0} i \int dx e^{iqx} \langle 0 | T \{ \bar{H}(x) H(0) \} | 0 \rangle &= 0, \end{aligned} \quad (\text{A.157})$$

where the dimensional transmutation formula:

$$\left\langle -\frac{b\alpha_s}{8\pi} G^2 \right\rangle = \text{const} \left[M_R \exp \left(-\frac{8\pi^2}{bg_0^2} \right) \right]^4, \quad (\text{A.158})$$

which comes from renormalisation group arguments, has been used. Holomorphy is analyticity of functions of complex variables. Holomorphy requires that a function of a complex variable, z , have independent functional dependence on z and z^* . We can immediately see that the fields H and \bar{H} decouple in the low energy theorems. This approach is motivated by fact that holomorphy is an exact property of the effective superpotential in the supersymmetric case. These details are mentioned here for completeness

¹In [9] the one-loop β -function was used but most of the discussion is formally correct keeping the full β -function.

and have some relevance to details discussed in the next section but are not essential for the understanding.

It can be seen that the n -point zero momentum correlation function of the operator H equals $(-4)^{n-1}\langle H \rangle$. Multi-point correlation functions of the operator \bar{H} are analogously expressed in terms of its vacuum expectation value $\langle \bar{H} \rangle$. At the same time, it is easy to check that the decoupling of the fields H and \bar{H} holds for arbitrary n -point functions of H and \bar{H} .

The goal of the construction is an effective Lagrangian that reproduces at tree level all the Low Energy Theorems for the composite fields H and \bar{H} . Consider the generating functional of connected Green functions with sources J and \bar{J} ²:

$$\exp [iW(J, \bar{J})] = \sum_{n' \in \mathcal{Z}} \int \mathcal{D}A \exp \left[\frac{i}{4g^2} \int dx G^2 + i \frac{\theta + 2\pi n'}{32\pi^2} \int dx G \tilde{G} + iJ \int dx H + i\bar{J} \int dx \bar{H} \right]. \quad (\text{A.159})$$

where A are the gauge fields in terms of which G is defined. Effective zero momentum fields, h and \bar{h} , are defined as:

$$\int dx h = \frac{dW}{dJ}, \quad \int dx \bar{h} = \frac{dW}{d\bar{J}}, \quad (\text{A.160})$$

which satisfy the equation:

$$\int dx h = \langle \int dx H \rangle, \quad \int dx \bar{h} = \langle \int dx \bar{H} \rangle. \quad (\text{A.161})$$

The effective action $\Gamma(h, \bar{h})$ is defined as the Legendre transformation of the generating functional $W(J, \bar{J})$:

$$\Gamma(h, \bar{h}) = -W(J, \bar{J}) + \int dx Jh + \int dx \bar{J}\bar{h}. \quad (\text{A.162})$$

²Note the summation over the integer, n' , which automatically ensures the 2π periodicity in θ and quantisation of topological charge. It is completely equivalent to the way that the vacuum angle, θ , originally appeared in YM theory[61].

The definition of generating functional (A.159), the Low Energy Theorems (A.157), and their extensions to arbitrary n-point functions can be combined to obtain the following set of equations for $W(J, \bar{J})$:

$$\begin{aligned} \frac{\partial^{n+1}}{\partial J^{n+1}} W|_{J=\bar{J}=0} &= i^n \int dx dx_1 \dots dx_n \langle T \{ H(x_1) \dots H(x_n) H(0) \} \rangle = (-4)^n \int dx \langle H \rangle, \\ \frac{\partial^{n+1}}{\partial \bar{J}^{n+1}} W|_{J=\bar{J}=0} &= i^n \int dx dx_1 \dots dx_n \langle T \{ \bar{H}(x_1) \dots \bar{H}(x_n) \bar{H}(0) \} \rangle = (-4)^n \int dx \langle \bar{H} \rangle, \\ \frac{\partial^{k+l}}{\partial J^k \partial \bar{J}^l} W|_{J=\bar{J}=0} &= 0. \end{aligned} \quad (\text{A.163})$$

The solution to these equations is:

$$W(J, \bar{J}) = -\frac{1}{4} \int dx \langle H \rangle e^{-4J} - \frac{1}{4} \int dx \langle \bar{H} \rangle e^{-4\bar{J}}, \quad (\text{A.164})$$

which substituted into (A.160) and solving for J, \bar{J} gives:

$$J = -\frac{1}{4} \log \left(\frac{h}{\langle H \rangle} \right), \quad \bar{J} = -\frac{1}{4} \log \left(\frac{\bar{h}}{\langle \bar{H} \rangle} \right). \quad (\text{A.165})$$

These expressions can then be substituted back into equation (A.164) to obtain W as a function of h, \bar{h} . The definition of Γ (A.162) now becomes a differential equation for the effective potential, $U(h, \bar{h}) \equiv -(1/V)\Gamma(h, \bar{h})$:

$$U - h \frac{\partial U}{\partial h} - \bar{h} \frac{\partial U}{\partial \bar{h}} = -\frac{1}{4}(h + \bar{h}). \quad (\text{A.166})$$

One solution to this equation is:

$$U_1(h, \bar{h}) = \frac{1}{4} h \log \frac{h}{C} + \frac{1}{4} \bar{h} \log \frac{\bar{h}}{\bar{C}} + D(h - \bar{h}), \quad (\text{A.167})$$

where C, \bar{C} and D are arbitrary constants. This function is not bounded from below and for complex argument is not single valued because of the branches of the logarithm. When dealing with the Veneziano-Yankielowicz effective Lagrangian [5] this problem was dealt with by summing over the branches of the logarithm [23]. In this case there exists yet another solution:

$$U_2(h, \bar{h}) = \frac{1}{4\alpha} h \log \left(\frac{h}{C} \right)^\alpha + \frac{1}{4\alpha} \bar{h} \log \left(\frac{\bar{h}}{\bar{C}} \right)^\alpha + D(h - \bar{h}), \quad (\text{A.168})$$

where α is an arbitrary real number. We consider the specific case:

$$U_3(h, \bar{h}) = \frac{1}{4}h \operatorname{Log} \frac{h}{C} + \frac{1}{4}\bar{h} \operatorname{Log} \frac{\bar{h}}{\bar{C}} + \frac{i\pi}{2} \left(k + n \frac{q}{p} \right) (h - \bar{h}), \quad (\text{A.169})$$

where Log stands for the principal branch of the logarithm, p and q ($p/q \equiv \alpha$) are relatively prime integers and n and k are integers in the ranges $n = 0, \pm 1 \dots$ and $k = 0, 1, \dots, q - 1$. This is the form of the function that will allow both the θ/N dependence and 2π periodicity discussed in Chapter 2. Therefore this is a natural place to discuss the introduction of the θ -parameter into the effective Lagrangian.

The form of the generating functional (A.159) contains an infinite sum over an integer parameter, n' , which enters in the combination $\theta + 2\pi n'$. The only term in Eq. (A.169) which can accommodate the θ -parameter in this form is the last since n runs over all integers and the θ -parameter is introduced in the combination: $\theta + 2\pi n$.

The final answer for the improved effective potential $W(h, \bar{h})$ (here “improved” refers to the necessity of summation over the integers n, k in Eq.(A.170), see below) reads[7]:

$$\begin{aligned} e^{-iVW(h, \bar{h})} &= \sum_{n=-\infty}^{+\infty} \sum_{k=0}^{q-1} \exp \left\{ -\frac{iV}{4} \left(h \operatorname{Log} \frac{h}{C_{\text{YM}}} + \bar{h} \operatorname{Log} \frac{\bar{h}}{\bar{C}_{\text{YM}}} \right) \right. \\ &\quad \left. + i\pi V \left(k + \frac{q}{p} \frac{\theta + 2\pi n}{2\pi} \right) \frac{h - \bar{h}}{2i} \right\}, \end{aligned} \quad (\text{A.170})$$

where the constants $C_{\text{YM}}, \bar{C}_{\text{YM}}$ can be taken to be real and expressed in terms of the vacuum energy in YM theory at $\theta = 0$, $C_{\text{YM}} = \bar{C}_{\text{YM}} = -2eE_v^{(\text{YM})}(0) = -2e\langle -b_{\text{YM}}\alpha_s/(32\pi)G^2 \rangle$, and V is the 4-volume. The integer numbers p and q are relatively prime and related to the parameter ξ introduced in Eq.(A.156): $q/p = 2\xi$. Thus, we expect that the parameter ξ defined in Equations(A.155), (A.156) is a rational number. This expectation is motivated by the fact that it turns out to be the case in all existing proposals to fix the value of ξ , to be discussed in the next section, and by experience with supersymmetric models. (In all likelihood, irrational values of ξ would produce a non-differentiable θ dependence for YM theory.) On general grounds, it follows that $p = \mathcal{O}(N_c)$ and $q = \mathcal{O}(N_c^0) = \mathcal{O}(1)$.

Now this result needs to be generalised to the case of full QCD with N_f light flavours and N_c colours. In the effective Lagrangian approach the light³ matter fields are described by the unitary matrix, U_{ij} , corresponding to the phases of the chiral condensate:

$$\langle \bar{\Psi}_L^i \Psi_R^j \rangle = -|\langle \bar{\Psi}_L \Psi_R \rangle| U_{ij}, \quad (\text{A.171})$$

with⁴:

$$U = \exp \left[i\sqrt{2} \frac{\pi^a \lambda^a}{f_\pi} + i \frac{2}{\sqrt{N_f}} \frac{\eta'}{f_{\eta'}} \right], \quad UU^\dagger = 1, \quad (\text{A.172})$$

where λ^a are the Gell-Mann matrices of $SU(N_f)$, π^a is the octet of pseudoscalar fields (pions, kaons and the eta meson), η' is the $SU(N_f)$ singlet pseudoscalar field (meson) and N_f is the number of quark flavours. We use the values $f_\pi = 132 \text{ MeV}$ [22] and $f_{\eta'} = 86 \text{ MeV}$ [20] for the meson decay constants⁵. The indices, i and j , of U_{ij} run over the quark flavor index, $i, j = 1 \dots N_f$, which correspond to the quark flavours up(u), down(d) and strange(s), respectively. As is well known, the effective potential for the U field is uniquely determined by the chiral anomaly and amounts to the substitution:

$$\theta \rightarrow \theta - i \text{Tr}(\log U), \quad (\text{A.173})$$

where Tr refers to the trace of the matrix. In the sense of anomalous conformal Ward Identities [20], QCD reduces to pure Yang-Mills theory with the substitutions $\langle G^2 \rangle_{QCD} \rightarrow \langle G^2 \rangle_{YM}$ and $b \equiv b_{QCD} \rightarrow b_{YM}$. Analogously, an effective Lagrangian for QCD should transform to that of pure Yang-Mills theory when the chiral fields, U , are “frozen”. Therefore the effective potential for QCD is given by:

$$e^{-iV^W(h,U)} = \sum_{n=-\infty}^{+\infty} \sum_{k=0}^{q-1} \exp \left\{ -\frac{iV}{4} \left(h \text{Log} \frac{h}{2eE} + \bar{h} \text{Log} \frac{\bar{h}}{2eE} \right) + i\pi V \left(k + \frac{q}{p} \frac{\theta - i \log \det U + 2\pi n}{2\pi} \right) \frac{h - \bar{h}}{2i} + \frac{i}{2} V \text{Tr}(MU + \text{h.c.}) \right\}, \quad (\text{A.174})$$

³Note that the η' is not really very light, but it enters the theory in this way.

⁴Note that mixing of the flavor eigenstates is ignored at this level.

⁵It should be noted that what we refer to as $f_\pi/\sqrt{2}$ is sometimes denoted f_π in the literature. As well, what we refer to as $f_{\eta'}$, is $f_{\eta'}/\sqrt{3}$ in the notation of [20].

where $M = \text{diag}(m_i |\langle \bar{\Psi}^i \Psi^i \rangle|)$, $E = \langle b \alpha_s / (32\pi) G^2 \rangle$, V is the 4-volume and the integers p and q are relatively prime and related to the parameter ξ from (A.155)(A.156) by $q/p = 2\xi$. The physical inputs to this equation are the values of the vacuum condensates $\langle \alpha_s / \pi G^2 \rangle = 0.012 \text{ GeV}^4$, $\langle \bar{\Psi}^u \Psi^u \rangle = \langle \bar{\Psi}^d \Psi^d \rangle = -(240 \text{ MeV})^3$ and $\langle \bar{\Psi}^s \Psi^s \rangle = -0.8 (240 \text{ MeV})^3$, and the quark masses (m_u , m_d and m_s).

As mentioned above, the sum over k prevents an ambiguity due to the multi-valued nature of the log function by summing over all branches of the effective potential[23][8]. The sum over n is the summation over all integer topological charges. The values of the parameters p and q are not definitely known as different proposals for their determining lead to different values which we will discuss in the next section. Wherever possible we will leave the values of p and q arbitrary but we should note that specific results in Chapter 3 use the the values $p = 11N_c - 2N_f$ and $q = 8$ and the whole basis of the false vacuum decay in that chapter requires $q \neq 1$. The numerical results in Chapter 4 use the values $p = N_c$ and $q = 1$ but the theory of that chapter is valid for arbitrary p and q .

Integrating out the heavy “glueball” fields, h and \bar{h} , by minimising the effective potential with respect to these variables one obtains the effective potential for the light chiral fields U and \bar{U} ⁶:

$$W_{eff}(U, U^+) = - \lim_{V \rightarrow \infty} \frac{1}{V} \log \left\{ \sum_{l=0}^{p-1} \exp \left[VE \cos \left[-\frac{q}{p} (\theta - i \log \text{Det } U) + \frac{2\pi}{p} l \right] + \frac{1}{2} V \text{Tr}(MU + M^+ U^+) \right] \right\}, \text{(A.175)}$$

which is Eq.(2.29) and the starting point of all the research presented in this thesis.

One should note that most of the results of Chapters 2 and 4 are not sensitive to the specific functional form of the $\cos[-q/p(\theta - i \log \text{Det } U)]$ term in the effective potential.

⁶Note that the summation variable k in (A.174) has been renamed l in this formula.

However, the requirement of Veneziano [19] for the resolution of the $U(1)$ problem:

$$\left. \frac{\partial^{2k} E_{vac}(\theta)}{\partial \theta^{2k}} \right|_{\theta=0} \sim \int \prod_{i=1}^{2k} dx_i \langle G\tilde{G}(x_1) \dots G\tilde{G}(x_{2k}) \rangle \sim \left(\frac{1}{N_c} \right)^{2k} \quad (\text{A.176})$$

supports the $\cos(\theta/N_c)$ behaviour of the potential.

The next section will discuss the values of the integer parameters p and q .

A.2 Determining the values of p and q

In the previous section we saw the anomalous effective potential depends on the integer parameters $p = \mathcal{O}(N_c)$ and $q = \mathcal{O}(N_c^0) = \mathcal{O}(1)$. There are different approaches to the fixing of these parameters that lead to very different vacuum structure. I will discuss the physical implications of these parameters and mention some of the different proposals for fixing their values.

The parameter ' p ' is the number of branches of the effective potential. It also corresponds to the number of distinct vacua before the infinite volume limit is taken. The parameter ' q ' determines the number of distinct vacua with different energies that exist before the infinite volume limit is taken. For q even there are $(q+2)/2$ different energy vacua; for q odd there are $(q+1)/2$ different energy vacua. For $q=1$ all of the p vacua are degenerate in energy. The parameter ' q ' is also the number of physically distinct vacua that exist at $\theta=0$ in the infinite volume limit.

It can be shown that the vacuum energy of the θ -vacuum has the following form:

$$E_v(\theta) \equiv \langle \theta | -\frac{b\alpha_s}{32\pi} G^2 | \theta \rangle = \langle 0 | -\frac{b\alpha_s}{32\pi} G^2 | 0 \rangle \cos(2\xi\theta) = -|E_v| \cos(2\xi\theta), \quad (\text{A.177})$$

where the ξ is a parameter from the following low energy theorem:

$$\lim_{q \rightarrow 0} i \int dx e^{iqx} \langle 0 | T \left\{ \frac{\alpha_s}{8\pi} G\tilde{G}(x) \frac{\alpha_s}{8\pi} G\tilde{G}(0) \right\} | 0 \rangle = \xi^2 \left\langle \frac{\beta(\alpha_s)}{4\alpha_s} G^2 \right\rangle. \quad (\text{A.178})$$

Comparing equation (A.177) with (2.31) for $\phi_i = 0$ and $l = 0$ we identify $2\xi = q/p$. Further, Equation (A.177) can only have 2π periodicity if θ is a rational number. Therefore restriction to q and p relatively prime integers is physically motivated.

The first method of fixing the values of p and q comes from a self duality hypothesis in [20] where it was suggested that gluodynamics should be a holomorphic in the composite operators: $G^2 \pm iG\tilde{G}$. Comparing with (A.155) and using $\beta(\alpha_s) = -b_{YM}\alpha_s^2/(2\pi)$, the Gell-Mann Low β -function for gluodynamics with $b_{YM} = (11/3)N_c$, we find that this corresponds to $q/p = 2\xi = 12/11N_c$.

The second approach is based on the analysis of softly broken supersymmetric theories by counting the number of degenerate vacua. A detailed discussion in the case of pure gluodynamics is given in [12]. The gluino condensate is given by: $\langle\lambda\lambda\rangle = \exp(i\theta/N_c + 2\pi k/N_c)$, $k = 0, \dots, N_c - 1$; this corresponds to N_c degenerate vacua. This sets the value of 'p' at N_c . The vacua are all degenerate which sets the value of 'q' at 1. The problem with this approach is that it is only valid when the gluon mass, $m_g \ll \Lambda_{SYM}$ where Λ_{SYM} is the dynamical mass scale; pure gluodynamics corresponds to the opposite limit, $m_g \gg \Lambda_{SYM}$. We should also mention that a non-standard non-soft supersymmetric breaking approach [62] leads to the value $p = 11N_c$.

Another approach was motivated by a suggestion in [63] that in QCD with massless quarks, nonperturbative matrix elements should be holomorphic in the Pauli Villars fermion mass, M_R . Assuming this holomorphy, they relate the proton matrix element of the topological density $\langle p|G\tilde{G}|p\rangle$ with the corresponding matrix element for the gluon scalar current $\langle p|G^2|p\rangle$. A similar approach was used in [21] for pure gluodynamics to relate the zero momentum two-point functions of $G\tilde{G}$ and G^2 . Pure gluodynamics was considered as the low energy limit of a theory including a heavy quark and holomorphy in the physical quark mass was argued to hold in the $m_q \rightarrow \infty$ limit. Holomorphy requires the values $p = 3b_{YM} = 11N_c$ and $q = 8$.

An inverse route was used in [64] to determine ‘ p ’ and ‘ q ’. This approach again relies on the fact that holomorphy of pure gluodynamics can be clarified by coupling it to a heavy fermion as in the previous method. The difference is that instead of starting from the coupled theory, in this approach the starting point is the holomorphic effective potential of pure gluodynamics and a heavy fermion is introduced at the effective Lagrangian level by the “integrating in” procedure familiar in the context of supersymmetric theories [65, 66]. The consistency condition used in [64], that the holomorphic structure of the pure gluodynamics should arise from the holomorphic structure of gluodynamics plus a heavy fermion, leads to the values $p = 3b_{YM} = 11N_c$, and $q = 8$. The agreement of this method with the previous approach is encouraging.

We do not pretend that the above discussion fully describes the methods or even lists all the possible ways of setting the values of the parameters ‘ p ’ and ‘ q ’. Our goal was simply to illustrate the uncertainty about the values and give the two main possibilities. The results can be summarised as follows. The self duality hypothesis, non-standard SUSY breaking and the consistency conditions of theories with and without a heavy fermion lead to the values $p = 3b_{YM} = 11N_c$ and $q = 8$ or 12 . For QCD the corresponding values are then $p = 3b_{QCD} = 11N_c - 2N_f$ and $q = 8$ or 12 . The soft SUSY breaking approach leads to the values $p = N_c$ and $q = 1$. As was stated at the beginning of this section, different values of these parameters can lead to some different qualitative results and are particularly important for the results of Chapter 3. Most of the results of Chapters 2 and 4 do not depend on specific values of these parameters.

Appendix B

Hyperspherical Harmonics in Four Dimensions

Hyperspherical coordinates in 4D dimensions are related to the Cartesian coordinates by:

$$x = r \sin(\psi) \sin(\theta) \sin(\phi), \quad (\text{B.179})$$

$$y = r \sin(\psi) \sin(\theta) \cos(\phi), \quad (\text{B.180})$$

$$z = r \sin(\psi) \cos(\theta), \quad (\text{B.181})$$

$$w = r \cos(\psi). \quad (\text{B.182})$$

The Laplacian in 4D in hyperspherical coordinates is:

$$\frac{1}{r^3} \partial_r (r^3 \partial_r) + \frac{1}{r^2 \sin^2 \psi} \partial_\psi (\sin^2 \psi \partial_\psi) + \frac{1}{r^2 \sin^2 \psi \sin \theta} \partial_\theta (\sin \theta \partial_\theta) + \frac{1}{r^2 \sin^2 \psi \sin^2 \theta} \partial_\phi^2. \quad (\text{B.183})$$

Assuming separable solutions and treating θ and ϕ coordinates in exactly the same way as in three dimensions we obtain the differential equation:

$$\Psi''(\psi) + 2 \cot(\psi) \Psi'(\psi) - l(l+1) \csc^2(\psi) \Psi(\psi) = \Lambda \Psi(\psi). \quad (\text{B.184})$$

With the substitution $u = \cos(\psi)$ this becomes:

$$(1 - u^2)U''(u) - 3uU'(u) - \frac{l(l+1)}{1 - u^2}U(u) = BU(u). \quad (\text{B.185})$$

If $B = n(n+2)$ and $l(l+1) = l'(l'+1)$ this can be identified as the differential equation satisfied by the associated type II Chebyshev functions. These can be obtained from the

type II Chebyshev differential equation in exactly the same way as associated Legendre functions are obtained from the Legendre differential equation.

As an aside notice that the type II Chebyshev equation is a special case of the Geigenbauer (Ultraspherical) equation:

$$(1-x^2)\frac{d^2}{dx^2}C_n^{(\alpha)}(x) - (2\alpha+1)x\frac{d}{dx}C_n^{(\alpha)}(x) - n(n+2\alpha)C_n^{(\alpha)}(x) = 0, \quad (\text{B.186})$$

with $\alpha = 1$. The Legendre polynomial equation corresponds to $\alpha = 1/2$. Hyperspherical coordinates in all higher dimensions will lead to associated Geigenbauer equations with integer or half integer α .

The hyperspherical harmonics in four dimensions are given by:

$$Y_{nlm}(\theta, \phi, \psi) = A(n, l, m) \begin{cases} Y_{lm}(\theta, \phi) U_n^l(\cos(\psi)) & 0 \leq l \leq n \\ Y_{|l|m}(\theta, \phi) U_n^{|l|-1}(\cos(\psi)) & -n \leq l \leq -1 \end{cases}, \quad (\text{B.187})$$

where $Y_{lm}(\theta, \phi)$ are the usual 3D spherical harmonics and U_n^l are associated Chebyshev type II functions defined by:

$$\begin{aligned} U_n^l(x) &= (1-x^2)^{l/2} \frac{d^l}{dx^l} U_n(x) \\ &= (1-x^2)^{l/2} \frac{(-1)^n (n+1) \sqrt{\pi}}{2^{n+1} (n+1/2)!} \frac{d^l}{dx^l} \left[(1-x^2)^{-1/2} \frac{d^n}{dx^n} \left\{ (1-x^2)^{n+1/2} \right\} \right] \end{aligned} \quad (\text{B.188})$$

for $l \geq 0$ and by:

$$U_n^l(x) = \frac{(-1)^n (n+1) \sqrt{\pi}}{2^{n+1} (n+1/2)!} (1-x^2)^{l/2} \frac{d^{n+l+1}}{dx^{n+l+1}} \left[(1-x^2)^{n+1/2} \right], \quad (\text{B.189})$$

for $l \leq -2$. These hyperspherical harmonics form a complete orthogonal basis for the functions of the angular variables in four dimensions:

$$\sum_{n=0}^{\infty} \sum_{l=-n}^n \sum_{m=-l}^l Y_{nlm}^*(r, \theta, \phi, \psi) Y_{nlm}(r', \theta', \phi', \psi') = \frac{\delta(\psi - \psi')}{\sin^2 \psi} \frac{\delta(\theta - \theta')}{\sin \theta} \delta(\phi - \phi'), \quad (\text{B.190})$$

$$\int_0^{\infty} \int_0^{\pi} \int_0^{\pi} \int_0^{2\pi} Y_{nlm}^*(r, \theta, \phi, \psi) Y_{n'l'm'}(r, \theta, \phi, \psi) = \delta_{nn'} \delta_{ll'} \delta_{mm'}. \quad (\text{B.191})$$